AD-A152 654 MULTIZONE MODULAR ARTILLERY PROPELLING CHARGE STUDIES 1/2
(U) ARMY BALLISTIC RESEARCH LAB ABERDEEN PROVING GROUND
MD C R RUTH ET AL. FEB 85 BRL-TR-2636 SBI-AD-F300 597

UNCLASSIFIED F/G 19/6 NL

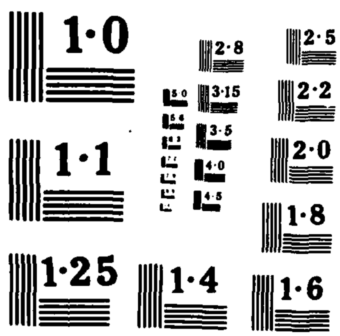
1·0
2·8
2·5
3·15
2·2
3·5
2·0
4·0
4·5
1·1
1·8
1·25
1·4
1·6

A152 005 97

(2)

AD-A152 654

AD

BRL

TECHNICAL REPORT BRL-TR-2636

MULTIZONE MODULAR ARTILLERY PROPELLING CHARGE STUDIES

Carl R. Ruth
Thomas C. Minor

February 1985

APPROVED FOR PUBLIC RELEASE; DISTRIBUTION UNLIMITED.

US ARMY BALLISTIC RESEARCH LABORATORY
ABERDEEN PROVING GROUND, MARYLAND

85

UNCLASSIFIED

SECURITY CLASSIFICATION OF THIS PAGE (When Data Entered)

REPORT DOCUMENTATION PAGE

READ INSTRUCTIONS BEFORE COMPLETING FORM

1. REPORT NUMBER: TECHNICAL REPORT BRL-TR-2636	2. GOVT ACCESSION NO.: AD-A152 654
3. RECIPIENT'S CATALOG NUMBER	
4. TITLE (and Subtitle): MULTIZONE MODULAR ARTILLERY PROPELLING CHARGE STUDIES	5. TYPE OF REPORT & PERIOD COVERED: Technical Report Oct 81 - Jul 83
	6. PERFORMING ORG. REPORT NUMBER
7. AUTHOR(s): Carl R. Ruth and Thomas C. Minor	8. CONTRACT OR GRANT NUMBER(s)
9. PERFORMING ORGANIZATION NAME AND ADDRESS: US Army Ballistic Research Laboratory, ATTN: AMXBR-IBD, Aberdeen Proving Ground, MD 21005-5066	10. PROGRAM ELEMENT, PROJECT, TASK AREA & WORK UNIT NUMBERS: 1L162618AH80
11. CONTROLLING OFFICE NAME AND ADDRESS: US Army Ballistic Research Laboratory, ATTN: AMXBR-OD-ST, Aberdeen Proving Ground, MD 21005-5066	12. REPORT DATE: February 1985
	13. NUMBER OF PAGES: 118
14. MONITORING AGENCY NAME & ADDRESS (if different from Controlling Office)	15. SECURITY CLASS. (of this report): Unclassified
	15a. DECLASSIFICATION/DOWNGRADING SCHEDULE

16. DISTRIBUTION STATEMENT (of this Report)

Approved for public release; distribution unlimited

17. DISTRIBUTION STATEMENT (of the abstract entered in Block 20, if different from Report)

18. SUPPLEMENTARY NOTES

Presented at 1983 JANNAF Propulsion Meeting

19. KEY WORDS (Continue on reverse side if necessary and identify by block number)

Interior Ballistics
Pressure Waves
Howitzers
Grain Geometry
Charge Geometry
Multizone Propelling Charges
Stick Propellant
Combustible Cases
Modular Charges

20. ABSTRACT (Continue on reverse side if necessary and identify by block number)

Many of the requirements for the design of a multizone, combustible-cased, modular charge for howitzer applications that will minimize pressure waves at all zone levels without compromising performance are essentially unknown at the present time. An unsuccessful development program for a 155-mm, multizone bagged charge (XM211) highlighted the need for careful selection of the interrelated components that comprise a multizone charge. In that development program, severe pressure waves in high-temperature firings at

DD FORM 1 JAN 73 1473 EDITION OF 1 NOV 65 IS OBSOLETE

UNCLASSIFIED

SECURITY CLASSIFICATION OF THIS PAGE (When Data Entered)

intermediate zone levels were noted. As a forerunner of the studies reported here, investigations of a similar charge at the Ballistic Research Laboratory demonstrated that severe pressure waves in high-temperature firings could be increased or somewhat mitigated by a change in the charge/chamber configuration and/or ignition stimulus.

Multizone, combustible-cased modular artillery propelling charges were fabricated with both granular and stick propellants and were used in this study to investigate the influence of charge interzone permeability, propellant bed permeability, distribution of ullage, and igniter brisance on the two-phase flow, interior ballistic process, in particular, on the formation of pressure waves. Test charges used to study these phenomena were fabricated to resemble the modular charge configurations proposed for future artillery applications. Gun tests with these charges were conducted using M549 Projectiles fired from an M199 Cannon instrumented to measure chamber and differential pressures. Representative data for each series fired in the standard gun are presented in detail. For the situations investigated here, in which a wide range of loading configurations, boundary permeabilities, and ignition stimuli were studied, the results demonstrated the superiority of stick propellant over granular propellant for this modular-charge application.

To better understand the events occurring early in the ignition cycle with these charges, and their relationship to the formation of pressure waves, multizone combustible-cased charges were fired in a 155-mm howitzer simulator which used plastic tubes in place of the M199 chamber. The simulator permitted direct visualization of the events transpiring within the chamber. Data obtained included pressures measured by gages at the spindle and projectile base; total force on the projectile base; flamefront movement, recorded by high-speed photography; and solid-phase motion, monitored via flash radiography. One granular- and one stick-propellant charge configuration, which were dramatically different in the levels of pressure waves produced in the gun firings, were selected for testing in the simulator.

TABLE OF CONTENTS

LIST OF ILLUSTRATIONS

LIST OF ILLUSTRATIONS (CON'T)

LIST OF TABLES

I. INTRODUCTION

A charge configuration that is frequently employed in Army howitzers is the multizone, artillery propelling charge. This type of charge, schematically illustrated in Figure 1, consists of several discrete packages of propellant bound together in some fashion, as with tie straps. The principal rationale for this charge design is that a particular velocity can be achieved dependent on the number of packages loaded into the weapon chamber, and this selectable velocity, coupled with the permitted variation of weapon launch angle, allows a wide range coverage by indirect fire weapons.

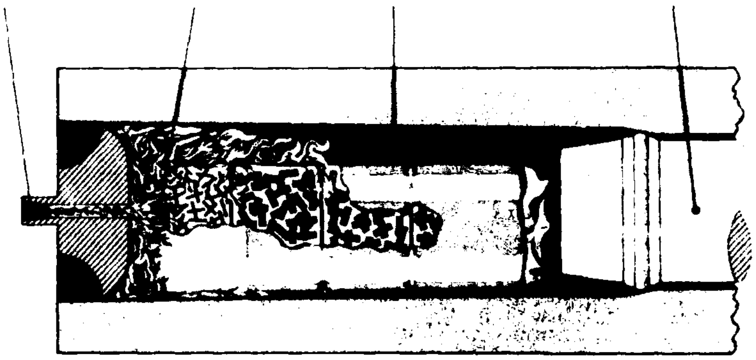

Figure 1. Granular-Propellant, Multiple-Increment, Bagged Charge

The requirements on the design of a multizone charge are demanding. The charge must exhibit reliable performance at the low-zone end without compromising performance at any other zone level.[1,2] A case in point is the now-terminated development program for the 155-mm, XM211, Propelling Charge.[3,4] The XM211 employed a small-web, single-perforation propellant in the base increment and a large-web, seven-perforation propellant in the upper-zone increments. Coupling a very rapidly burning localized-ignition

---

1 I. W. May, "The Role of Ignition and Combustion: A Survey of Developmental Efforts," 13th JANNAF Combustion Meeting, CPIA Publication 281, Vol. I, pp. 315-340, September 1976.

2 I. W. May and A. W. Horst, "Charge Design Considerations and Their Effect on Pressure Waves in Guns," ARBRL-TR-02277, Ballistic Research Laboratory, USA ARRADCOM, Aberdeen Proving Ground, MD, December 1980 (AD A095342).

3 T. C. Minor and J. DeLorenzo, "Charge Design Approaches to the Reduction of Low Zone Stickers," 1976 JANNAF Propulsion Meeting, CPIA Publication 280, Vol. III, pp. 403-434, December 1976.

4 R. J. DeKleine, "155-mm XM211 Propelling Charge Zones 3-6 Design Review Minutes," Office of Project Manager, Cannon Artillery Weapons Systems, Dover, NJ, April 1980.

source to forward packages of less rapidly burning propellant in the XM211 led to the formation of axial pressure waves, particularly at the Zone-5 level with charges conditioned to 63°C. From this program, we once again learned that it is necessary to consider all the interrelated components that make up the charge in order to obtain satisfactory performance at all zone levels.

The phenomenology of a multiple-increment, bagged charge similar to that of Figure 1 was considered in detail previously.[5,6] It was shown that in addition to well-documented problems usually associated with pressure waves in high-loading-density M203 charges, the deleterious effect in low-loading-density charges of the impact of large quantities of propellant on the projectile base on the projectile's safety and performance is also of concern. Even though pressure waves themselves in this-low-loading-density charge were not a hazard to tube or breech integrity, they have adversely affected more delicate weapon mechanisms.

To eliminate many, if not all, the aforementioned problems, the charge design community is seriously considering modular, energetic packaging configurations for both granular and stick propellants with special emphasis being placed on the stick configuration. The use of stick propellant in both high- and medium-performance artillery charges is finding increased application.[7] The Army is currently introducing stick propellant into the product-improved 155-mm, M203 (Zone 8S) charge. As future advanced artillery weapons systems come along, the use of stick propellant is virtually assured.

The main advantages of charges made with stick propellant are: reduced pressure-wave generation leading to improved safety; increased loading density, permitting the use of lower flame temperature propellants that may reduce wear, flash, and blast; simplicity of the ignition system with reduced ignition delay; and simplified loading, assembling and packaging procedures. In Figure 2, a multizone, modular charge consisting of three zones is shown.

As illustrated in Figure 3, one of the main advantages of modular-charge configurations over bag-charge configurations is a rigid package consisting of interlocking components, thus facilitating automatic loading in new weapons systems planned for the 1990s to augment the M198 Howitzer

---

5 T. C. Minor and A. W. Horst, "Experimental Studies of Ignition Phenomena in One-Dimensional Propelling Charges," ARBRL-TR-02315, Ballistic Research Laboratory, USA ARRADCOM, Aberdeen Proving Ground, MD, April 1981 (AD A100298).

6 C. R. Ruth and T. C. Minor, "Multizone Artillery Propelling Charge Studies," ARBRL-TR-02486, Ballistic Research Laboratory, USA ARRADCOM, Aberdeen Proving Ground, MD, May 1983 (AD A128285).

7 T. C. Minor, "Mitigation of Ignition-Induced, Two-Phase Flow Dynamics in Guns Through the Use of Stick Propellant," ARBRL-TR-02508, Ballistic Research Laboratory, USA ARRADCOM, Aberdeen Proving Ground, MD, August 1983 (AD A133685).

shown in Figure 4. Furthermore, since the modular-charge system will consist of a small number of discrete module types, the propelling charge corresponding to a desired performance level can be built up from the increments at firing time, rather than discarding bags of propellant as is currently done with multizone artillery charges, resulting in a propellant and cost savings. New processing techniques might allow for the incorporation of additives such as wear-reducing, decoppering, flash-reducing, etc., directly into the case, and the increased strength of loaded, rigidized combustible cartridge cases, as compared to bag charges, will minimize handling and transportation problems.

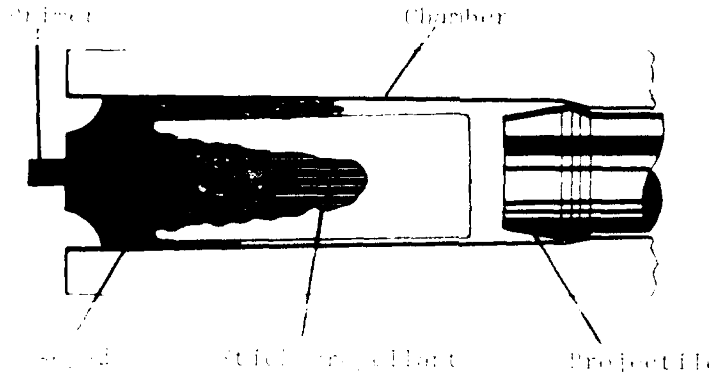

Figure 2. Stick-Propellant, Multiple-Increment, Modular Charge

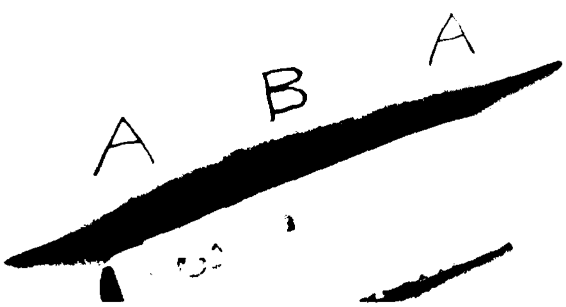

Figure 3. Comparison of Modular and Bagged Charges

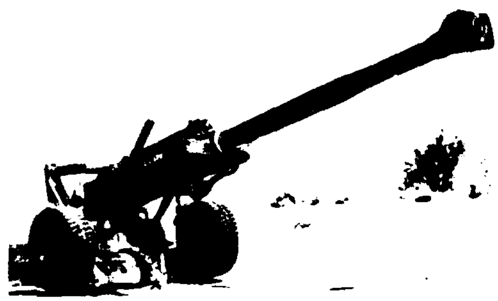

Figure 4. M198 Howitzer System

Let us now examine, with reference to Figure 2, some of the potential events in the early portion of the interior ballistic cycle with a combustible-cased, modular propelling charge. The output of a primer impinges on a basepad, and the burning basepad ignites the rear case wall of the module. Upon burn-through of the rear case wall, the rear of the propellant bed is exposed to hot igniter gases, and is heated to ignition. These hot gases then join those from the igniter and case to produce a convectively driven ignition wave, resulting in flamespread through the charge. In the situation of granular propellant, resistance to the gas flow may lead to the formation of a pressure gradient in the propellant bed, and perhaps even movement of the solid phase, as we have previously seen for bagged granular charges.[5] With the use of stick propellant yielding a much smaller resistance to gas flow, essentially no pressure gradient is formed in the propellant bed, and we would not expect

the solid phase to experience much movement. However, even with the stick propellant, there will be substantial resistance to the flow of the gases offered by the relatively impermeable interzone barriers presented by the case end walls, possibly leading to the acceleration of entire packages of propellant toward the projectile base. Complicating characterization of these phenomena, but perhaps resulting in better ignition of the charge, the igniter gases may take the path of least resistance and flow into the annular ullage surrounding the charge, which will almost certainly be present in order to facilitate loading. We have noted such behavior in other combustible-cased charges employing stick propellant.[8] In this manner, the case may begin to burn along its length, and if the case collapses due to pressurization of the ullage, the propellant bed itself may be exposed to these hot gases along a substantial portion of its axial extent, promoting uniform ignition of the charge. Lastly, we cannot overlook the potential for fracture of the propellant, either granular or stick. Such fracture may occur not only as a result of impact of a package of propellant on the projectile base, but also due to attack of an overly brisant igniter on the rear of the charge. Furthermore, stick propellant may rupture due to a pressure differential established between the interior and exterior of the long grain. All of these processes serve to create unprogrammed burning surfaces, which may lead to high local pressurization and the formation of pressure waves, should even the natural flow channels presented by stick propellant be obstructed.

The experimental investigations reported herein attempted to assess the influence of loading conditions and variations of the interrelated components which comprise a medium-performance, large-caliber, combustible-cased, multizone propelling charge on pressure-wave formation. These investigations were conducted via test firings of the charges in both a well-instrumented 155-mm howitzer and a howitzer simulator.

II. TEST SETUP

A. Weapon

A 155-mm, M199 tube modified with pressure ports at thirteen axial locations was the test weapon for all the firings. The standard muzzle brake was replaced with a special pressure-gage adapter used in support of a muzzle-pressure program that was conducted concurrently with the multi-zone firings. For this weapon, the standard, lanyard-operated, spring-driven firing pin was replaced by a gas-activated firing pin.[9] The gas necessary to drive the modified firing pin into the M82 percussion primer

---

8 T. C. Minor and A. W. Horst, "Ignition Phenomena in Developmental Stick-Propellant, Combustible-Cased, 155-mm, M203E2 Propelling Charges," ARBRL-TR-02568, Ballistic Research Laboratory, USA ARRADCOM, Aberdeen Proving Ground, MD, July 1984.

9 J. J. Rocchio, R. A. Hartman, and N. J. Gerri, "An Electric Primer-Operated Firing Pin Actuator for Large Caliber Guns," ARBRL-MR-02897, Ballistic Research Laboratory, USA ARRADCOM, Aberdeen Proving Ground, MD, January 1979 (AD A069109).

TABLE 4. FIRING RESULTS FOR ULLAGE VARIATIONS/GRANULAR PROPELLANT*

Series No.	Charge Variations	Spindle Pressure (MPa)	$-\Delta P_i$ (MPa)	Velocity (m/s)	No. Rds.	Ign. Del. (ms)
8.	CBI basepad on Module A/ Hole of endcaps on Modules A, B, and A" opened from 22 to 51 mm/ Holes of fronts of Modules A and B opened from 22 to 51 mm/ Vent holes (5.6-mm diam) put in Modules A and A" (50 holes) and in Module B (40 holes)/ NC spacers connected to Modules A and B, and to B and A"	281 (5.5)	23 (18.2)	695 (2.6)	3	51 (19.1)
9.	Similar to Series 8 except that vent holes 3.8-mm in diameter	283**	34**	696 (2.1)	3	40 (5.5)
10.	Same as Baseline Series 1 except that modules separated in chamber with no spacers keeping them from moving	276**	26**	696**	2	47
11.	Same as Series 1 except that modules were placed at maximum standoff - 10 cm from spindle face	322	65	701	1	56

*Standard deviations are given in parentheses for series with 3 or more rounds

**Average of two rounds

To determine the effects of maximum standoff, another Baseline Series 1 charge was fabricated and test-fired (Series 11, Figure 14). The results for the one round firing are shown in Table 4. The peak pressure and $-\Delta P_i$ of 322 and 65 MPa, respectively, were much higher than observed with the baseline series. The change in standoff from 2 to 10 cm apparently alters the flow of igniter and initial combustion gases significantly. Though only one round was fired, this configuration gave the highest level of pressure waves of all the series tested using a one-basepad ignition source.

C. Modular Case/Stick Propellant

1. Baseline Series/Stick Propellant. To fabricate the baseline series, the Type-[illegible], NC containers were used. Two of the long A modules and one of the short B modules were loaded with 2.9 kg and 2.0 kg, respectively, of the [illegible], slotted-stick propellant. Endcaps were placed on all three containers before they were fitted together into a charge consisting of Basepad/Module A/Module B/Module A" (Figure 15). As in the previous tests, Module A was next to the basepad and Module A" was at the front of the

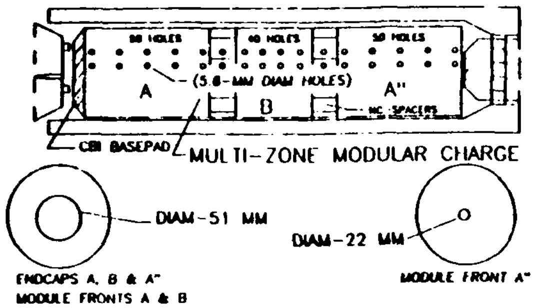

(Series 8)

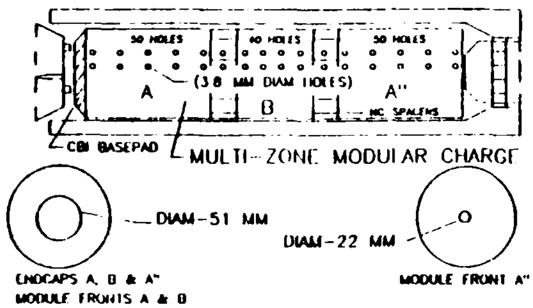

(Series 9)

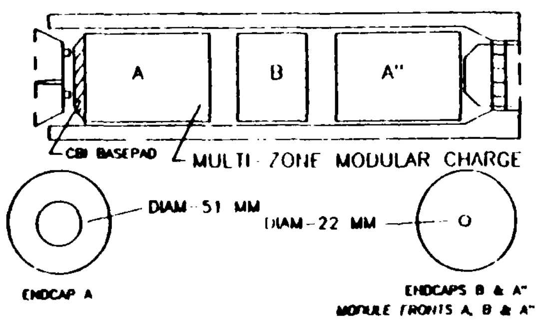

(Series 10)

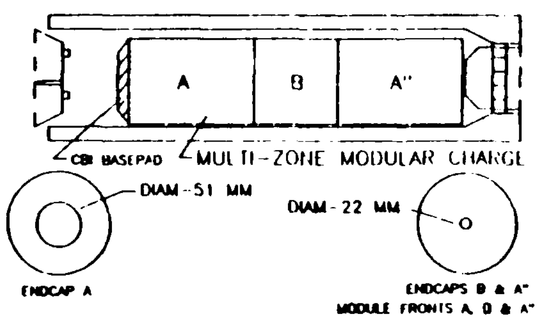

(Series 11)

Figure 14. Charge/Chamber Configuration for Modular Case/Granular Propellant with Ullage Variations

vent-hole size from 5.6 mm to 2.8 mm produced a four-fold reduction in access area of igniter and early combustion gases to propellant surfaces. Such a reduction impeded uniform axial ignition of the charge, and, as expected, resulted in a higher level of pressure waves.

3. Ullage Variations/Granular Propellant. Since the length of the charge and that of the chamber differed by only 10 cm, there could be no dramatic altering of the charge/chamber interface. Two basic configurations, charge at maximum standoff and charge modules equally separated with NC spacers interconnecting the modules in the chamber, were selected. Perturbations on each of these two series were also fired. Results are noted in Table 4.

Series 8 was similar to Series 5, except that NC spacers made it almost full-chamber length (Figure 14). As in Series 5, the holes in the three endcaps and the front of Modules A and B were opened from 22 to 51 mm, and 50 vent holes in Modules A and A" and 40 vent holes in Module B, all 5.6 mm in diameter, were added to insure maximum axial and radial penetration of igniter gases into the propellant bed. After the charge was fabricated, two NC spacers, one connected to Modules A and B, the other connected to Modules B and A", were inserted. This increase in charge length reduced the possible axial movement of the charge from 10 to 2 cm. The results (Table 4) of this restriction on charge movement did little to peak pressure in comparison to Series 5 (281 MPa versus 277 MPa), but substantially increased the level of pressure waves (23 versus 8 MPa). The large standard deviation in $-\Delta P_i$ of 18 MPa and in ignition delay of 19 ms attested to the large variation within the three rounds. Charge integrity was weakened by the five-module system (Module A/NC spacer/Module B/NC spacer/Module A") since the two 5-cm long spacers, fabricated from an existing module, did not interlock as tightly as the modules. This could have contributed to erratic ignition and flow of igniter and combustion gases through the system.

To determine the effect of reduced radial penetration of igniter gases into a charge that had the same overall axial and radial dimensions as those of Series 8, Series 9 (Figure 14) was fabricated with vent holes 3.8 mm in diameter, all other characteristics of the charge being the same as Series 8. This reduced the radial, initial vent area by a factor of two. The results (Table 4) were essentially the same as Series 8 for pressure, velocity and ignition delay. The $-\Delta P_i$ was about 30 percent higher, again, a not-surprising result.

In Series 10 (Figure 14), the effect of initial increment position on pressure-wave formation was addressed. The charge fabrication used unmodified NC modules as in the baseline series, wherein the hole in the endcap of only Module A was opened up from 22 to 51 mm. The increments were positioned so that Module A" was forward against the base of the projectile; Module B was mid-chamber approximately 5 cm from the base of Module A"; and Module A was 2 cm from the spindle face, approximately 5 cm from Module B. No spacers were positioned between modules to keep them from moving after ignition occurred. The averaged results (Table 4) for a two-round series gave a peak pressure of 276 MPa and a $-\Delta P_i$ of 26 MPa which were similar to those observed in Series 8 and 9. Although peak pressure was about the same as the baseline series, the level of pressure waves was considerably less, indicating a more uniform ignition of the charge.

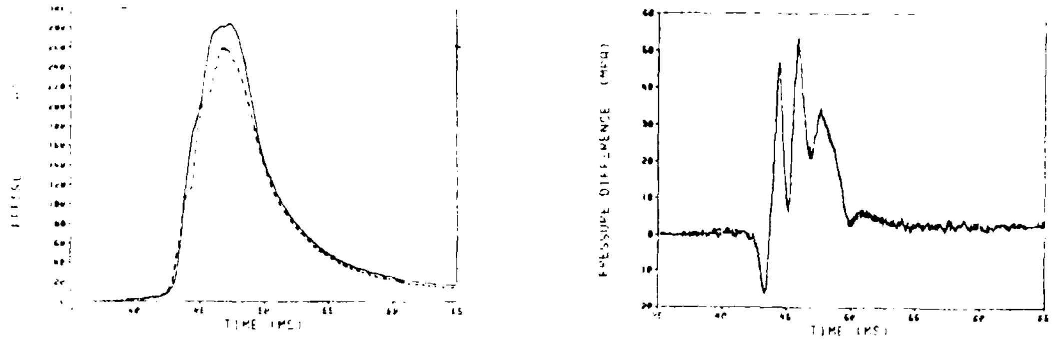

Figure 12. Spindle and Forward Chamber Pressure and Pressure Difference versus Time for Medium Pressure Waves

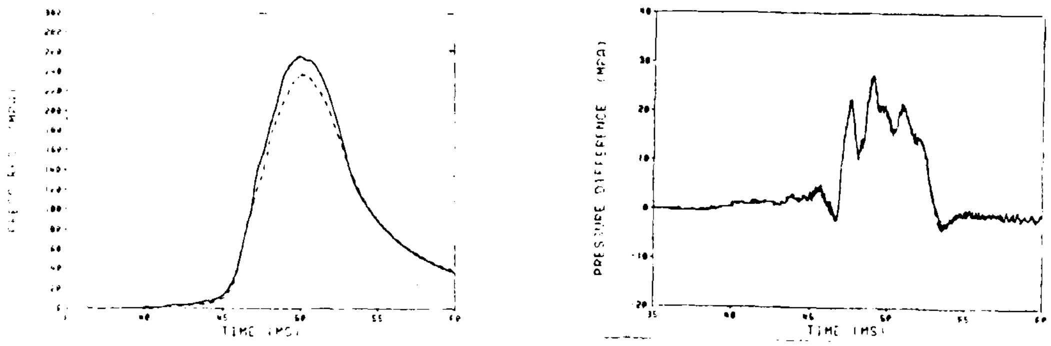

Figure 13. Spindle and Forward Chamber Pressure and Pressure Difference versus Time for Small Pressure Waves

versus 279 MPa) but a dramatic drop in the $-\Delta P_i$ (8 versus 46 MPa). This combination of both axial and radial enhancement of igniter gas flow into the charge reduced pressure-wave levels sixfold. Examples of both medium pressure waves (10 to 20 MPa) and small pressure waves (0 to 10 MPa) are shown, respectively, in Figures 12 and 13.

In each series, it was necessary to place a thin cloth covering over either the 22-mm or 51-mm hole to prevent propellant from moving from one module to another. In those series with 51-mm openings, the integrity of the cloth in preventing propellant from moving from one module to another was suspect. In Series 6 (Figure 9), we kept the small 22-mm opening and yet still maintained the large radial and axial flow of igniter gases as in Series 5. This was done by altering the three endcaps and fronts of Modules A and B with 150 holes 5.6 mm in diameter, rather than opening the 22-mm hole to 51 mm. The results (Table 3) for the one round agreed well with those from the Series 5 firings. Peak pressure was 281 MPa and $-\Delta P_i$ was 10 MPa, only slightly higher than the 8 MPa of Series 5.

To further clarify the importance of the radial and axial vent holes in the charge, another round similar to Series 6 was fabricated and test-fired. In Series 7, the holes in both the module sides, fronts and endcaps were reduced from 5.6 mm to 2.8 mm in diameter (Figure 9). Peak pressure was about the same as Series 6 (Table 3). The initial reverse-pressure gradient at 16 MPa was higher than the 10 MPa of Series 6. The change in

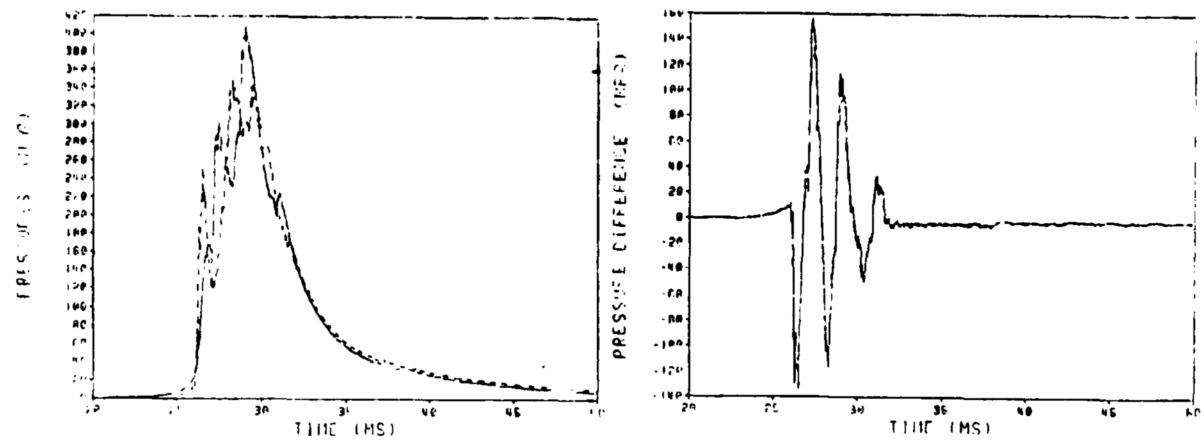

Figure 11. Spindle and Forward Chamber Pressure and Pressure Difference versus Time for Very Large Pressure Waves

To maximize the flow of igniter gases through the charge, rounds were constructed which minimized interior boundaries between modules. In Series 3 (Figure 9), not only was the hole of the endcap on Module A opened from 22 to 51 mm, but the endcaps on Modules B and A" were eliminated. In addition, the holes on the front of Modules A and B were also opened up to 51 mm. The results (Table 3) indicate a more uniform ignition of the propellant. Peak pressure was about the same as in the baseline series, but the $-\Delta P_i$ was much lower, 17 MPa versus 46 MPa. Velocity and ignition delay were in the same range as the baseline series.

In an effort to further enhance the rapid ignition of all propellant grains in the modular charges, NC centercore tubes were added in Series 4 (Figure 9). The 22-mm hole in both the three endcaps and the front of the modules was maintained so as to hold the centercore tubes in place. To have similar axial flow of igniter gases as in Series 3, several small cutouts were made in the three endcaps and the fronts of Modules A, B and A". The addition of the centercore tubes not only changed the flow characteristics of the ignition gases but somewhat redistributed the propellant in relation to both the charge and initial combustion gases. There was no improvement in the results (Table 3) of this configuration over that of Series 3. The peak pressure at 288 MPa was slightly higher while the $-\Delta P_i$ of 14 MPa was slightly lower than in Series 3. Both the increase in pressure and the lower $-\Delta P_i$ resulted in a higher muzzle velocity for Series 4 of 698 m/s.

In Series 5 (Figure 9), the charge design was a further modification of Series 3. Endcaps with 51-mm rather than 22-mm holes were on each of the modules. The holes in the front of Modules A and B were also opened up from 22 to 51 mm. A layer of cloth was placed over each of these holes to keep propellant from moving between modules. To increase radial flow of igniter gases into the charge, vent holes 5.6 mm in diameter were placed in each of the modules. Fifty holes in Modules A and A", and 40 holes in Module B were symmetrically placed around the cylindrical walls. The results (Table 3), when compared with the baseline series, show no change in peak pressure (277

TABLE 3. FIRING RESULTS FOR IGNITION VARIATIONS/GRANULAR PROPELLANT* (CON'T)

Series No.	Charge Variations	Spindle Pressure (MPa)	$-\Delta P_i$ (MPa)	Velocity (m/s)	No. Rds.	Ign. Del. (ms)
6.	CBI basepad on Module A/ Endcaps and fronts of Modules A and B both have 150 holes (5.6-mm diam) and standard 22-mm hole/ Vent holes (5.6-mm diam) put in Modules A and A" (50 holes) and in Module B (40 holes)	281	10	694	1	45
7.	Similar to Series 6 except the holes in sides, fronts, and endcaps are 2.8-mm diam	279	16	694	1	40

*Standard deviations are given in parentheses for series with 3 or more rounds.

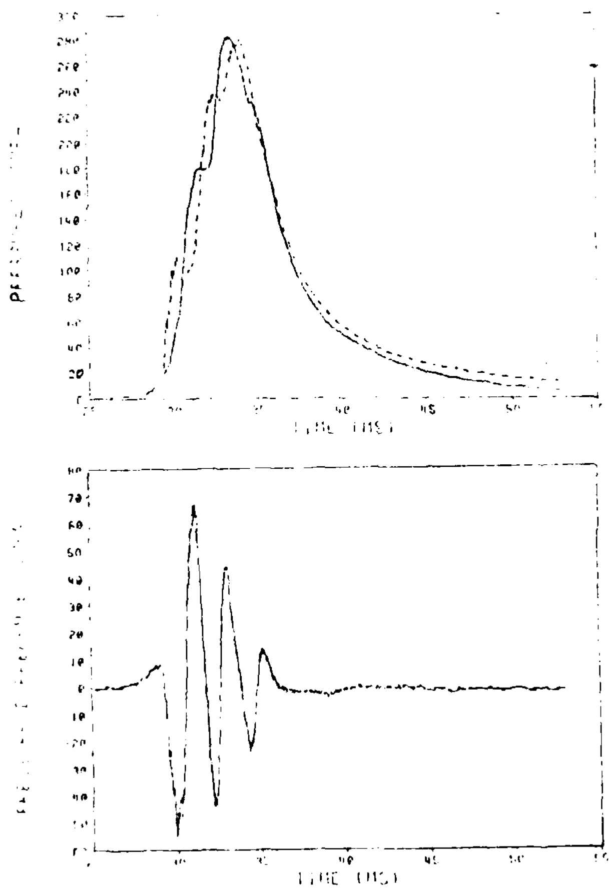

Figure 10. Spindle and Forward Chamber Pressure and Pressure Difference versus Time for Large Pressure Waves

TABLE 3. FIRING RESULTS FOR IGNITION VARIATIONS/GRANULAR PROPELLANT*

Series No.	Charge Variations	Spindle Pressure (MPa)	$-\Delta P_i$ (MPa)	Velocity (m/s)	No. Rds.	Ign. Del. (ms)
1.	CBI basepad on Module A/ Hole in endcap of Module A opened from 22 to 51 mm/ Modules A, B, and A" and Endcaps B and A" unmodified (Baseline Series)	279 (5.3)	46 (5.5)	686 (0.8)	4	28 (1.9)
2.	Three CBI basepads - one each at base of Modules of A, B, and A"/ Hole in endcaps A, B, and A" opened from 22 to 51 mm	402	115	717	1	25
3.	CBI basepad and one endcap on Module A/ No endcaps on Modules B and A"/ Holes in endcap of Module A and front of Modules A and B opened from 22 to 51 mm	282 (1.0)	17 (5.1)	690 (1.5)	3	31 (3.1)
4.	CBI basepad on Module A/ Endcaps and fronts of modules had 22-mm hole unmodified to support centercore tubes/ Cutouts on endcaps and fronts of Modules A, B and A" to mimic 51-mm hole in Series 1, 2, and 3	288 (2.6)	14 (8.4)	698 (0.6)	3	32 (0.6)
5.	CBI basepad on Module A/ Holes of endcaps on Modules A, B, and A" opened from 22 to 51 mm/ Holes of fronts of Modules A and B opened from 22 to 51 mm/ Vent holes (5.6-mm diam) put in Modules A and A" (50 holes) and in Module B (40 holes)	277 (2.5)	8 (3.5)	693 (1.7)	3	34 (2.0)

*Standard deviations are given in parenthesis for series with 3 or more rounds.

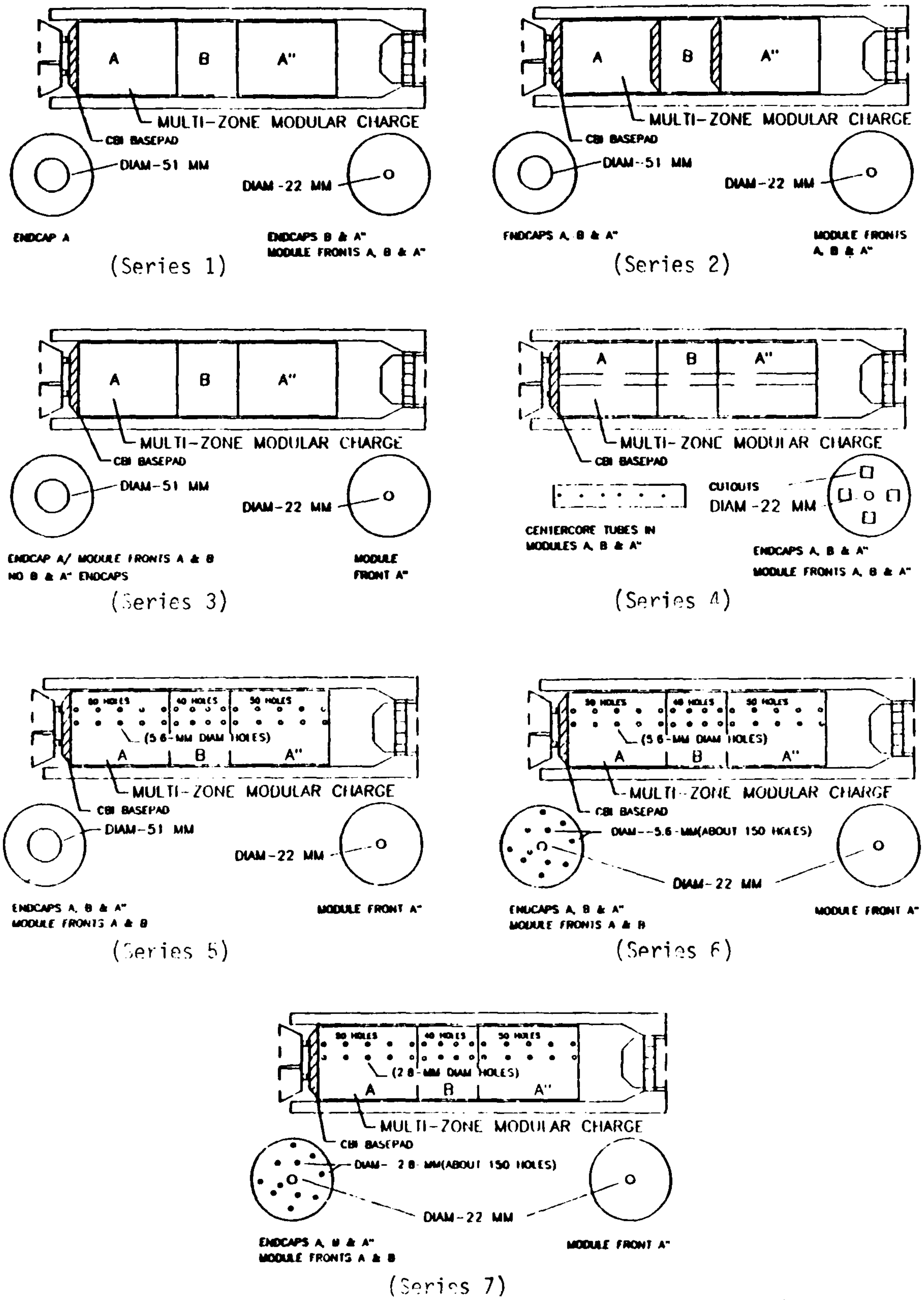

Figure 9. Charge/Chamber Configuration for Modular Case/Granular Propellant with Ignition Variations

In inventory was some 1.14-mm web M1MP propellant which was calculated to give a peak pressure substantially less than the 0.91-mm web M1MP. Since peak pressure and perhaps the level of pressure waves would be lower, and thus less threatening to the integrity of the gun, this propellant was selected as the candidate propellant pending outcome of the initial firing tests.

B. Modular Case/Granular Propellant

1. Baseline Series/Granular Propellant. To fabricate the baseline series, two of the long A modules were each loaded with 2.9 kg of propellant and one of the short B modules was loaded with 2.0 kg of propellant. Endcaps were placed on all three containers before they were fitted together into a charge consisting of Basepad/Module A/Module B/Module A". Although modules A and A" were identical, the module at the front of the charge will be referred to as A" and the module next to the basepad as A. The total weight of the charge was 7.8 kg of the 1.14-mm web, M1MP propellant, 85 g Clean Burning Igniter (CBI) in a basepad, and approximately 0.84-kg Type-1, NC container. The hole in the endcap between the basepad and Module A was opened up from 22 to 51 mm to enhance igniter gas flow through the charge. Standoff for all four charges in Series 1 was 25 mm (Figure 9). The results from this baseline series are given in the first entry in Table 3. The peak pressure of 279 MPa and $-\Delta P_i$ of 46 MPa were well within the acceptable limits of gun safety for continuation of further tests with this propellant. Typical plots of spindle and forward chamber pressure and pressure difference versus time for large pressure waves (20 to 60 MPa) are shown in Figure 10. Coil velocity and ignition delay were 686 m/s and 28 ms, respectively.

2. Ignition Variations/Granular Propellant. Limited availability of Type-1 NC modular components required limiting series size to three rounds. For three of the six ignition variations, only one round was fired, either to simply establish a trend or because of gun safety considerations.

Series 2 fabrication (Figure 9) paralleled that of Series 1 except that three basepads were used instead of one. The three basepads, one each at the base of Modules A, B, and A", were all on the outside of the module with the base endcap located between basepad and propellant. The opening in the Series 2 endcaps all were enlarged to 51 mm. Thus, the charge consisted of Basepad/Module A/Basepad/Module B/Basepad/Module A". Again, the charge standoff was 25mm. Propellant was restrained in each module by placing a thin cloth covering over the vent openings. Results were dramatically different from Series 1. Peak pressure and $-\Delta P_i$ rose from 279 and 46 MPa, respectively to 402 and 115 MPa. The average pressure difference for the second and third negative excursions were 97 and 43 MPa, respectively, indicating an extremely severe pressure-wave phenomenon. This very large reverse pressure difference (greater than 60 MPa) is shown graphically in Figure 11. The effect of the two additional basepads behind Modules B and A" did not enhance ignition of the granular propellant in all modules as intended, but rather reinforced the vigorous, localized ignition of the cha ge, perhaps at several sites. Firings were discontinued after one shot since both peak pressure and pressure-wave levels were large enough to damage the tube and/or related components. All further testing was done using one basepad.

to by a substantial increase in $-\Delta P_i$ (Series E) which was accompanied by a slight increase in peak pressure. Since this large $-\Delta P_i$ in conjunction with a large peak pressure posed serious safety problems for the various parts of the howitzer, either another web of M1MP or another type of propellant had to be considered. The influence of case confinement on pressure-wave formation (Series C thru E) prompted retesting of the M31E1MP in modular containers (Series F). Although pressure waves were present, their feedback into peak pressure was not apparent in this limited testing.

TABLE 2. PRELIMINARY FIRINGS WITH GRANULAR PROPELLANTS*

Charge	Rationale	Spindle Pressure (MPa)	$-\Delta P_i$ (MPa)	No. Rds.	Series
M31E1MP bagged charges	Effect of 7.8-kg propellant on pressure and $-\Delta P_i$	132 (1.3)	0 (0.0)	4	A
M1MP bagged charges	Effect of 7.8-kg propellant on pressure and $-\Delta P_i$	341 (2.9)	21 (12.9)	4	B
M1MP sub-caliber NC-sleeved cylinder	Effect of 7.8-kg propellant on pressure and $-\Delta P_i$/ Effect of no axial inhibition of gas flow, radial ullage	379 (2.9)	14 (5.6)	4	C
M1MP full-bore NC-sleeved cylinder	Effect of 7.8-kg propellant on pressure and $-\Delta P_i$/ Effect of no axial inhibition of gas flow, reduced radial ullage	381 (7.2)	26 (10.3)	3	D
M1MP full-bore modular case (Type 1)	Effect of 7.8-kg propellant in modular case on pressure and $-\Delta P_i$/ Effect of fully combustible-cased packaging	387	50	2	E
M31E1MP full-bore modular case (Type 1)	Effect of 7.8-kg propellant in modular case on pressure and $-\Delta P_i$/ Effect of fully combustible-cased packaging	130 (1.6)	12 (3.9)	3	F

*Standard deviations are given in parentheses for series with 3 or more rounds

TABLE 1. GRANULAR MULTI-PERFORATED PROPELLANT AVAILABLE FOR TESTS

Propellant	Web (mm)	Length (mm)	Diameter (mm)	Diameter Perf (mm)
M1SP	0.33	4.04	1.75	0.10
M1MP	0.91	11.20	4.83	0.38
M31E1MP	1.52	20.20	8.15	0.69
M1MP	1.14	13.49	5.92	0.43

Interior ballistic calculations for each of these available granular propellant charges were performed using an updated version of the Baer-Frankle lumped parameter code.[11] The calculation for 7.8 kg of M1SP propellant indicated that it would give pressures too high for reasonable safety. Charges with two different webs of M1MP and one web of M31E1MP were predicted to give a wide range of peak pressures well within the safety limits of the gun, and thus were selected for initial testing. Pertinent data from the initial tests with M1MP (0.91-mm web) and M31E1MP (1.52-mm web) are listed in Table 2 along with a rationale for each particular test.

Although the M31E1MP would have brought a continuity of propellant formulation to the program in going from initial tests with granular propellant to final tests with stick propellant, the web of the readily available M31E1MP granular propellant was too large as reflected by the peak pressure (Series A). The M1MP seemed promising since both the peak pressure and the pressure difference were at acceptable levels for manipulating conditions within both the charge and charge/chamber interface (Series B).

Since rigid, NC-cased modules loaded with granular propellant might alter peak pressure and $-\Delta P_i$, an increasingly more stringent set of NC-case-confinement conditions was imposed on the propellant. The initial change from bag to NC-cylinder confinement with no change in axial or radial charge/chamber configuration, but with some change in radial flow of initial combustion gases because of the difference in bag versus case permeability, increased peak pressure while reducing $-\Delta P_i$ (Series C). When radial ullage was reduced by increasing the NC cylinder diameter to approximately that of the modular cases to be used later in the program, the peak pressure remained unchanged, but the level of $-\Delta P_i$ rose substantially (Series D), surpassing that of the bag charges (Series B). When modular charges with front and rear NC surfaces were used in place of NC-sleeved cylinders, the passage of igniter and initial combustion gases through the granular bed of propellant was further restricted as attested

11 P. G. Baer and J. M. Frankle, "Simulation of the Interior Ballistics of Guns by Digital Computer Program," R1183, Ballistic Research Laboratories, Aberdeen Proving Ground, MD, December 1962 (AD299980).

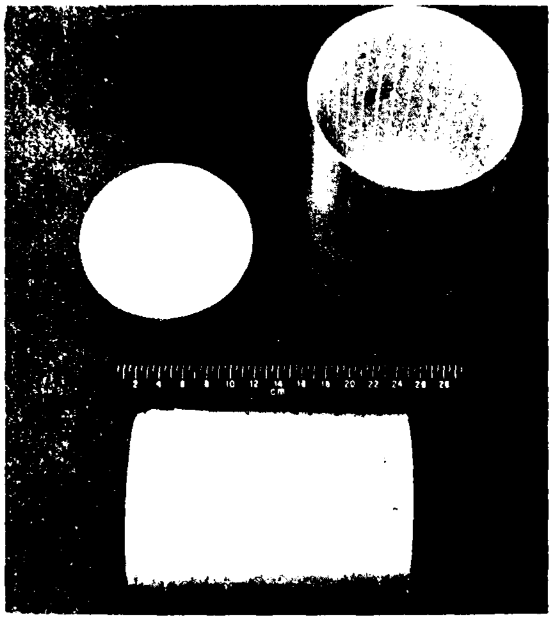

Figure 7. NC Container, Type 2

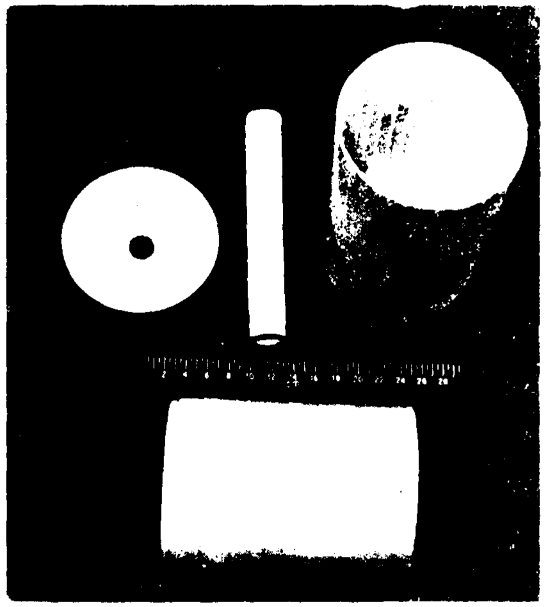

Figure 8. NC Container, Type 1

III. RESULTS

Preliminary firings were done with the Type-1, NC modules[10] and several granular propellant formulations and webs under consideration for testing. After selection of the baseline granular propellant, variations in charge/chamber interface, ullage distribution, ignition intensity, etc., were made in both the granular and the follow-on stick propellants to ascertain the extent to which they influenced pressure-wave formation as indicated by the initial reverse pressure gradients, $-\Delta P_i$. Additional tests on the more interesting cases, as determined from the gun firings, were repeated in the 155-mm howitzer simulator.

A. Preliminary Firings for Selection of Granular Propellant

The modular, Zone-3 charge used for all these tests contained 7.8 kg of propellant, a substantial increase in propellant weight over our previous work on multizone combustion phenomena.[6] To ascertain the interactive affects of different propellant weights and types with different packaging configurations, several granular propellant formulations, locally available, were used for initial testing while awaiting the fabrication of the M31E1 slotted-stick propellant. Their physical characteristics are shown in Table 1.

[10] S. Einstein, B. Pellington, S. Westley, "Charge Design Technology," Large Caliber Weapon Systems Laboratory, USA ARRADCOM, September 1980.

velocities required for the 155-mm, M198 and M109A2/A3 Howitzers. The charge is built from two combustible-cased increments, one with a propellant weight of 2.9 kg (Module A) and the other with a weight of 2.0 kg (Module B). The 1.3-mm web, slotted-stick propellant consisted of two different lengths, 24 cm for the Module . and 17 cm for the Module B units. For our tests, the 24-cm and 17-cm long stick propellants were reduced in length to 23 cm and 16 cm, respectively, so that the module endcaps could be firmly snapped in place. In this concept, the two basic increments, one 27-cm long, the other 21-cm long both being 15 cm in diameter and having wall thicknesses of 3 mm, would be added together to obtain the required velocities rather than discarding increments as is done with the present standard, bagged, multizone charge. The propelling charge may be fired as a Zone 1 (Module A), a Zone 2 (Modules A and B), or a Zone 3 (Modules A, B, and A). A photograph of the granular M1MP and the slotted-stick M31E1 propellants used for these tests is shown in Figure 6. Copies of the Propellant Description Sheets for these propellants are given in Appendix A.

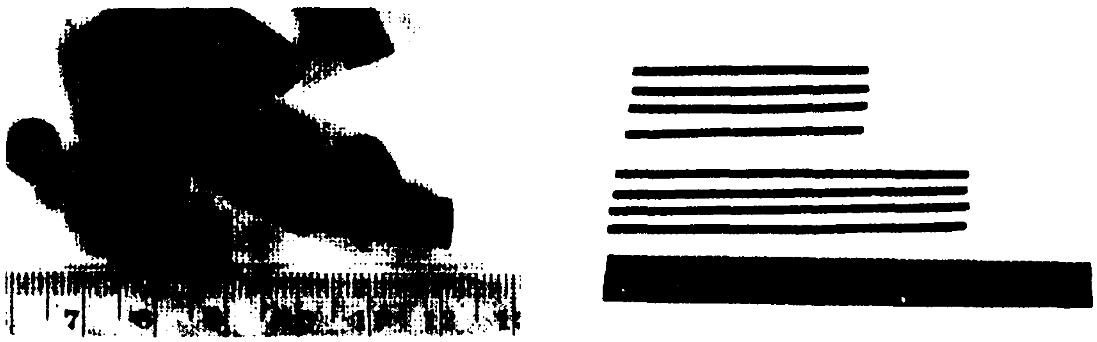

Figure 6. Granular Propellant, M1MP, and Slotted-Stick Propellant, M31E1

Two types of nitrocellulose (NC) modules were used for the tests. The present version (Type 2) is a molded NC cylindrical container (72-percent NC) open at one end to allow for loading of propellant. An unvented endcap fits snugly into the open end of the cylinder. This version, shown in Figure 7, was used for all tests with stick propellant. The previous version (Type 1), shown in Figure 8, was a molded NC cylindrical container (55-percent NC) which had a 22-mm vent hole in both the base of the cylinder and in the endcap. Extensions were structurally designed into both the base and endcap to allow for the placement of an NC centercore tube. When the tube was not used, a thin cloth covering was placed over the fore and aft holes to contain the propellant. Since this early version was readily available, it was used for all tests with granular propellant while awaiting the manufacture and shipment of both the modular containers and M31E1 slotted-stick propellant. Depending on the test condition, modifications were made to the NC modular structure and/or the charge/chamber interface. The modular NC containers were purchased from the EFMC Corporation, CA. The stick propellant was purchased under contract from Radford Army Ammunition Plant, Radford, VA, whereas the M1MP was obtained on post from available lots at Aberdeen Proving Ground, MD. All charges were conditioned at 63°C for at least 24 hours prior to firing.

was obtained from an M52A3B1 electric detonating cap. The rapid and reproducible functioning of the M52A3B1 enabled instrumentation to be accurately timed by this firing system. After the M52A3B1 cap was detonated, there was approximately a 1-ms delay until the M82 primer functioned. An M158 recoil mechanism in conjunction with the upper carriage from a 155-mm, M59 gun was used to mount the APG Medium B Sleigh which housed the 155-mm, M199 Cannon. All tests with this system were done at the Sandy Point Firing Facility (Range 18) located at the Ballistic Research Laboratory.

B. Instrumentation

Instrumentation on all tests consisted of six Kistler 607C piezoelectric pressure transducers housed in the gun chamber: two each, side-by-side in the spindle; two each, 180 degrees apart at mid chamber; and two each, 30 degrees apart at a forward chamber location (Figure 5). These six gages were sufficient to yield a measure of the pressure profile in the chamber. By differencing either of the spindle and forward-chamber gages (P1-P5, P1-P6, P2-P5, P2-P6), the initial negative pressure difference, $-\Delta P_i$, was determined. Projectile velocity was calculated using the distance between and the projectile arrival times at two solenoid coils located approximately 20 and 35 meters, respectively, forward of the gun muzzle. Ignition delay was defined as the time interval between the firing pulse and a spindle pressure of 7 MPa.

Generally, the data were recorded in real time by the Ballistic Data Acquisition System under the control of a PDP 11/45 mini-computer. If the data were not recorded on-line because of an unusually long ignition delay or a computer malfunction, they were later digitized from an analog recording made of each test firing.

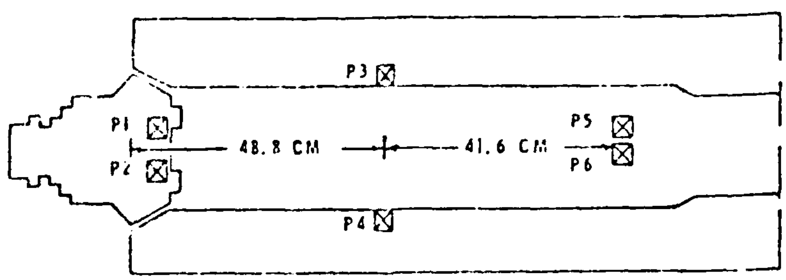

Figure 5. Locations of Pressure Transducers in M199 Chamber

C. Firing Components

M549A1 Projectiles from Lot 10878E001S066, inert loaded with wax to 43.6 kg, were used for all tests. Projectile weight and rotating band condition (burrs, indentations, etc.) were ascertained prior to loading into the howitzer; projectile seating distance was measured prior to loading the propelling charge.

The XM216 Propelling Charge, a version of which is shown in Figure 3, is currently under development by the Large Caliber Weapon Systems Laboratory to serve as the next-generation zoning solution for the midrange

charge. The total weight of the charge was 7.8 kg of propellant, 85 g of CBI igniter, and approximately 0.84 kg of Type-2, NC container. Standoff for the three rounds in the series was 2.5 cm. Combustion irregularities were almost nonexistent as attested by the small $-\Delta P_i$ of 2 MPa (Table 5). Both spindle and forward chamber pressure traces were smooth with only a slight pressure-wave undulation superimposed on the pressure. Coil velocity for the series was 699 m/s. Ignition delay at 40 ms was slightly larger than for the baseline series with granular propellant.

Since pressure-wave phenomena were almost nonexistent, modifications to the modules as in the earlier tests with granular propellant to change the flow of igniter and early combustion gases into the charge were deemed not necessary. Therefore, ullage rather than igniter variations were examined first to see if pressure-wave phenomena of a serious nature could be induced.

2. Ullage Variations/Stick Propellant. Variations in charge/chamber configuration were limited because the charge was radially almost as large as the chamber (14.7 cm versus 16.5 cm for the chamber), and axially only 13.6 cm shorter than the chamber. Within these limited confines, three additional series were tested.

Series 2 was fabricated exactly like the baseline series. The charge was positioned at maximum (13.6-cm) rather than standard (2.5-cm) standoff (Figure 15). Firing results are shown in Table 5. Both peak pressure and $-\Delta P_i$ increased substantially from the baseline series. Spindle pressure and $-\Delta P_i$ were, respectively, 276 and 12 MPa. Although there was a six-fold increase in $-\Delta P_i$ it was still low in relation to those encountered with granular propellants. The increase in peak pressure was manifested also in a coil velocity of 704 m/s, which was considerably higher than Series 1. Ignition delay at 46 ms was about the same as the baseline series.

For Series 3, the modules were spaced in the chamber so that Module A was at 2.5-cm standoff, Module B was approximately 6 cm forward of Module A, and Module A" was 6 cm forward of Module B, just touching the base of the projectile. There were no spacers between the three modules to prevent movement after initial ignition of the charge (Figure 15). Results (Table 5) were essentially midway between Series 1 and 2 with a peak pressure and $-\Delta P_i$, respectively, of 266 and 8 MPa. Again, slight changes in the charge/chamber configuration made noticeable changes in the combustion characteristics of the charge. Coil velocity and ignition delay were 695 m/s and 43 ms, respectively.

To ascertain whether initial increment placement rather than increment movement could induce large pressure waves, a slight variation on Series 3 was made. Series 4 was similar to Series 3, except that 6-cm long, cardboard spacers were inserted between Modules A and B and between Modules B and A" to impede increment movement after initial ignition of the charge (Figure 15). Results, which are listed in Table 5, indicate that pressure, velocity, and ignition delay were essentially the same as Series 3. The $-\Delta P_i$ was reduced somewhat from 8 MPa in Series 3 to 5 MPa in this series. The lower standard deviation on all variables except ignition delay may be an indication of slightly more stability for the restricted modules over the unrestricted ones.

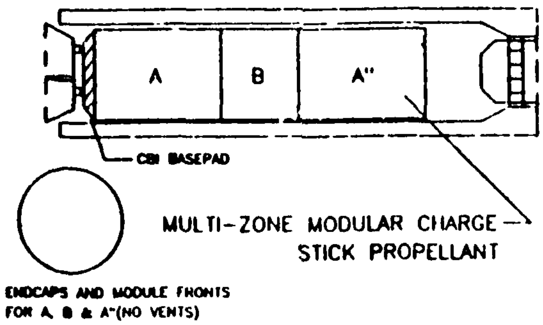

(Series 1)

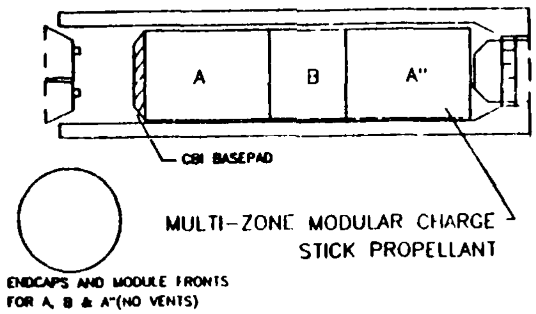

(Series 2)

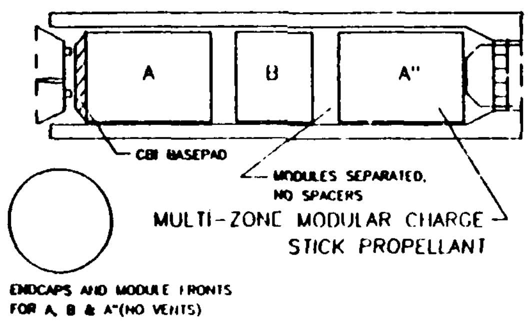

(Series 3)

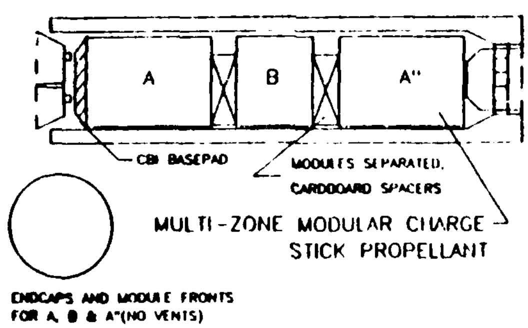

(Series 4)

Figure 15. Charge/Chamber Configuration for Modular Case/Stick Propellant with Ullage Variations

TABLE 5. FIRING RESULTS FOR ULLAGE VARIATIONS/STICK PROPELLANT*

Series No.	Charge Variations	Spindle Pressure (MPa)	$-\Delta P_i$ (MPa)	Velocity (m/s)	No. Rds.	Ign. Del. (ms)
1.	CBI basepad on Module A/ Endcaps on Modules A, B, and A"/ 2.5-cm standoff/ Baseline Series	260 (3.8)	2 (1.0)	699 (2.1)	3	40 (5.5)
2.	Charge configuration same as Series 1/ Charge at maximum standoff (13.6 cm)	276 (7.0)	12 (3.6)	704 (3.1)	3	46 (4.0)
3.	Module loading same as Series 1/ Modules separated by 5 cm/ Module A at 2-cm standoff/ Module A" touching base of projectile	266 (8.5)	8 (3.8)	695 (10.4)	3	43 (1.5)
4.	Charge configuration same as Series 3/ Cardboard spacers used to keep modules separated	268 (1.5)	5 (1.7)	698 (2.9)	3	38 (5.5)

*Standard deviations are given in parentheses for series with 3 or more rounds

3. Ignition Variations/Stick Propellant. Five basepad variations were tested to determine the effect of initial ignition stimulus on charge performance. The intent was to dramatically change the ignition characteristic of the charge so as to induce, if possible, ignition variations leading to pressure-wave formation.

Series 5 (Figure 16) was fabricated exactly like the baseline series except that the basepad was 85 g of Class 1 Black Powder instead of CBI. Charge standoff was 2.5 cm. The results are shown in Table 6. Peak pressure at 268 MPa, $-\Delta P_i$ at 2 MPa and coil velocity at 697 m/s, were essentially the same as the baseline series. As expected, ignition delay was reduced substantially over the baseline series.

To create a more brisant ignition source, 85 g of Class 5 Black Powder was used in Series 6. All other characteristics of the system were the same as in Series 5 (Figure 16). Peak pressure and velocity were about the same as in Series 5 (Table 6). Although $-\Delta P_i$ at 7 MPa was threefold higher than Series 5, it was still much lower than that observed with most of the granular charges. The ignition delay of 16 ms was the lowest observed for any series tested in this project.

With the advent of modular charges that are to be loaded into howitzers by automatic mechanisms, the possibility exists that modules could be

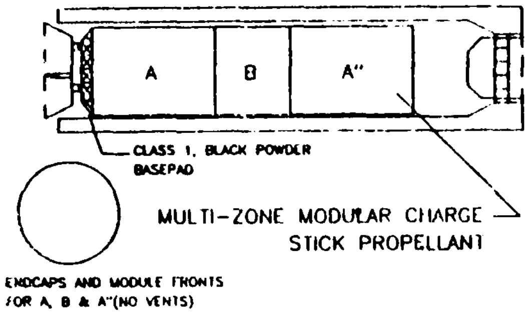

(Series 5)

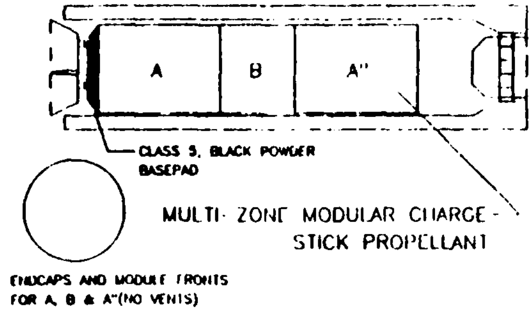

(Series 6)

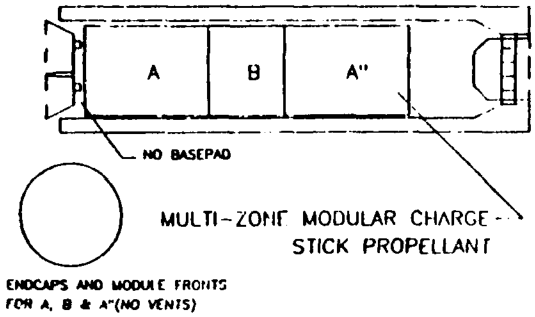

(Series 7)

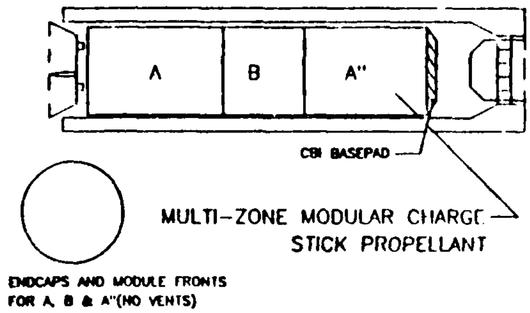

(Series 8)

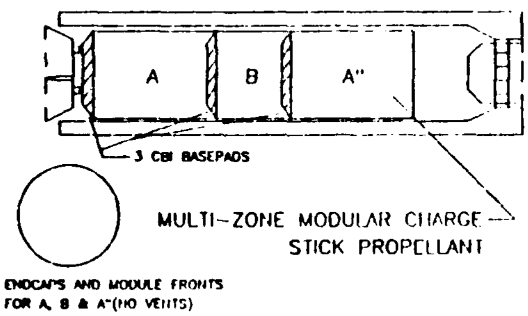

(Series 9)

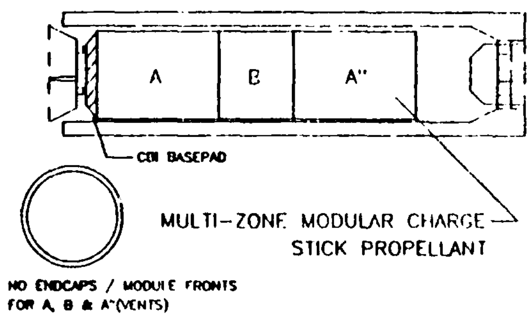

(Series 10)

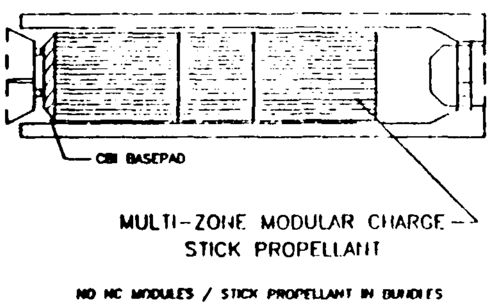

(Series 11)

Figure 16. Charge/Chamber Configuration for Modular Case/Stick Propellant with Ignition Variations

misloaded with the basepad at a mid- or forward-chamber position or possibly not in the system at all. To ascertain the effects on ignition and combustion of charges with no basepad, Series 7 was constructed exactly as Series 5 except that the basepad was eliminated (Figure 16). Results, as shown in Table 6 indicate no change in peak pressure or velocity. The initial reverse pressure gradient at 1 MPa was reduced twofold over Series 5; sevenfold over Series 6 and, thus, was one of the lowest recorded for any series tested in this project. As expected, the ignition delay increased substantially to 200 ms.

TABLE 6. FIRING RESULTS FOR IGNITION VARIATIONS/STICK PROPELLANT*

Series No.	Charge Variations	Spindle Pressure (MPa)	$-\Delta P_i$ (MPa)	Velocity (m/s)	No. Rds.	Ign. Del. (ms)
5.	Class 1 Black Powder basepad on Modules A/ Endcaps on Modules A, B, and A"/ 2.5-cm standoff	268 (5.5)	2 (0.6)	697 (1.5)	3	29 (3.1)
6.	Charge configuration same as Series 5/Class 5 Black Powder basepad	266 (7.2)	7 (5.1)	698 (2.9)	3	16 (1.5)
7.	Charge configuration same as Series 5/ No basepad	266 (3.2)	1 (2.3)	698 (3.8)	3	200 (57.1)
8.	Charge configuration same as Series 1 except CBI basepad on front of Module A"	275	0	706	1	342
9.	Three CBI basepads - one each at base of Modules A, B, and A"/ Modules and endcaps unmodified	259 (6.8)	4 (3.2)	704 (3.6)	3	38 (7.2)
10.	CBI basepad on Module A/ No endcap on Module A, B, and A"/ Fronts of Modules A, B, and A" opened up with 11-cm hole	264**	2**	698**	2	32**
11.	No NC module/ Stick Propellant tied in bundles/ CBI basepad	232**	0**	670**	2	66**

*Standard deviations are given in parentheses for series with 3 or more rounds

**Average of two rounds

The single firing for Series 8 depicts the effect of having the CBI basepad at the front of the charge. Pressure and velocity at 275 MPa and 706 m/s, respectively, were similar to Series 2 where the charge was at maximum standoff. Unlike Series 2, $-\Delta P_i$ did not increase but was 0 MPa. Ignition delay at 342 ms was the longest for any series fired even surpassing that of Series 7 where no basepad was used. Series 9 shows the opposite extreme from Series 7 wherein 3 basepads, one each at the base of Modules A, B, and A", were loaded into the howitzer (Figure 16). The results (Table 6) of this test, simulating another case of misloading the howitzer, again suggest a very safe and forgiving charge. Pressure, ignition delay and $-\Delta P_i$ at 259 MPa, 38 ms and 4 MPa, respectively, were similar to Series 1, the baseline configuration. Velocity at 704 m/s was 5 m/s higher than the baseline series thus being more comparable to Series 2 (charge at maximum standoff) and Series 8 (CBI basepad in front of Module A").

As suggested by the very low $-\Delta P_i$ for all of the series tested, near simultaneous ignition of the stick propellant charges appears to be occurring even though the propellant is packaged in unvented NC modules. In Series 10, rapid axial flow of igniter gases over the propellant sticks was enhanced by eliminating both the endcaps and opening up the fronts of Modules A, B, and A" with an 11-cm hole (Figure 16). These results (Table 6), when compared to those from Series 1, suggest that the effects of axial confinement preventing rapid flow of igniter gases into a stick propellant charge that is not tightly constrained within the NC tube are minimal. When the NC container was completely eliminated (Series 11, Figure 16) the reduced energy of the system in conjunction with a slightly larger free volume reduced, substantially, the peak pressure and thus the velocity (Table 6), a result corroborated by lumped-parameter interior ballistic calculations. Ignition delay increased 30 percent over the baseline series to 66 ms. Not only were pressure-wave phenomena nonexistent, the pressure-time profile was the smoothest for any series fired. Apparently, even to generate the small pressure waves noted in most of the series, the stick propellant has to either be confined in the NC module or tightly constrained in bundles thus reducing the radial flow of igniter gases through the charge. Neither condition was present for the two rounds in Series 11.

D. 155-mm Howitzer Simulator Tests

The apparatus used to conduct a variety of studies at the BRL of the detailed phenomenology of propelling charges is shown in Figure 17. The massive mount, constructed of armor plate, accepts either plastic chambers or axially reinforced, filament-wound fiberglass chambers. The plastic chambers used were commercially available cast acrylic tubing with inner and outer diameters of 165 mm and 191 mm, respectively. Although the clear plastic fractures at significantly lower pressures than the fiberglass chambers, they offer a much better view of the events transpiring within, and thus were used for this study. The muzzle end of the chamber was closed by a projectile seated in a section of gun tube machined to the dimensions of the M199 Cannon. The breech end of the chamber was closed by a spindle similar to the mushroom configuration of the M185 Cannon with the centrally venting primer spithole. The spindle accepted three piezoelectric pressure transducers. An instrumented projectile permitted gas pressure, total force, and acceleration measurements to be made at the projectile base.

Figure 17. 155-mm Howitzer Simulator, Plastic Chamber

Photographic data were recorded with a high-speed 16-mm camera. Data were recorded at a framing rate of approximately 5000 pictures per second. A one-kHz timing signal was placed on the film by electronics internal to the camera, and the firing fiducial (time at which the firing voltage was applied to the gun) was also placed on the films to aid in correlation of the film data with other data.

Flash X-rays were used on these tests to monitor the movement of the solid phase. For one shot, a total of four, 300-kV X-ray heads was used, two at one axial location, separated by approximately twenty degrees (see Figure 18), and another two at a further axial location, similarly separated, to cover the length of the tube. The overlapping images from the two sets of heads were recorded on a single sheet of film, yet it was possible to determine the X-ray source of each image. One image was created by X-rays triggered at a predetermined spindle pressure, and the second image was made by the X-ray heads triggered at a predetermined time delay after the first. For the stick-propellant test, only one image was recorded using two X-ray heads to improve the clarity of the radiograph. The radiographs were recorded on Kodak XR-5 film using Dupont Lightning Plus intensifier screens. The film was protected from the blast of the disposable chamber by a wooden cassette, with the forward face composed of layers of air spaces and sacrificial wooden plates.

The two charges selected for testing in the fixture were the baseline configurations for both the modular/granular (Series 1, Table 3) and modular/stick (Series 1, Table 5) propellants. These charges represented a tenfold variation in $-\Delta P_i$ and a threefold variation in ignition delay. An overview of the data is presented below.

Data were obtained for the granular-propellant charge up to a spindle pressure of 17 MPa. The high-speed film showed the functioning of the M82 Primer at about 1.5 ms after application of the firing voltage. At 2 ms, the rear ullage was full of flame. By 5 ms, a luminous front traversed the length of the chamber in the top annular ullage, and was then reflected

toward the spindle. After arrival of this reflection in the spindle region, all luminosity disappeared, and several oscillations of smoke in the annular ullage were seen. The chamber remained dark until after 50 ms, but by 55 ms there was a very bright luminosity at the spindle end of the charge. At 58 ms, a plume of flame escaped from the front of the charge in the area of the hole in the forward end of Module A". The luminosity increased such that it was very intense at both ends of the chamber at 60 ms, and the flame started moving into the annular ullage from the rear of the charge at about 61 ms. The flame then continued to fill the chamber until the plastic tube ruptured, without any obvious indication of combustible case fracture or substantial movement of the charge. The flash X-ray recorded at about 4 MPa showed that the charge had moved forward approximately 50 mm. The rear of the charge was lifted off the bottom of the chamber so that it touched the top of the chamber. The "A" module was raised slightly off the bottom of the chamber. The granular propellant was seen to fill nearly the entire volume of the modules, and the walls of the cases appeared to be intact, including the endcap of Module A which was next to the basepad igniter. There were no obvious traces remaining of the igniter itself. A flash X-ray recorded at a pressure of approxiamtely 8 MPa showed the same features as the one shot at 4 MPa, except that the charge had moved forward an additional 5 mm.

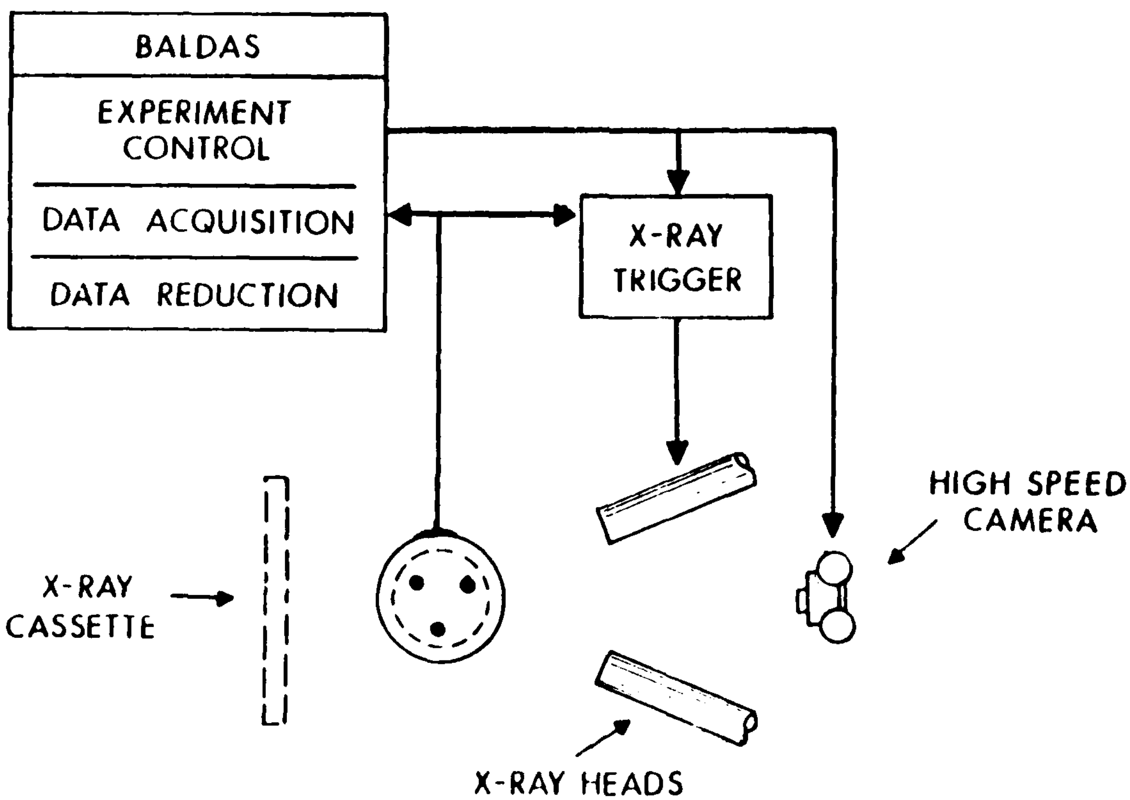

Figure 18. System for Experiment Control, Data Acquisition, and Data Reduction, 155-mm Howitzer Simulator

Data were obtained for the stick-propellant charge up to a spindle pressure of 16 MPa. As with the granular charge, the high-speed movie showed the functioning of the primer, ignition of the basepad, and an oscillation of luminous gases in the annular ullage, at about the same times. However, the intensity of the luminosity of the combustion of the basepad appeared to be much less intense than with the previous shot. Again after the luminous oscillation, the chamber became dark with only smoke visible. At 38 ms, luminosity appeared at the spindle and front of the chamber, without traversing the annular ullage in view of the camera. By 40 ms, the flame at the front of the chamber was very bright, and started moving through the annular ullage toward the rear of the chamber. At 42 ms, the rear of the charge was lifted from the bottom of the chamber, and the top casewall of Module A perhaps was ruptured. By 44 ms, luminous gases were swirling into the annular ullage from the rear of the charge, and it appeared that the case of Module B perhaps was collapsed. Just prior to failure of the plastic chamber, it appeared that the casewall of Module A was blown out to the wall of the chamber through the top annular ullage. Also prior to the failure of the chamber, the intense luminosity inside the modules illuminated them from within, and though propellant grains could not be seen, the reinforced areas of the modules at their overlap points were readily discernible. Due to a test failure, a radiograph was not recorded for the shot just described, but a second test firing of an identical charge in the simulator provided a flash X-ray recorded at about 7 MPa. It showed that the rear of the charge was elevated well off the bottom of the chamber and the forward end was slightly lifted. The charge moved axially about 50 mm from the initial loading position. The top of the case of Module A was pushed out into the annular ullage, the case of Module B remained intact, and the top sidewall of Module A" was collapsed down upon the stick-propellant bed. There were some twists of either propellant or case material in the annular ullage in the region of the juncture of Modules B and A". The endwall of Module A, initially next to the basepad, was not in evidence.

IV. CONCLUSIONS

In this study, the influence of charge interzone permeability, distribution of ullage, charge increment movement, igniter brisance and/or placement on the formation of pressure waves for modular charges employing both granular and stick propellant was investigated. These parameters were noted as those likely to cause ignition and early combustion problems, based on our previous work with bagged, multizone configurations.

Within the range of parameters studied and sample sizes of the series, the results indicate a distinct performance difference between modular charges employing granular and stick propellants. The modular charges fabricated with granular propellant, regardless of the charge/chamber configuration, generally gave large pressure-wave levels. Only after extensive modifications to the modular container to enhance both the radial and axial flow of igniter gases into the body of the granular-propellant bed did the level of pressure waves lessen from large to medium or small levels. The stick propellant, regardless of charge/chamber configuration, type of basepad igniter or, indeed, no igniter at all, gave pressure-wave levels that were small without any modifications being made to the modular container.

The overwhelming conclusion reached from this study is that the multizone, modular charge with stick propellant has good ignition and combustion characteristics that are not affected, substantially, by the charge/chamber interface or by ignition variations. Future studies will concentrate on the effects of low temperature and parasitic components in the module on ignition and combustion characteristics of the charge.

ACKNOWLEDGEMENTS

The authors wish to express their gratitude to Mr. Scott Westley of the Large Caliber Weapon Systems Laboratory, USA ARRADCOM, Dover, NJ, for supplying the combustion modules used in some of the tests and to the Sandy Point Firing Facility personnel (Messrs, J. Bowen, J. Hewitt, and J. Stabile) who conducted the test firings and recorded the data.

REFERENCES

1. I. W. May, "The Role of Ignition and Combustion: A Survey of Developmental Efforts," 13th JANNAF Combustion Meeting, CPIA Publication 281, Vol. I, pp. 315-340, September 1976.

2. I. W. May and A. W. Horst, "Charge Design Considerations and Their Effect on Pressure Waves in Guns," ARBRL-TR-02277, Ballistic Research Laboratory, USA ARRADCOM, Aberdeen Proving Ground, MD, December 1980 (AD A095342).

3. T. C. Minor and J. DeLorenzo, "Charge Design Approaches to the Reduction of Low Zone Stickers," 1976 JANNAF Propulsion Meeting, CPIA Publication 280, Vol. III, pp. 403-434, December 1976.

4. R. J. DeKleine, "155-mm XM211 Propelling Charge Zones 3-6 Design Review Minutes," Office of Project Manager, Cannon Artillery Weapons Systems, Dover, NJ, April 1980.

5. T. C. Minor and A. W. Horst, "Experimental Studies of Ignition Phenomena in One-Dimensional Propelling Charges," ARBRL-TR-02315, Ballistic Research Laboratory, USA ARRADCOM, Aberdeen Proving Ground, MD, April 1981 (AD A100298).

6. C. R. Ruth and T. C. Minor, "Multizone Artillery Propelling Charge Studies," ARBRL-TR-02486, Ballistic Research Laboratory, USA ARRADCOM, Aberdeen Proving Ground, MD, May 1983 (AD A128285).

7. T. C. Minor, "Mitigation of Ignition-Induced, Two-Phase Flow Dynamics in Guns Through the Use of Stick Propellant," ARBRL-TR-02508, Ballistic Research Laboratory, USA ARRADCOM, Aberdeen Proving Ground, MD, August 1983 (AD A133685).

8. T. C. Minor and A. W. Horst, "Ignition Phenomena in Developmental, Stick-Propellant, Combustible-Cased, 155-mm, M203E2 Propelling Charges," ARBRL-TR-02568, Ballistic Research Laboratory, USA ARRADCOM, Aberdeen Proving Ground, MD, July 1984.

9. J. J. Rocchio, R. A. Hartman, and N. J. Gerri, "An Electric Primer-Operated Firing Pin Actuator for Large Caliber Guns," ARBRL-TR-02897, Ballistic Research Laboratory, USA ARRADCOM, Aberdeen Proving Ground, MD, January 1979 (AD A069109).

10. S. Einstein, B. Pellington, S. Westley, "Charge Design Technology," Large Caliber Weapon Systems Laboratory, USA ARRADCOM, September 1980.

11. P. G. Baer and J. M. Frankle, "Simulation of the Interior Ballistics of Guns by Digital Computer Program," R1183, Ballistic Research Laboratories, Aberdeen Proving Ground, MD, December 1962 (AD 299980).

APPENDIX A

Propellant Description Sheets

PROPELLANT DESCRIPTION SHEET

REPORT CONTROL SYMBOL EXEMPT PARA 7-2a AR 335-15

... POWDER, TYPE II (ACTUAL LOT)	DA LOT NUMBER RAD82L005-006
TYPE ...-P-60356 dtd 14 Jan 82	PACKED AMOUNT 18,020 lbs.
RADFORD ARMY AMMUNITION PLANT, RADFORD, VA.	CONTRACT NUMBER DAAA09-77-C-4007

NITROCELLULOSE

ACCEPTED BLEND NUMBERS	NITROGEN CONTENT	KI STARCH (65.5°C)	STABILITY (134.5°C)
...Y; 204Y; 221Y	MAX 13.19 %	MIN	MIN
	MIN 13.11 %	MIN	MIN
	AVG 13.15 %	45+ MIN	30 MIN
			EXPLOSION HR

MANUFACTURE OF SOLVENT PROPELLANT

... POUNDS SOLVENT PER POUND NC/DRY WEIGHT INGREDIENTS CONSISTING OF 30 POUNDS ALCOHOL AND 70 POUNDS ... SOLVENT PERCENTAGE REMIX TO WHOLE 10

PROCESS—SOLVENT RECOVERY AND DRYING

	DAYS	HOURS
... AIR DRY		
... TEMPERATURE 5°F PER HOUR		
... TEMPERATURE		24

TESTS OF FINISHED PROPELLANT

	PERCENT FORMULA	PERCENT TOLERANCE	PERCENT MEASURED	STABILITY AND PHYSICAL TESTS	FORMULA	ACTUAL
	98.0	MINIMUM	98.43	HEAT TEST SP, 134.5°C	NO CC 30'	CC 60'+
	1.50	...	1.57	NO EXPLOSION	NE 5 HRS.MIN	NE 5 hrs
			100.00	FORM OF PROPELLANT		FLAKE
	0.3	MAX.	0.20	NO. OF PERFORATIONS		1
	1.3	±0.5	0.98			
	0.4	MAX.	0.12	BULK DENSITY, lbs/cu.ft	27.0 ±3.0	25.0
... FREE BASIS.						

...CLOSED BOMB

...	TEMP °F	RELATIVE QUICKNESS	RELATIVE FORCE
		100.00%	100.00%

... CLOSED BOMB TEST

PROPELLANT DIMENSIONS (inches)

	SPECIFICATION	DIE	FINISHED	STD DEV in % of Mean Dimensions SPEC	ACTUAL
LENGTH (L)	0.004	0.004	0.004		
DIAMETER (D)	0.055	0.080	0.056		
PERF DIA (d)	0.010	0.018	0.011		

DATES	
PACKED	11/24/82
SAMPLED	11/24/82
TEST FINISHED	12-22-82
OFFERED	12-27-82
DESCRIPTION SHEETS FORWARDED	1-6-83

... CERTIFICATION.

SIGNATURE OF CONTRACTOR REPRESENTATIVE	SIGNATURE OF GOVERNMENT QUALITY ASSURANCE REPRESENTATIVE
R. D. S...	... E. Bland

DA FORM 2148 10 AUG 77

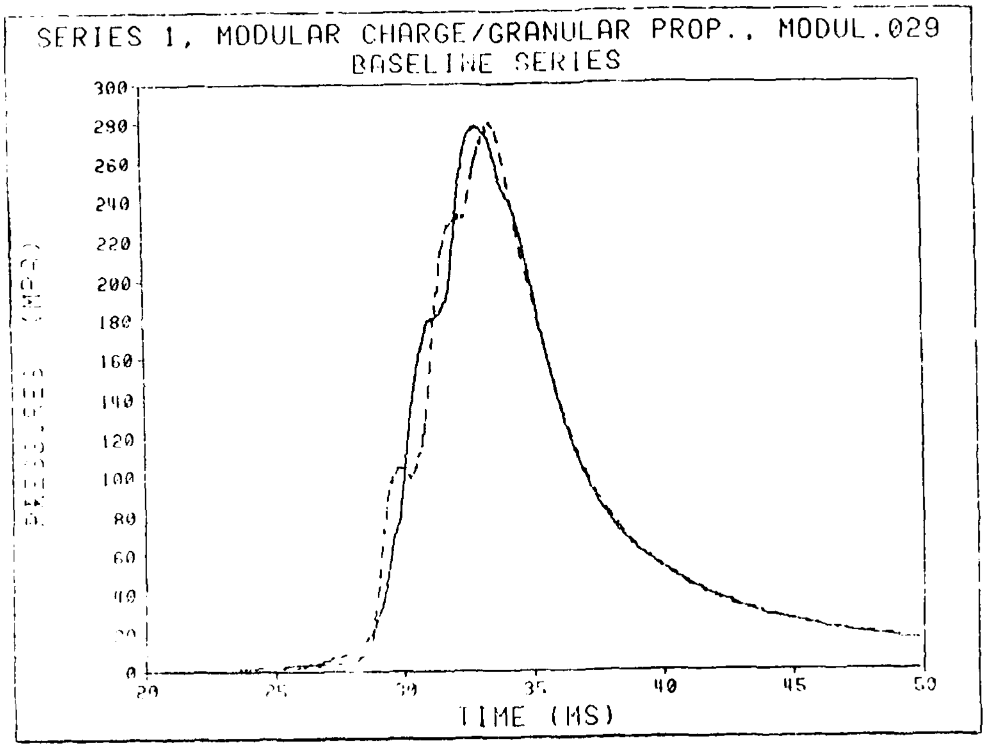
SERIES 1, MODULAR CHARGE/GRANULAR PROP., MODUL.029
BASELINE SERIES
300
280
260
240
220
200
180
160
140
120
100
80
60
40
0
40
45
50
TIME (MS)

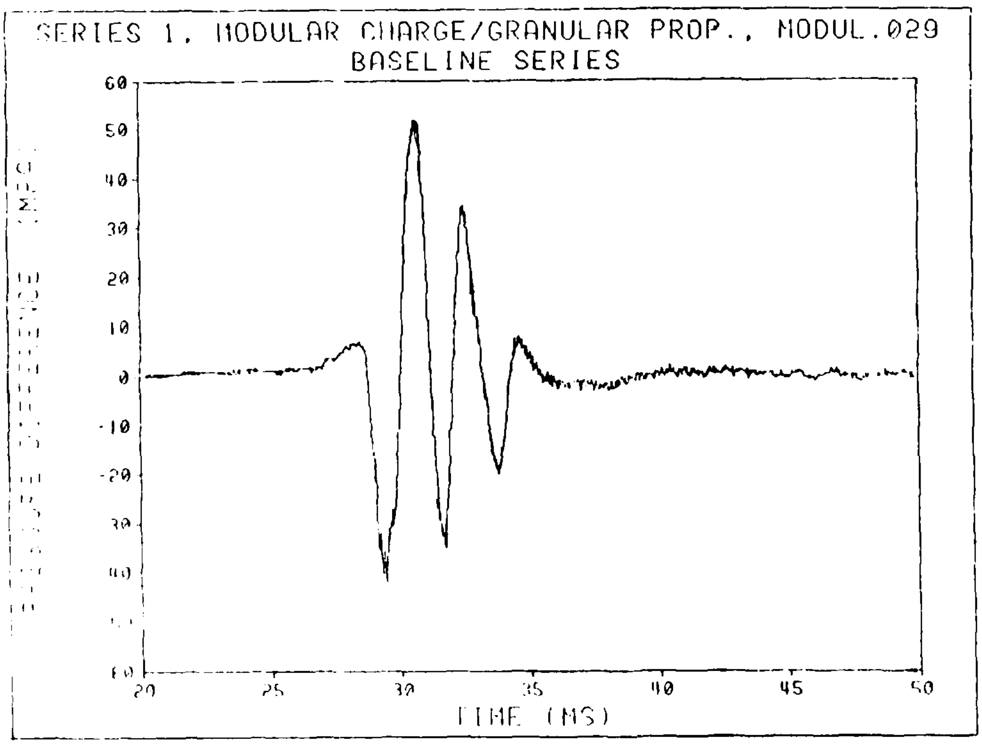
SERIES 1, MODULAR CHARGE/GRANULAR PROP., MODUL.029
BASELINE SERIES
60
50
40
30
20
10
0
-10
-20
30
40
45
50
TIME (MS)

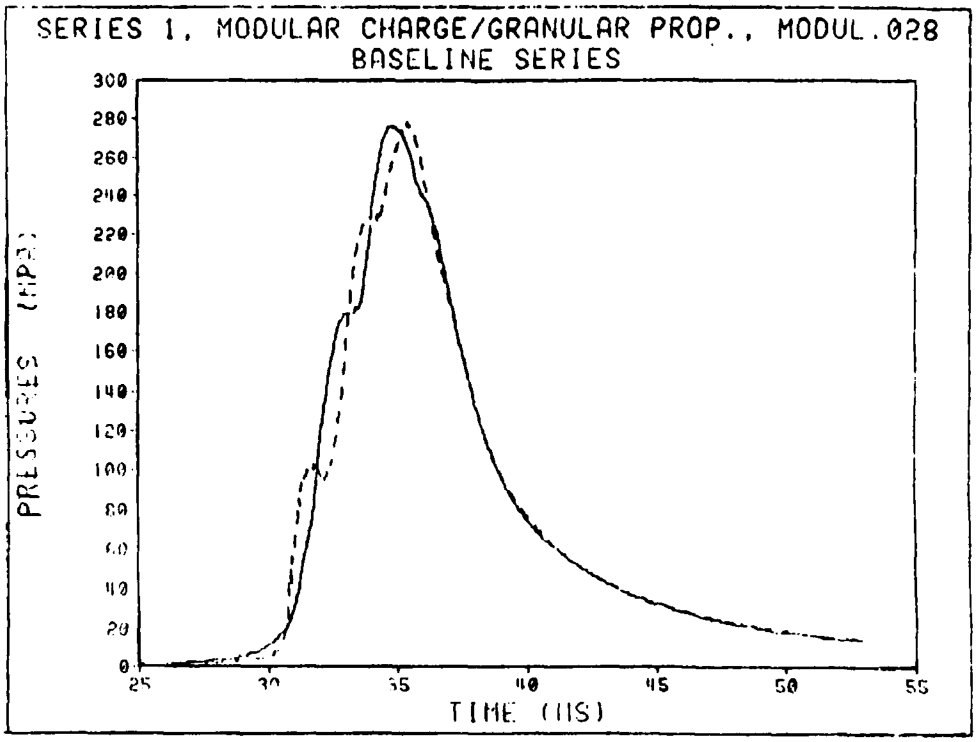
SERIES 1, MODULAR CHARGE/GRANULAR PROP., MODUL.028
BASELINE SERIES
PRESSURES (MPA)
TIME (MS)
0
20
40
60
80
100
120
140
160
180
200
220
240
260
280
300
25
30
35
40
45
50
55

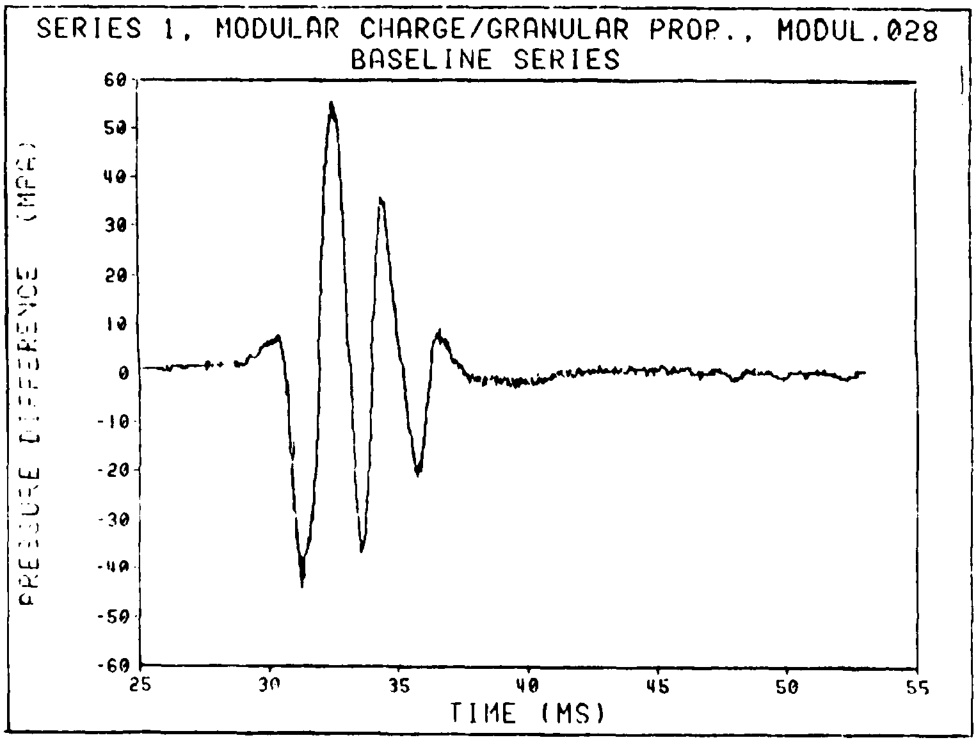
SERIES 1, MODULAR CHARGE/GRANULAR PROP., MODUL.028
BASELINE SERIES
PRESSURE DIFFERENCE (MPA)
TIME (MS)
60
50
40
30
20
10
0
-10
-20
-30
-40
-50
-60
25
30
35
40
45
50
55

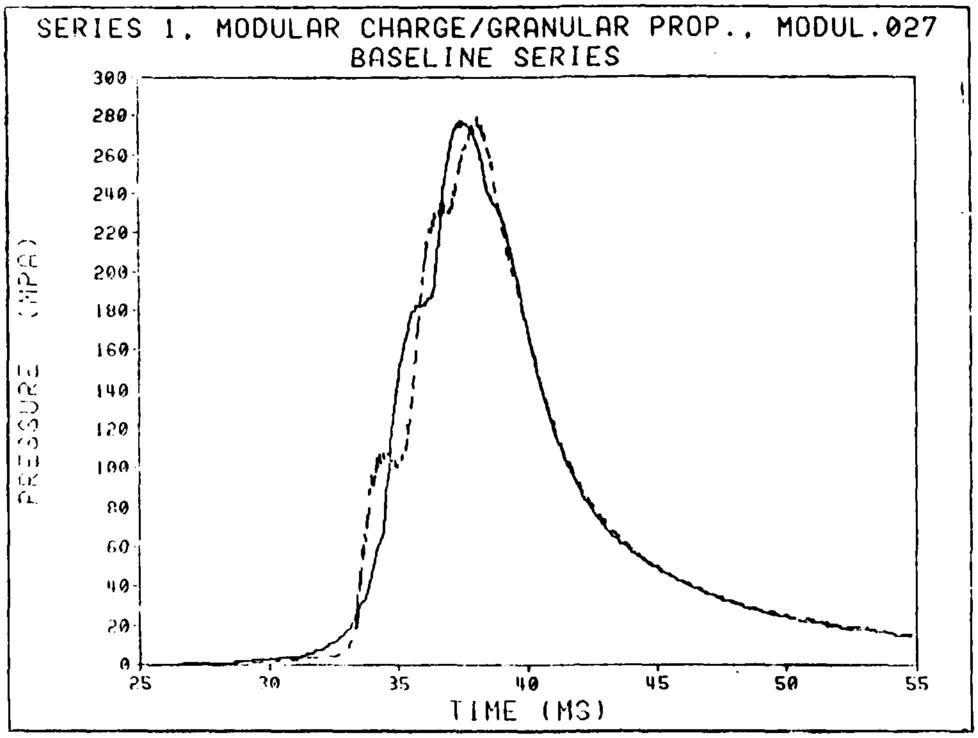
SERIES 1, MODULAR CHARGE/GRANULAR PROP., MODUL.027
BASELINE SERIES
PRESSURE (MPA)
TIME (MS)
0
20
40
60
80
100
120
140
160
180
200
220
240
260
280
300
25
30
35
40
45
50
55

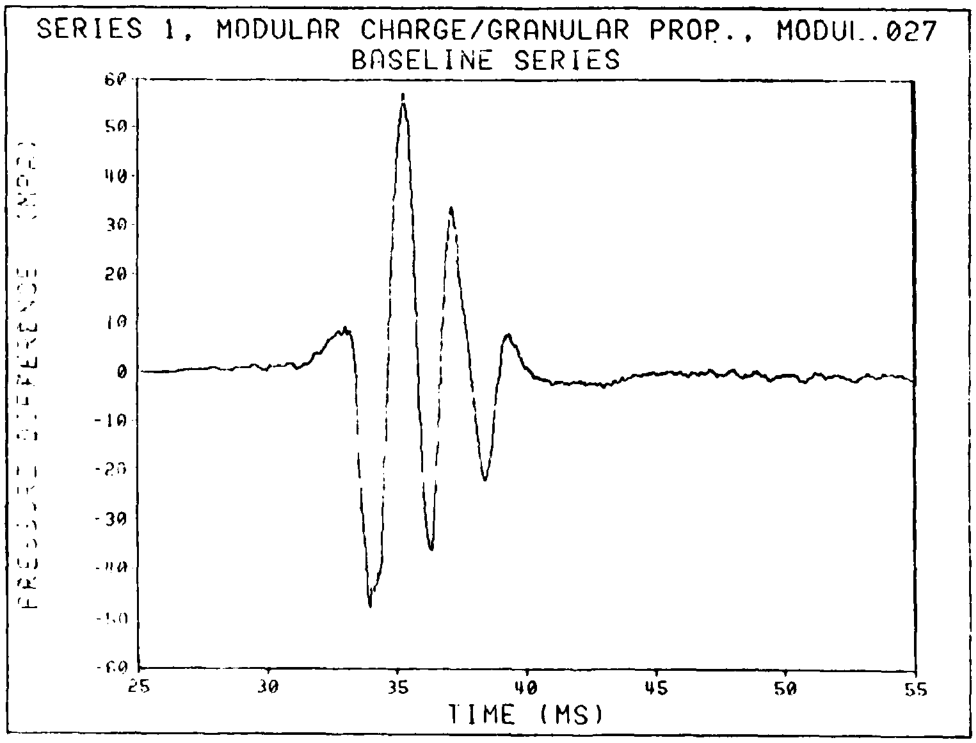
SERIES 1, MODULAR CHARGE/GRANULAR PROP., MODUL.027
BASELINE SERIES
PRESSURE DIFFERENCE (MPA)
TIME (MS)
60
50
40
30
20
10
0
-10
-20
-30
-40
-50
-60
25
30
35
40
45
50
55

APPENDIX C

Plots of Spindle Pressure (Solid Line), Forward Chamber Pressure (Dashed Line), and Pressure Difference Versus Time

TABULATION OF FIRING DATA/STICK PROPELLANT (cont)

Series	Code	Charge Configuration*	Charge Standoff (cm)	NC Module Weight (kg)	Pressures P_1 (MPa)	Pressures P_5 (MPa)	Delta Pressure $-\Delta P_i$ (P_1-P_5) (MPa)	Velocity (m/s)	Ignition Delay (ms)
	MODUL								
10	084	CBI basepad on Module A/ No endcaps	2.5	0.65	263	246	3	698	33
	085	on Modules A, B, and A"/ Front		0.68***	266***	247***	2***	699***	30***
		holes of Modules A, B, and A"	Avg.	0.66	264	246	2	698	32
		opened up to 11 cm	(Std Dev)	—					
	MODUL								
11	086	No NC modules/ Stick propellant	2.5	0.0	234	218	0	672	76
	087	with CBI basepad		0.0	229***	212***	0***	668***	57***
			Avg.	0.0***	232	215	0	670	66
			(Std Dev)	--	---	---	--	---	--

* Propellant and projectile weights were 7.8 and 43.6 kg, respectively. Projectile seating distance was 911 mm unless noted otherwise. Basepads contained 85 g CBI unless noted otherwise.

*** Average of 2 rounds

TABULATION OF FIRING DATA/STICK PROPELLANT (cont)

Series	Code	Charge Configuration*	Charge Standoff (cm)	NC Module Weight (kg)	Pressures P_1 (MPa)	Pressures P_5 (MPa)	Delta Pressure $-\Delta P_i$ (P_1-P_5) (MPa)	Velocity (m/s)	Ignition Delay (ms)
	MODUL								
5	065	Charge configuration same as	2.5	0.83	274	242	3	699	26
	066	Series 1 except that basepad was		0.84	264	238	2	696	32
	067	85 g Class 1 Black Powder		0.82	265	238	2	697	28
			Avg.**	0.83	268	239	2	697	29
			(Std Dev)	(0.01)	(5.5)	(2.3)	(0.6)	(1.5)	(3.1)
	MODUL								
6	068	Charge configuration same as	2.5	0.87	258	234	3	695	18
	069	Series 1 except that basepad was		0.85	272	248	13	700	16
	070	85 g Class 5 Black Powder		0.83	268	239	6	700	15
			Avg.**	0.85	266	240	7	698	16
			(Std Dev)	(0.02)	(7.2)	(7.1)	(5.1)	(2.9)	(1.5)
	MODUL								
7	074	Charge configuration same as	2.5	0.85	265	238	4	696	179
	075	Series 1 except no basepad was		0.81	270	246	0	702	265
	076	used		0.87	264	237	0	695	157
			Avg.**	0.84	266	240	1	698	200
			(Std Dev)	(0.03)	(3.2)	(4.9)	(2.3)	(3.8)	(57.1)
	MODUL								
8	083	CBI basepad on front end of Module A"/ Charge configuration same as Series 1	2.5	0.85	273	253	0	706	342
	MODUL								
9	080	Three CBI basepads - one each at	2.5	0.81	257	243	5	703	34
	081	base of Modules A, B, and A"/		0.83	254	244	6	701	33
	082	Modules an endcaps unmodified		0.81	267	252	0	708	46
			Avg.**	0.82	259	246	4	704	38
			(Std Dev)	(0.01)	(6.8)	(4.9)	(3.2)	(3.6)	(7.2)

* Propellant and projectile weights were 7.8 an 43.6 kg, respectively. Projectile seating distance was 911 mm unless noted otherwise. Basepads contained 85 g CBI unless noted otherwise.

** Standard deviations are given in parentheses for series with 3 or more rounds.

TABULATION OF FIRING DATA/STICK PROPELLANT

Series	Code	Charge Configuration*	Charge Standoff (cm)	NC Module Weight (kg)	Pressures P_1 (MPa)	Pressures P_5 (MPa)	Delta Pressure $-\Delta P_i$ (P_1-P_5) (MPa)	Velocity (m/s)	Ignition Delay (ms)
	MODUL								
1	077	Basepad on Module A/ Endcaps on	2.5	0.86	263	244	1	701	43
	078	Modules A, B, and A"/ No modifi-		0.85	256	239	2	697	44
	079	cations to modules or endcaps		0.86	262	243	3	700	34
			Avg**	0.86	260	242	2	699	40
			(Std Dev)	(0.01)	(3.8)	(2.6)	(1.0)	(2.1)	(5.5)
	MODUL								
2	059	Charge configuration same as	13.6	0.83	284	260	16	707	42
	060	Series1/ Charge at maximum		0.83	273	251	11	703	50
	061	standoff		0.83	271	244	9	701	46
			Avg.**	0.83	276	252	12	704	46
			(Std Dev)	(0.00)	(7.0)	(8.0)	(3.6)	(3.1)	(4.0)
	MODUL								
3	062	Charge configuration same as	2.5	0.83	256	234	12	683	43
	063	Series 1/ Modules equally spaced		0.85	272	244	6	701	44
	064	in chamber - no spacers		0.83	269	242	5	701	41
			Avg.**	0.84	266	240	8	695	43
			(Std Dev)	(0.01)	(8.5)	(5.3)	(3.8)	(10.4)	(1.5)
	MODUL								
4	071	Charge configuration same as	2.5	0.87	270	243	6	700	38
	072	Series 1/ Modules equally spaced		0.80	268	243	6	695	33
	073	in chamber - spacers		0.88	267	242	3	700	44
			Avg.**	0.85	268	243	5	698	38
			(Std Dev)	(0.01)	(1.5)	(0.6)	(1.7)	(2.9)	(5.5)

* Propellant and projectile weights were 7.8 and 43.6 kg, respectively. Projectile seating distance was 911 mm unless noted otherwise. Basepads contained 85 g CBI unless noted otherwise.

** Standard deviations are given in parentheses for series with 3 or more rounds.

TABULATION OF FIRING DATA/GRANULAR PROPELLANT (cont)

Series	Code	Charge Configuration*	Charge Standoff (cm)	NC Module Weight (kg)	Pressures P_1 (MPa)	Pressures P_5 (MPa)	Delta Pressure $-\Delta P_i$ (P_1-P_5) (MPa)	Velocity (m/s)	Ignition Delay (ms)
	MODUL								
8	041	One basepad on Module A/ Endcap	2.5	0.75	276	276	12	693	45
	042	holes on Modules A, B, and A"		0.74	287	293	44	698	35
	043	opened from 22 to 51 mm/ Front		0.74	281	293	13	694	72
		holes of Modules A and B opened	Avg.**	0.74	281	283	23	695	51
		from 21 to 51 mm/ Vent holes	(Std Dev)	(0.01)	(5.5)	(8.7)	(18.2)	(2.6)	(19.1)
		(5.6-mm diam) put in Module A and							
		A" (50 holes) and in Module B							
		(40 holes)/ NC spaces connected							
		to Module A and B and to B and A"							
	MODUL								
9	044	Similar to Series 8 except that	2.5	0.76	282	285	36	698	34
	045	vent holes were 3.8-mm in		0.74	284	288	33	697	40
	046	diam		0.74	--	280	--	694	45
			Avg.**	0.75	283***	284	34***	696	40
			(Std Dev)	(0.01)	--	(4.0)	--	(2.1)	(5.5)
	MODUL								
10	D52	Same as Series 1 except that	2.5	0.82	277	275	23	696	46
	D53	modules separated in chamber		0.79	275	278	30	696	48
		with no spacers keeping them from	Avg.	0.80***	276***	276***	26***	696***	47***
		moving	(Std Dev)	--	--	--	--	--	--
	MODUL								
11	D54	Same as Series 1 except that modules were at maximum standoff	10.0	0.84	322	290	23	696	46

* Propellant and projectile weights were 7.8 and 4.6 respectively. Projectile seating distance was 911 mm unless noted otherwise. Basepads contained 85 g CBI used unless otherwise noted.

** Standard deviations are given in parentheses for series with 3 or more rounds.

*** Average of 2 rounds.

TABULATION OF FIRING DATA/GRANULAR PROPELLANT (cont)

Series	Code	Charge Configuration*	Charge Standoff (cm)	NC Module Weight (kg)	Pressures P_1 (MPa)	Pressures P_5 (MPa)	Delta pressure $-\Delta P_i$ $(P_1 - P_5)$ (MPa)	Velocity (m/s)	Ignition Delay (ms)
5	MODUL 038	One basepad on Module A/ Endcap holes on Modules A, B, and A" opened from 22 to 51 mm/ Fronts of Modules A and B opened from 22 to 51 mm/ Vent holes (5.6 mm diam) put in Modules A and A" (50 holes) and in Module B (40 holes)	2.5	0.64	275	276	4	692	36
	039			0.67	280	280	10	695	32
	040			0.68	277	279	10	692	34
			Avg.**	0.66	277	278	8	693	34
			(Std Dev)	(.02)	(2.5)	(2.1)	(3.5)	(1.7)	(2.0)
6	MODUL 047	One basepad on Module A/ Endcaps and fronts of Modules A and B both had 150 holes (5.6-mm diam) and standard 22-mm hole/ Vent holes (5.6-mm diam) put in Modules A and A" (50 holes) and in Module B (40 holes)	2.5	0.78	281	279	10	694	45
7	MODUL 048	Similar to Series 6 except the holes in sides, fronts, and end-caps were 2.8-mm diam	2.5	0.80	279	278	16	694	40

* Propellant and projectile weights were 7.8 and 43.6 kg, respectively. Projectile seating distance was 911 mm unless noted otherwise.

** Standard deviations are given in parentheses for series with 3 or more rounds.

TABULATION OF FIRING DATA/GRANULAR PROPELLANT

Series	Code	Charge Configuration*	Charge Standoff (cm)	NC Module Weight (kg)	Pressures P_1 (MPa)	Pressures P_5 (MPa)	Delta Pressure $-\Delta P_i$ (P_1-P_5) (MPa)	Velocity (m/s)	Ignition Delay (ms)
	MODUL								
1	027	One basepad on Module A/ Endcap	2.5	0.83	276	276	48	686	31
	028	hole of Module A opened from 22 to		0.84	276	278	42	687	29
	029	51-mm/ Modules A, B, and A" and		0.84	278	280	40	686	27
	030	Endcaps B, and A" unmodified		0.84	287	281	52	685	27
		(Baseline Series)	Avg**	0.84	279	279	46	686	28
			(Std Dev)	(0.01)	(5.3)	(2.2)	(5.5)	(0.8)	(1.9)
	MODUL								
2	031	Three basepads - one each at base of Modules A, B, and A"/ Endcap holes of A, B, and A" opened from 22 to 51 mm	2.5	0.72	402	340	115	717	25
	MODUL								
3	032	One basepad and one endcap on	2.5	0.63	281	276	11	689	34
	033	Module A/ No endcaps on Modules B		0.65	282	280	18	690	30
	034	and A"/ Endcap hole of A and		0.64	283	281	21	692	28
		front of Modules A and B opened	Avg.**	0.64	282	279	17	690	31
		from 22 to 51 mm	(Std Dev)	(0.01)	(1.0)	(2.6)	(5.1)	(1.5)	(3.1)
	MODUL								
4	035	One basepad on Module A/ Endcaps	2.5	0.80	290	283	10	698	32
	036	and fronts of modules had 22-mm		0.79	289	282	9	698	31
	037	hole unmodified/ Cutouts on		0.78	285	288	24	699	32
		endcaps and fronts of Modules A,	Avg.**	0.79	288	284	14	698	32
		B, and A"	(Std Dev)	(0.01)	(2.6)	(3.2)	(8.4)	(0.6)	(0.6)

* Propellant and projectile weights were 7.8 and 43.6 kg, respectively. Projectile seating distance was 911 mm unless noted otherwise. Basepads contained 85 g CBI used unless otherwise noted.

** Standard deviations are given in parentheses for series with 3 or more rounds.

APPENDIX B

Tabulation of Firing Data for Modular Case/Granular Propellant and Modular Case/Stick Propellant for all Series Configurations

PROPELLANT DESCRIPTION SHEET

REPORTS CONTROL SYMBOL: EXEMPT-PARA 7-2a AR 335-15

COMPOSITION: M31A1E1 Slotted Stick (NOMINAL LOT)	DA LOT NUMBER: RAD-PE-480-90
SPECIFICATION: COR 1ttr SARRA-EN dtd 10/6/82 & 11/29/82	PACKED AMOUNT: 10,200 Pounds
MFG AT: RADFORD ARMY AMMUNITION PLANT, RADFORD, VA.	CONTRACT NUMBER: DAAA09-77-C-4007

NITROCELLULOSE

ACCEPTED BLEND NUMBERS			NITROGEN CONTENT	KI STARCH (65.5°C)	STABILITY (134.5°C)
B30955	B30956	B30960	MAX 12.58 %	___ MIN	___ MIN
			MIN 12.50 %	___ MIN	___ MIN
B30963	B30964	B30966	AVG 12.52 %	45+ MIN	30 MIN
					EXPLOSION ___ HR

MANUFACTURE OF SOLVENT PROPELLANT

0.178 POUNDS SOLVENT PER POUND NC/DRY WEIGHT INGREDIENTS CONSISTING OF 60 POUNDS ALCOHOL AND 40 POUNDS Acetone PER 100 POUNDS SOLVENT PERCENTAGE REMIX TO WHOLE ___

PROCESS—SOLVENT RECOVERY AND DRYING

TEMPERATURES ° FROM	TO	PROCESS	TIME DAYS	HOURS
Ambient	Ambient	Ambient Conditioning		48
Ambient	120	Increase at 5° per Hour		
120	120	Hold		2
120	ambient			

TESTS OF FINISHED PROPELLANT

PROPELLANT COMPOSITION

CONSTITUENT	PERCENT FORMULA	PERCENT TOLERANCE	PERCENT MEASURED
Nitrocellulose	22.20	±1.3	21.91
Nitroglycerin	19.00	±1.0	19.48
Nitroguanidine	53.70	±1.0	53.28
Dibutylphthalate	2.70	±0.3	2.98
Ethyl Centralite	1.40	±0.3	1.32
Potassium Sulfate	1.00	±0.3	1.03
Total	100.00	-	
Total Volatiles (TV)	n/a	n/a	0.15
Carbon Black	0.09	±0.01	0.11*

STABILITY AND PHYSICAL TESTS

	FORMULA	ACTUAL
HEAT TEST No CC	40'	60+
No Fumes	60'	60
FORM OF PROPELLANT		
HOE cal/gm	n/a	86.50
Avg Stick wt-gms	n/a	30.00
Std Dev -gms	n/a	0.931
No Trials	n/a	100
Absolute Density g/cc		1.63

CLOSED BOMB

TEST	LOT NUMBER	TEMP °F	RELATIVE QUICKNESS	RELATIVE FORCE
	PE-480- 90	+90	103.16	120.95
STANDARD	70077		100.00%	100.00%

REMARKS

PROPELLANT DIMENSIONS (inches)

	SPECIFICATION	DIE	FINISHED	STD. DEV. in % of Mean Dimensions SPEC	ACTUAL
LENGTH (L)	29	29	28.81	n/a	0.33
DIAMETER (D)	0.234	0.259	0.237	n/a	1.26
PERF. DIA. (d)	0.079	0.086	.079		
Web	0.078	0.087	.080		
Web Difference /Std. Dev. in % of Web Avg.	N/A		N/A		
L:D	123.93	111.97	12[illegible]56		
D:d	2.96	3.01	2.[illegible]		

DATES

- PACKED 1/13/83
- SAMPLED 1/13/83
- TEST FINISHED 2/8/83
- OFFERED
- DESCRIPTION SHEETS FORWARDED 3-7-83

TYPE OF PACKING CONTAINER

REMARKS

* include ash

SIGNATURE OF CONTRACTOR'S REPRESENTATIVE	SIGNATURE OF GOVERNMENT QUALITY ASSURANCE REPRESENTATIVE
[signature]	James E Blan[signature]

ARRCOM FORM 214R 10 AUG 77

PROPELLANT DESCRIPTION SHEET

Lot No. 69275 (ACTUAL LOT) 74 Composition No. M1, MP, 155MM HOW., FOR PROPELLING CHARGE, M4A2

ITEM VI-30623

RADFORD ARMY AMMUNITION PLANT, RADFORD, VA. Packed Amount 461,487 LBS.

DAAA09-71-C-0329 Date 6-20-71 Specification No. MIL-P-60397 (MU) W/FCPA'S 49206-2, 51049-2, 52153-2, 53472-2, FAN 7000588-2 AND T&X SMCAP-AMM-62142088

NITROCELLULOSE

Blend numbers: 231Y; 237Y; 252Y; 253Y; 256Y; 260Y; 262Y; 263Y; 268Y; 282Y; 288Y; 295Y;

	Nitrogen Content	KI Starch (65.5°C)	Stability (134.5°C)
Maximum	13.20 %	45+ Mins	30 +
Minimum	13.11 %	Mins	30
Average	13.16 %	Mins	30 + Mins
			Explosion Mins

SULFITE CELLULOSE

MANUFACTURE OF PROPELLANT

per Pound XX / Dry Weight Ingredients Consisting of 35 Pounds Alcohol and 65 Pounds ETHER per 100 Pounds Solvent

PROCESS-SOLVENT RECOVERY AND DRYING

	Time Days	Time Hours
HEAT SOLVENT RECOVERY TANK		
INCREASE SOLVENT RECOVERY TEMPERATURE		12
HOLD SOLVENT RECOVERY TEMPERATURE		24
WATER DRY CYCLE	4	
AIR DRY CYCLE		16

TESTS OF FINISHED PROPELLANT

Percent Formula	Percent Tolerance	Percent Measured
85.00	±2.00	84.97
10.00	±2.00	9.73
5.00	±1.00	5.30
100.00		100.00
1.00	[illegible]	1.08
1.00	±0.30	1.10
		0.79
0.60	±0.20	0.45
1.32	MAX.	0.34

...AMINE-, AND POTASSIUM SULFATE-FREE BASIS.

STABILITY AND PHYSICAL TESTS

	Formula	Actual
Heat Test S.P., 134.5°C	NO CC 40'	60'
NO EXPLOSION	5 HRS. MIN	5 hrs.
Form of Propellant		GRAIN TYPE I
NO. OF PERFORATIONS		7
COMPRESSIBILITY	30% MIN	43

CLOSED BOMB

Temp °F	Relative Quickness	Relative Force
+90	99.62 %	99.85 %
+90	100.00%	100.00%

...WITH MIL-STD-286B, METHOD 801.1, CLOSED BOMB. TEST FOR ... ONLY.

PROPELLANT DIMENSIONS (inches)

	Specification	Die	Finished	Mean Variation in % of Mean Dimensions: Spec	Actual
Length (L)		0.447	0.4322	6.25 MAX.	1.73
Diameter (D)		0.279	0.1943	6.25 MAX.	2.66
Perf Dia (d)		0.023	0.0152		
WEB					
INNER		0.0535	0.0361		
OUTER		0.0515	0.0387		
AVERAGE		0.0525	0.0374		
Difference/ in % Average	15 MAX.		7.1		
L/D	2.10 to 2.50		2.22		
D/d	5.0 to 15		12.8		

DATES

Packed	4/22/74
Sampled	4/22/74
Test Finished	4-29-74
Offered	4-30-74
Description Sheets Forwarded	5-2-74

FIBER DRUMS PER MIL-STD-652B

... CHEMICAL AND PHYSICAL REQUIREMENTS OF THE APPLICABLE SPECIFICATION.

H. L. Dickinson

Government Quality Assurance Representative

JAMES E. ELAND

Rev. 3 9/71

CERTIFICATE OF COMPLIANCE AND ANALYSIS

BLACK POWDER, POTASSIUM NITRATE (Nominal Lot)
SODIUM NITRATE

DATE PACKED 8/1981

LOT NUMBER NOMINAL

SPECIFICATION Mil P223

GRADE/CLASS C-5

CHEMICAL AND PHYSICAL REQUIREMENTS

	SPECIFICATION LIMITS MAXIMUM	MINIMUM	ANALYTICAL RESULTS SAMPLE 1	SAMPLE 2
MOISTURE	0.70 %	%	0.527 %	0.511 %
ANALYSIS - DRY BASIS:				
Potassium Nitrate	75.0 %	73.0 %	73.6 %	74.2 %
Sodium Nitrate				
Sulfur	11.4	9.4	10.5	10.5
Charcoal	16.6	14.6	15.9	15.3
Calcium Carbonate				
Semi-Bituminous Coal				
Total	xx	xx	100.0 %	100.0 %
ASH	0.80 %	%	0.5 %	0.4 %
SPECIFIC GRAVITY	1.80	1.72	1.777	1.781
APPARENT DENSITY	↔	↔	1.02	1.01
GRITTY OR FIBROUS PARTICLES	None	None	None	None
GLAZE				
GRANULATION:				
On U.S. Std. 16	3.0 %	%	1.9 %	2.1 %
On U.S. Std.				
Thru U.S. Std.				
Thru U.S. Std. 40	5.0		3.0	2.7

Date Tested 8/6/81

Book No.

Order No.

Customer

Tested by: James Mills

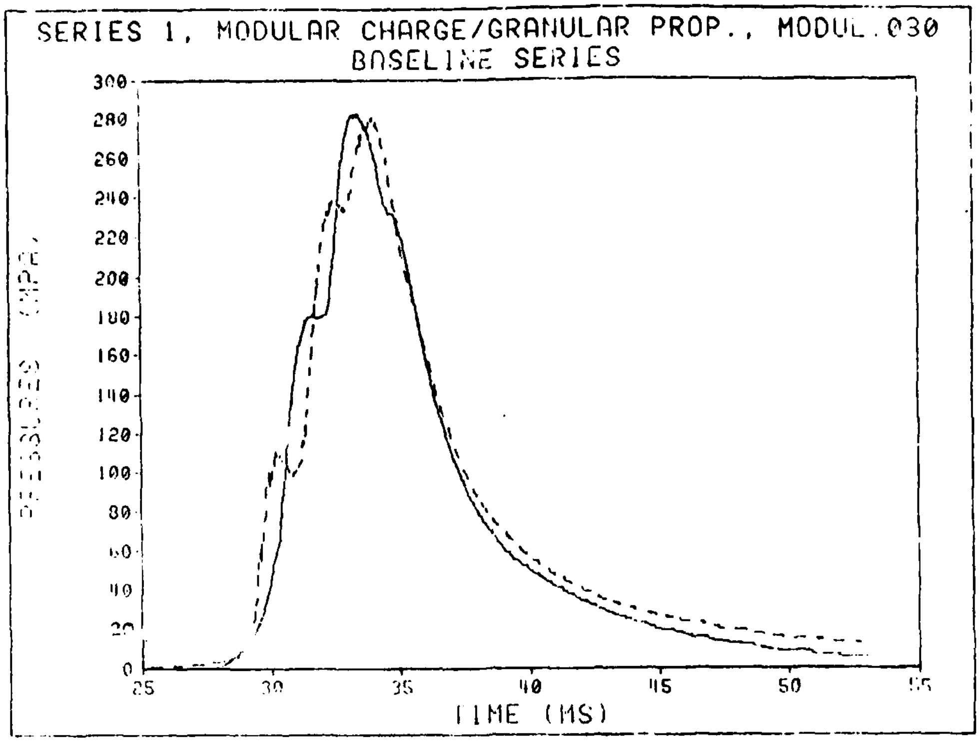
SERIES 1, MODULAR CHARGE/GRANULAR PROP., MODUL.030
BASELINE SERIES
TIME (MS)

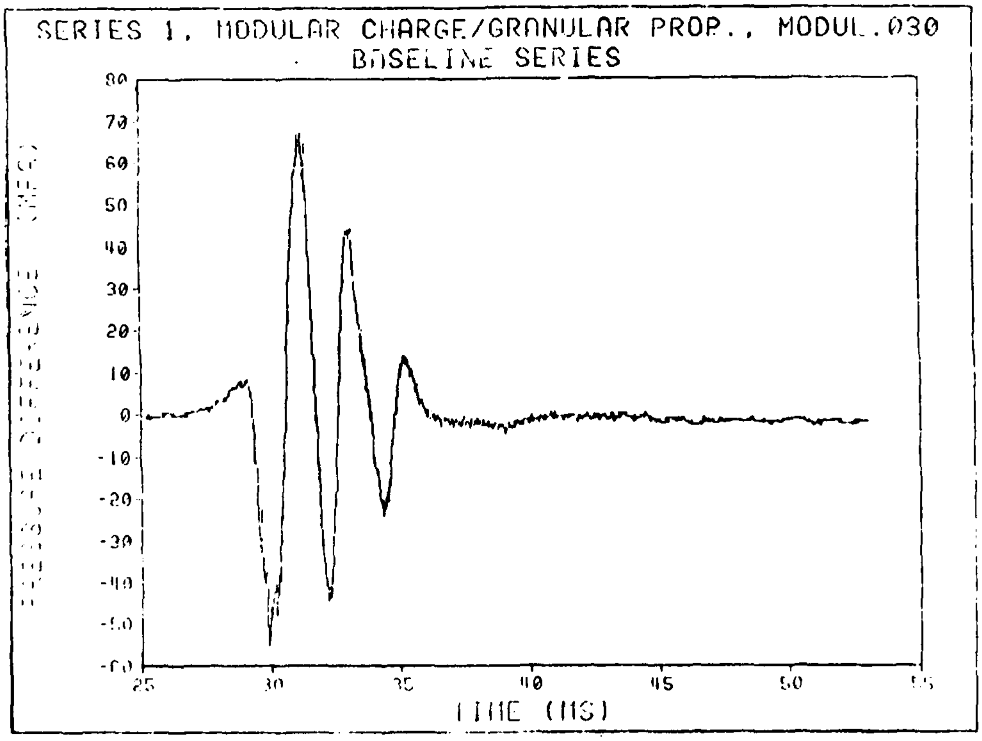
SERIES 1, MODULAR CHARGE/GRANULAR PROP., MODUL.030
BASELINE SERIES
TIME (MS)

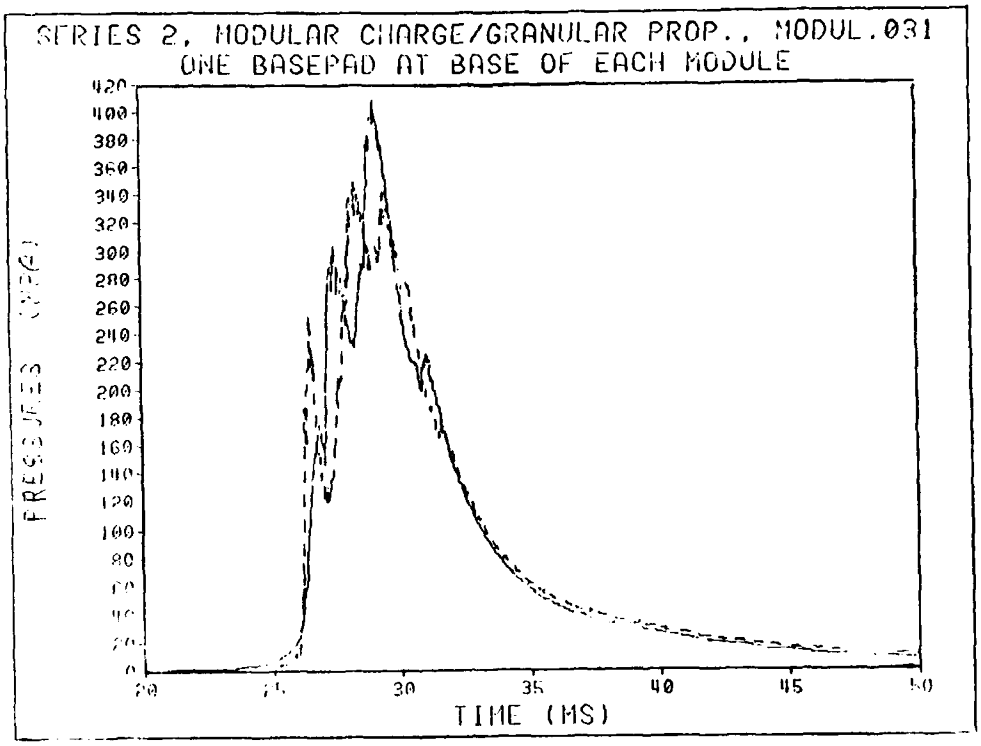
SERIES 2, MODULAR CHARGE/GRANULAR PROP., MODUL.031
ONE BASEPAD AT BASE OF EACH MODULE
TIME (MS)

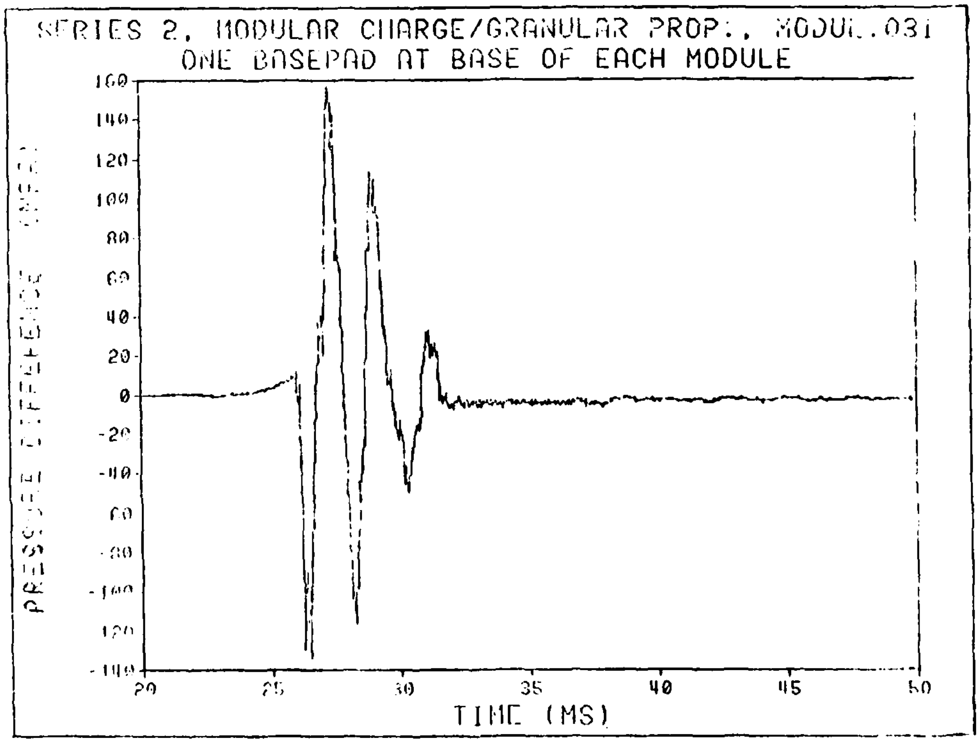
SERIES 2, MODULAR CHARGE/GRANULAR PROP., MODUL.031
ONE BASEPAD AT BASE OF EACH MODULE
TIME (MS)

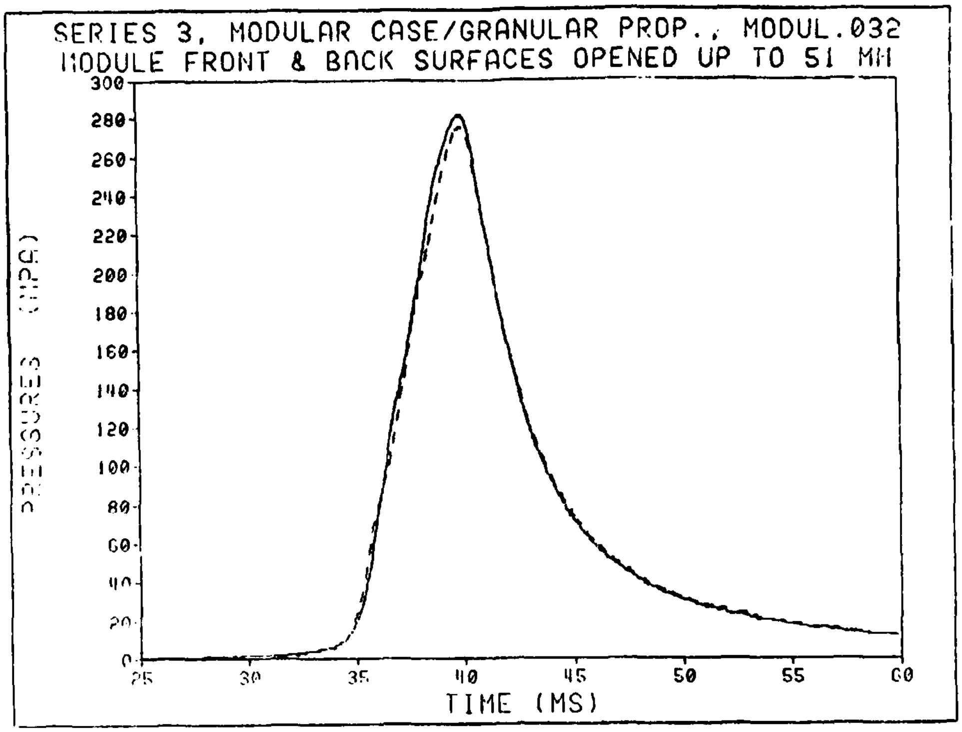

SERIES 3, MODULAR CASE/GRANULAR PROP., MODUL.032
MODULE FRONT & BACK SURFACES OPENED UP TO 51 MM
PRESSURES (MPA)
TIME (MS)

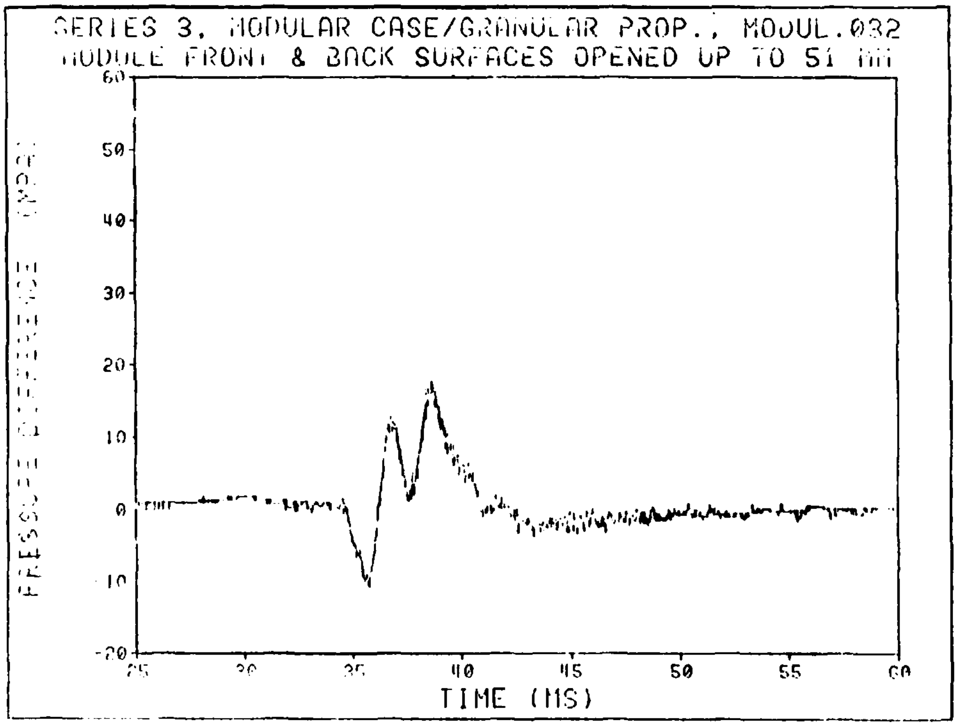

SERIES 3, MODULAR CASE/GRANULAR PROP., MODUL.032
MODULE FRONT & BACK SURFACES OPENED UP TO 51 MM
TIME (MS)

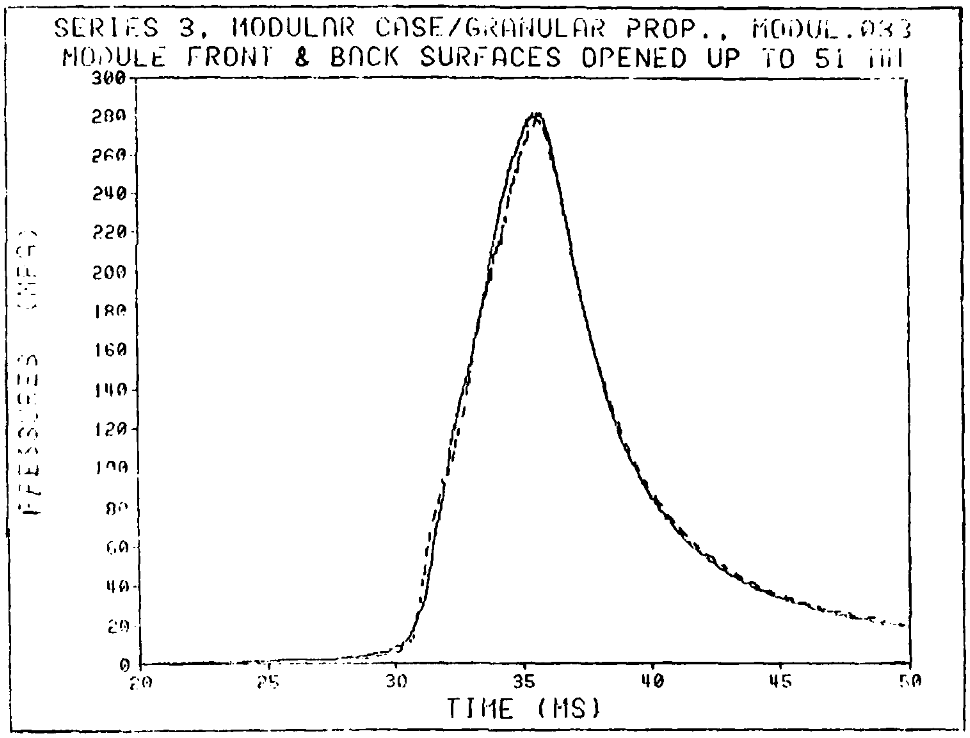
SERIES 3, MODULAR CASE/GRANULAR PROP., MODUL.033
MODULE FRONT & BACK SURFACES OPENED UP TO 51 MM
TIME (MS)

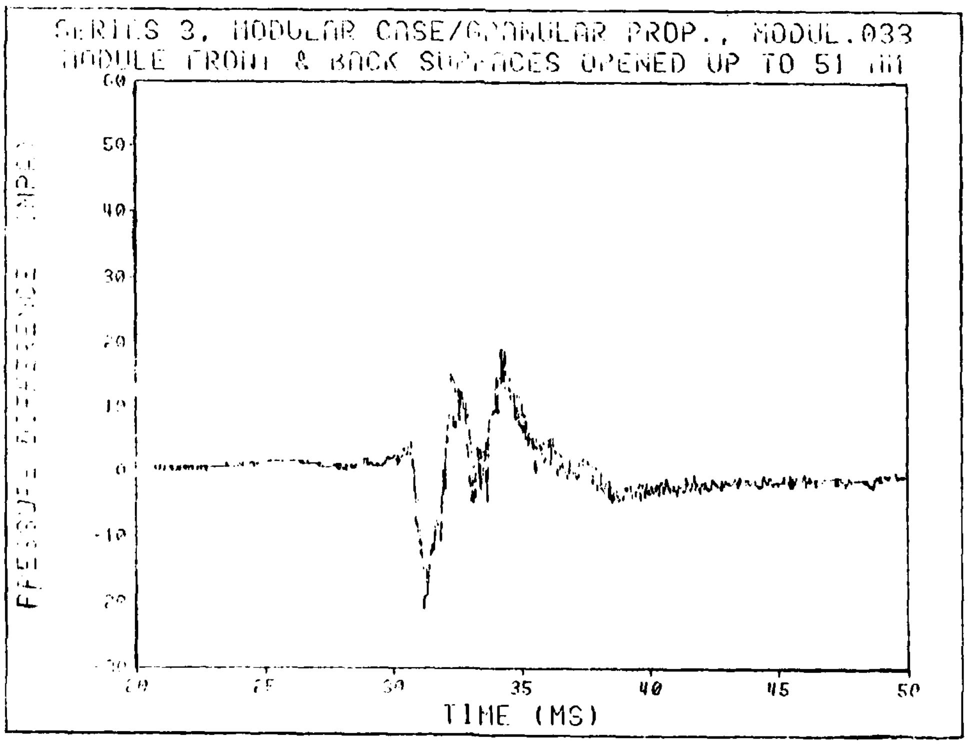
SERIES 3, MODULAR CASE/GRANULAR PROP., MODUL.033
MODULE FRONT & BACK SURFACES OPENED UP TO 51 MM
TIME (MS)

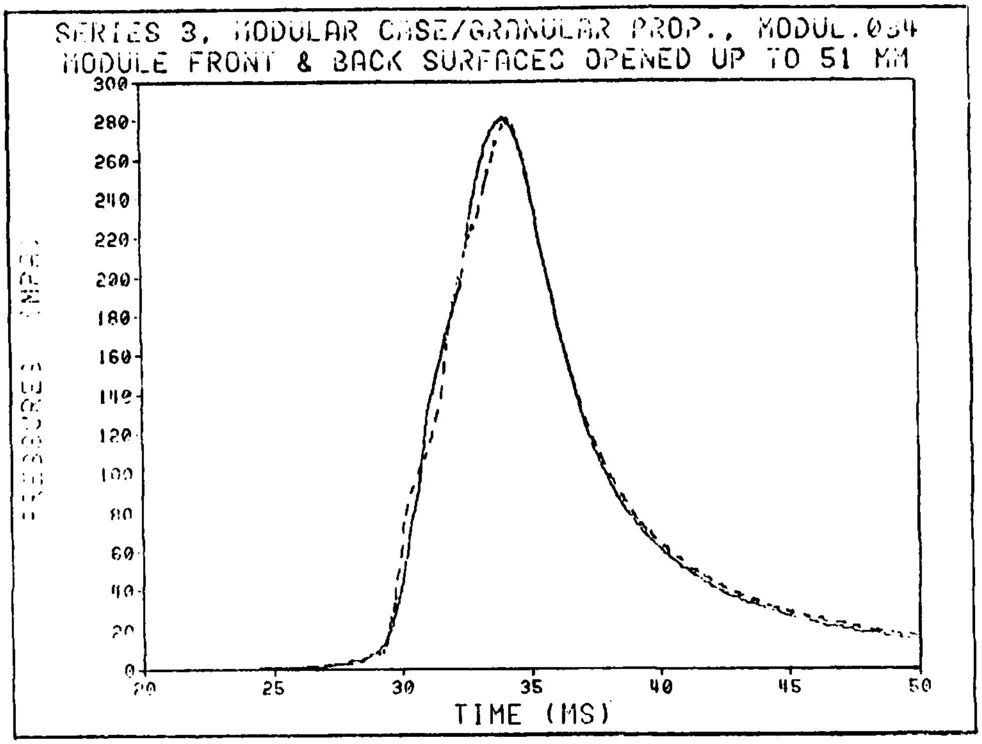
SERIES 3, MODULAR CASE/GRANULAR PROP., MODUL.034
MODULE FRONT & BACK SURFACES OPENED UP TO 51 MM
PRESSURES (MPA)
TIME (MS)

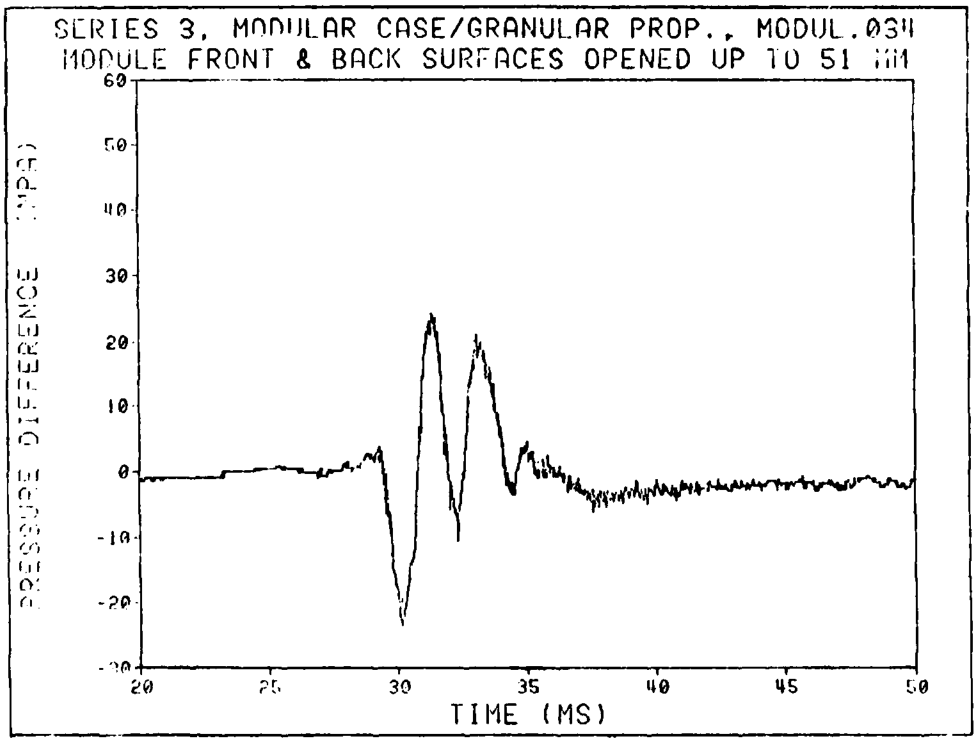
SERIES 3, MODULAR CASE/GRANULAR PROP., MODUL.034
MODULE FRONT & BACK SURFACES OPENED UP TO 51 MM
PRESSURE DIFFERENCE (MPA)
TIME (MS)

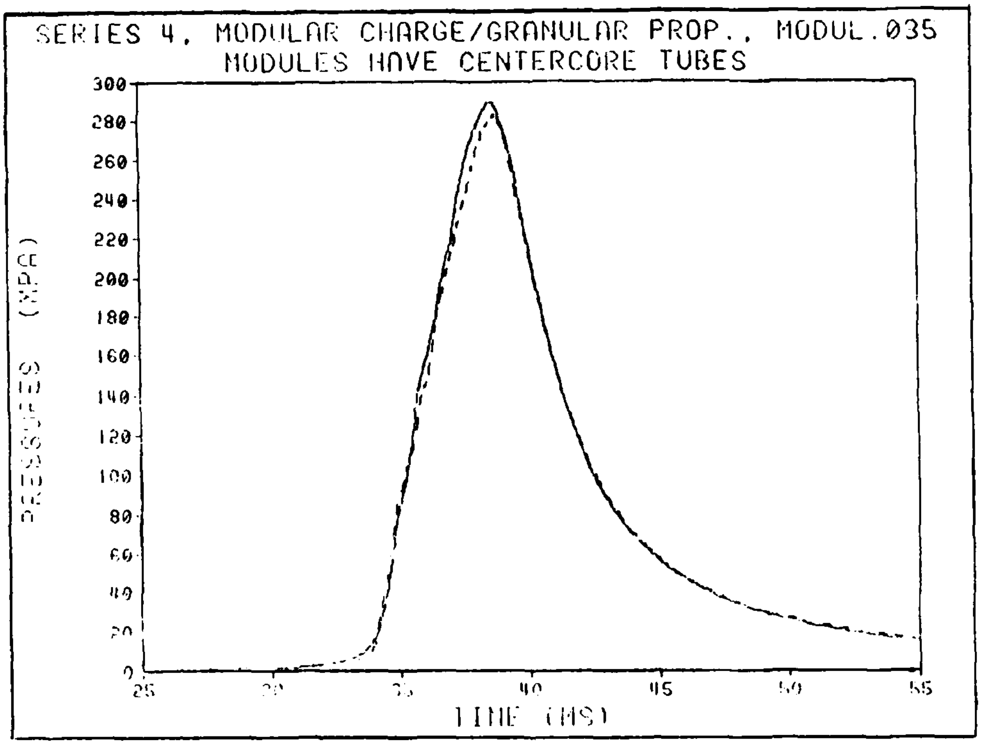
SERIES 4, MODULAR CHARGE/GRANULAR PROP., MODUL.035
MODULES HAVE CENTERCORE TUBES
PRESSURES (MPA)
TIME (MS)

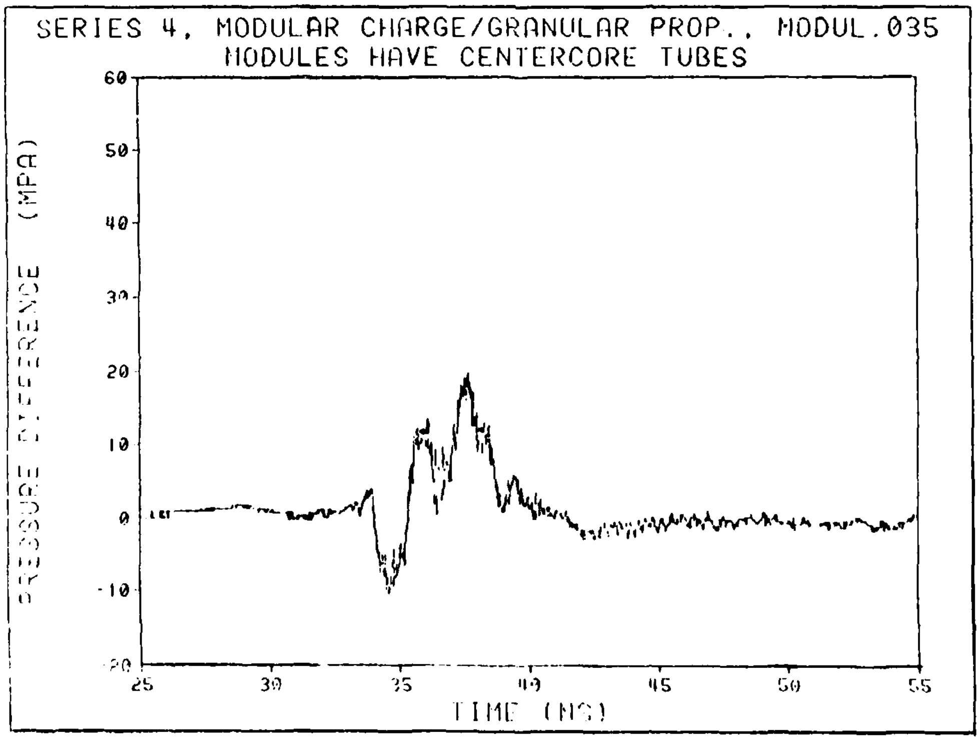
SERIES 4, MODULAR CHARGE/GRANULAR PROP., MODUL.035
MODULES HAVE CENTERCORE TUBES
PRESSURE DIFFERENCE (MPA)
TIME (MS)

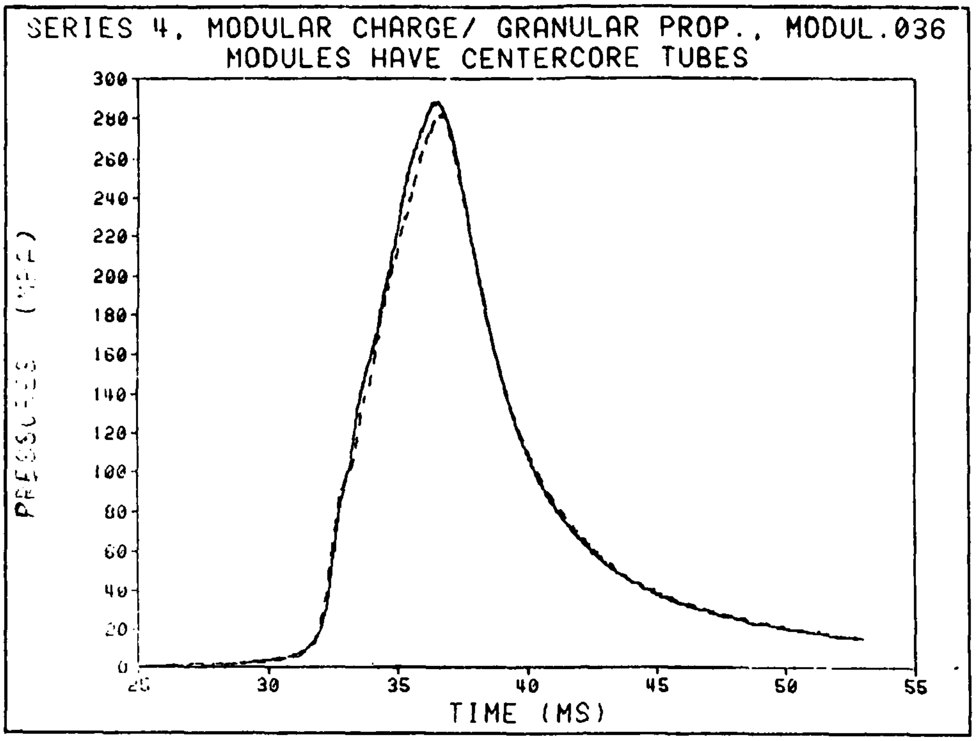
SERIES 4, MODULAR CHARGE/ GRANULAR PROP., MODUL.036
MODULES HAVE CENTERCORE TUBES
TIME (MS)

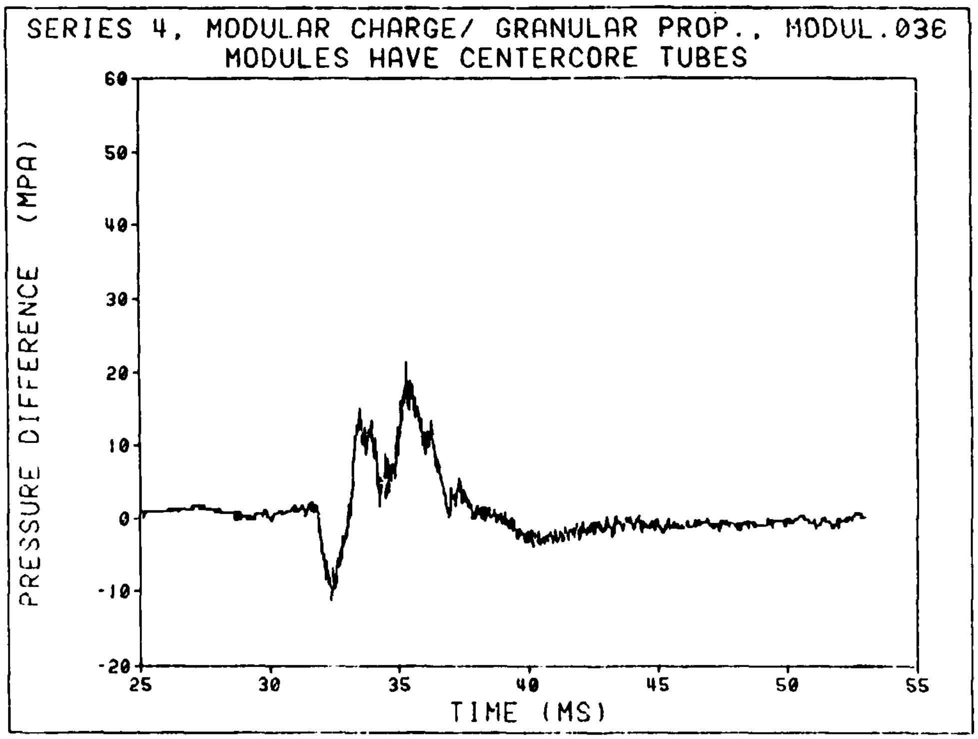
SERIES 4, MODULAR CHARGE/ GRANULAR PROP., MODUL.036
MODULES HAVE CENTERCORE TUBES
PRESSURE DIFFERENCE (MPA)
TIME (MS)

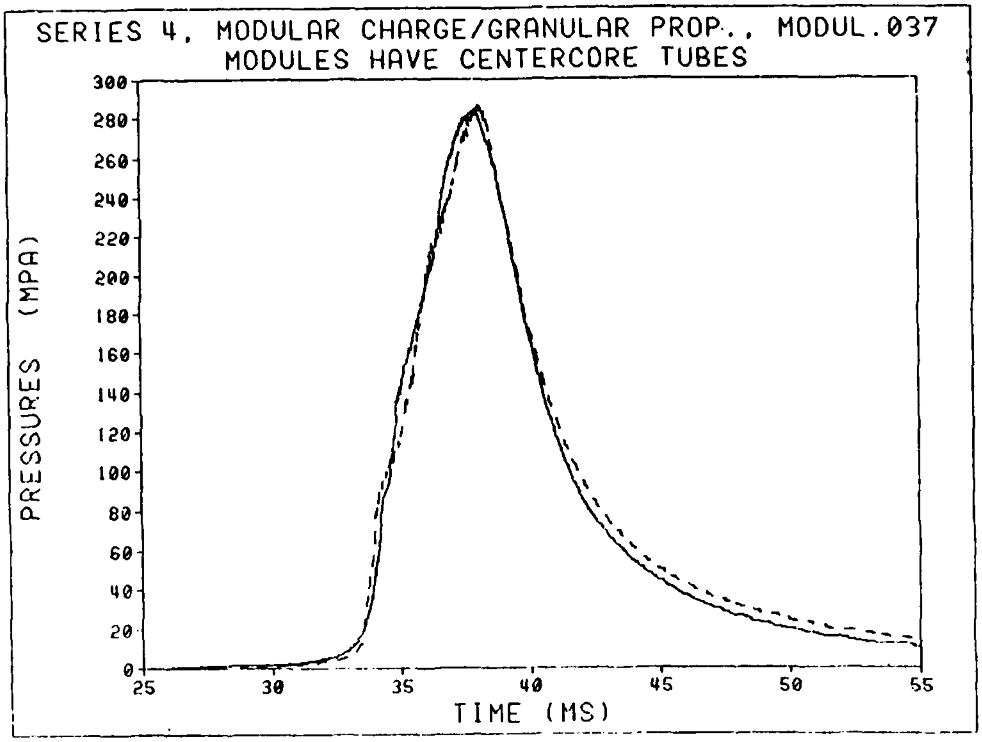
SERIES 4, MODULAR CHARGE/GRANULAR PROP., MODUL.037
MODULES HAVE CENTERCORE TUBES
PRESSURES (MPA)
0
20
40
60
80
100
120
140
160
180
200
220
240
260
280
300
25
30
35
40
45
50
55
TIME (MS)

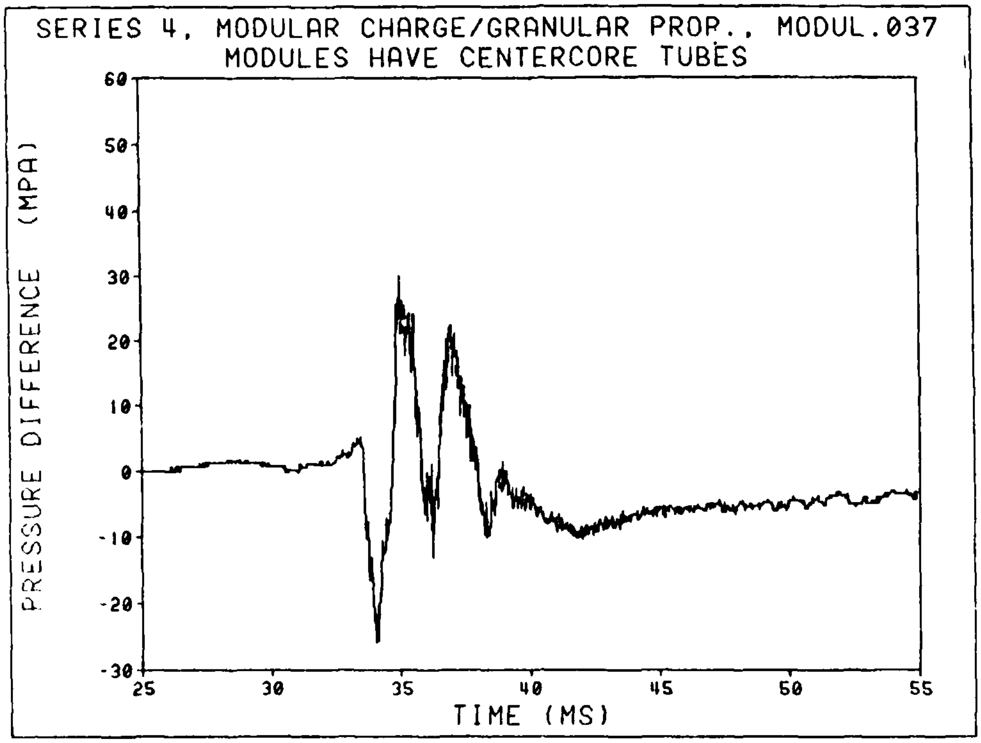
SERIES 4, MODULAR CHARGE/GRANULAR PROP., MODUL.037
MODULES HAVE CENTERCORE TUBES
PRESSURE DIFFERENCE (MPA)
-30
-20
-10
0
10
20
30
40
50
60
25
30
35
40
45
50
55
TIME (MS)

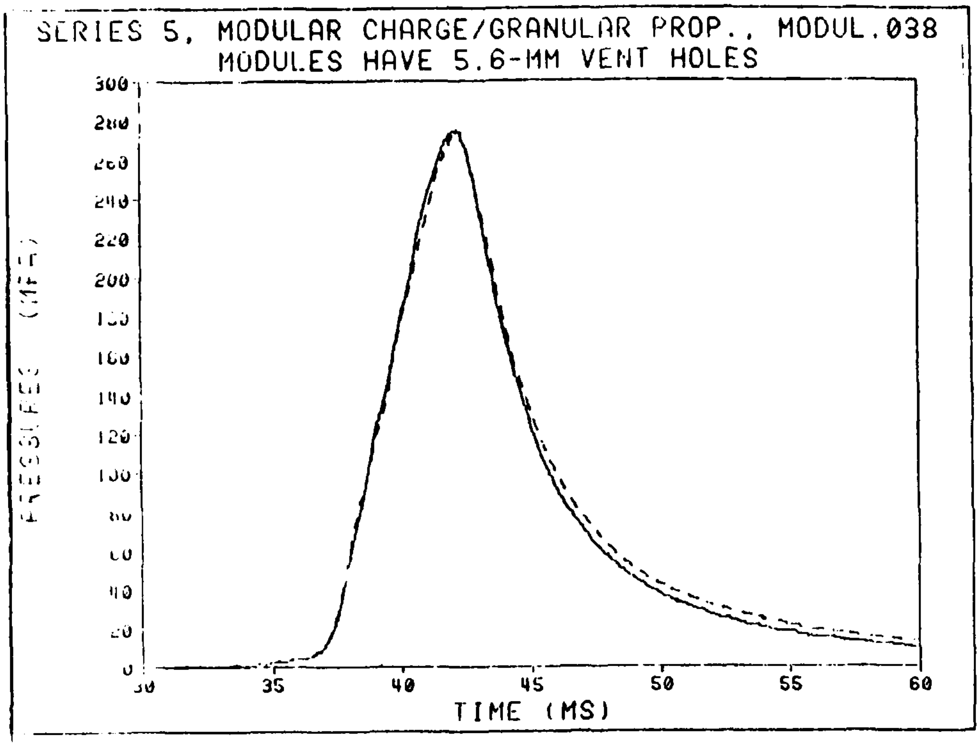
SERIES 5, MODULAR CHARGE/GRANULAR PROP., MODUL.038
MODULES HAVE 5.6-MM VENT HOLES
PRESSURES (MPA)
TIME (MS)

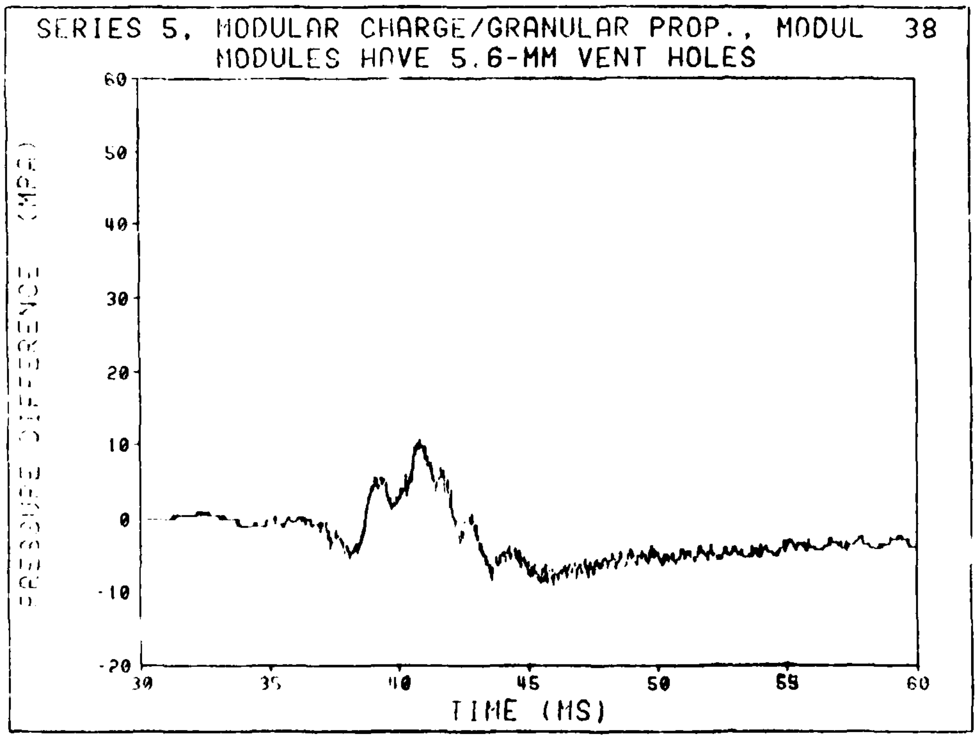
SERIES 5, MODULAR CHARGE/GRANULAR PROP., MODUL 38
MODULES HAVE 5.6-MM VENT HOLES
PRESSURE DIFFERENCE (MPA)
TIME (MS)

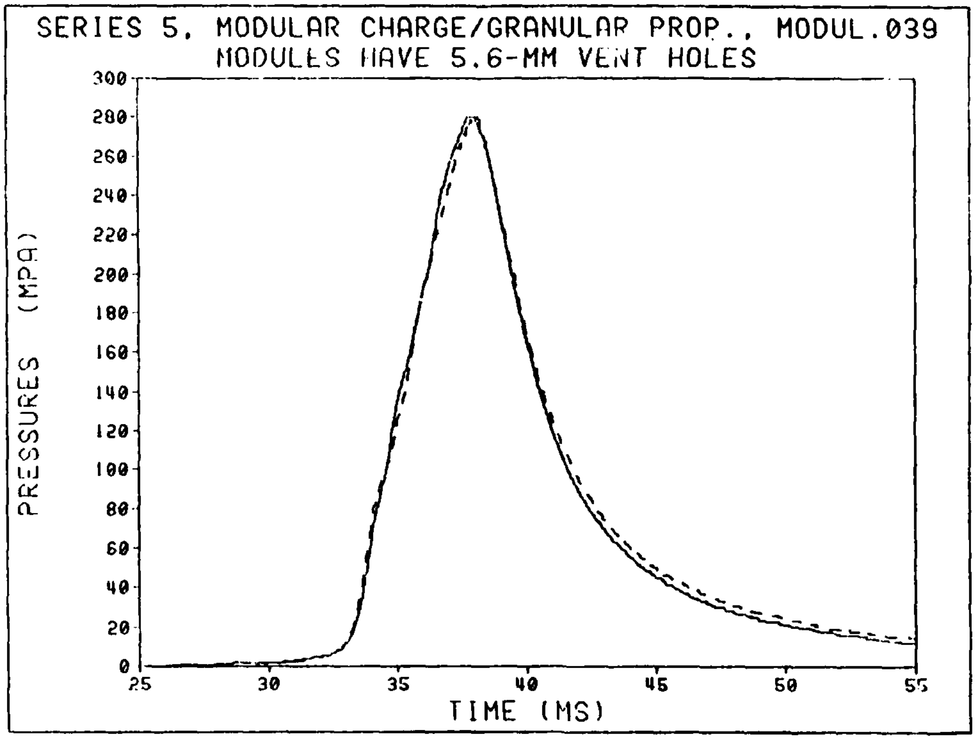
SERIES 5, MODULAR CHARGE/GRANULAR PROP., MODUL.039
MODULES HAVE 5.6-MM VENT HOLES
PRESSURES (MPA)
TIME (MS)
300
280
260
240
220
200
180
160
140
120
100
80
60
40
20
0
25
30
35
40
45
50
55

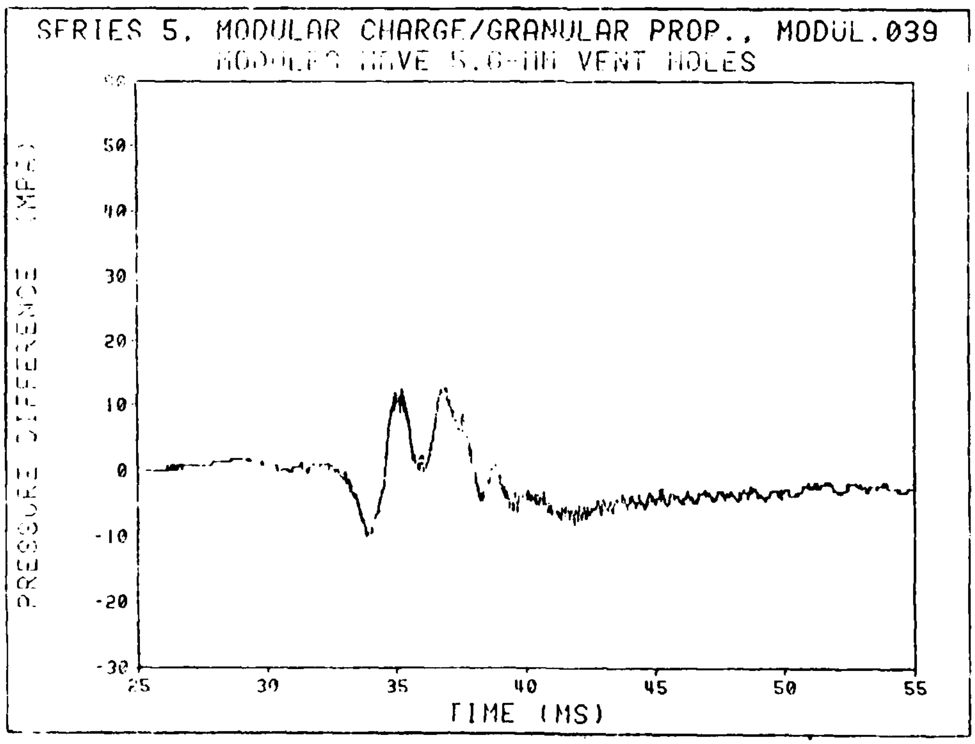
SERIES 5, MODULAR CHARGE/GRANULAR PROP., MODUL.039
PRESSURE DIFFERENCE (MPA)
TIME (MS)
50
40
30
20
10
0
-10
-20
-30
25
30
35
40
45
50
55

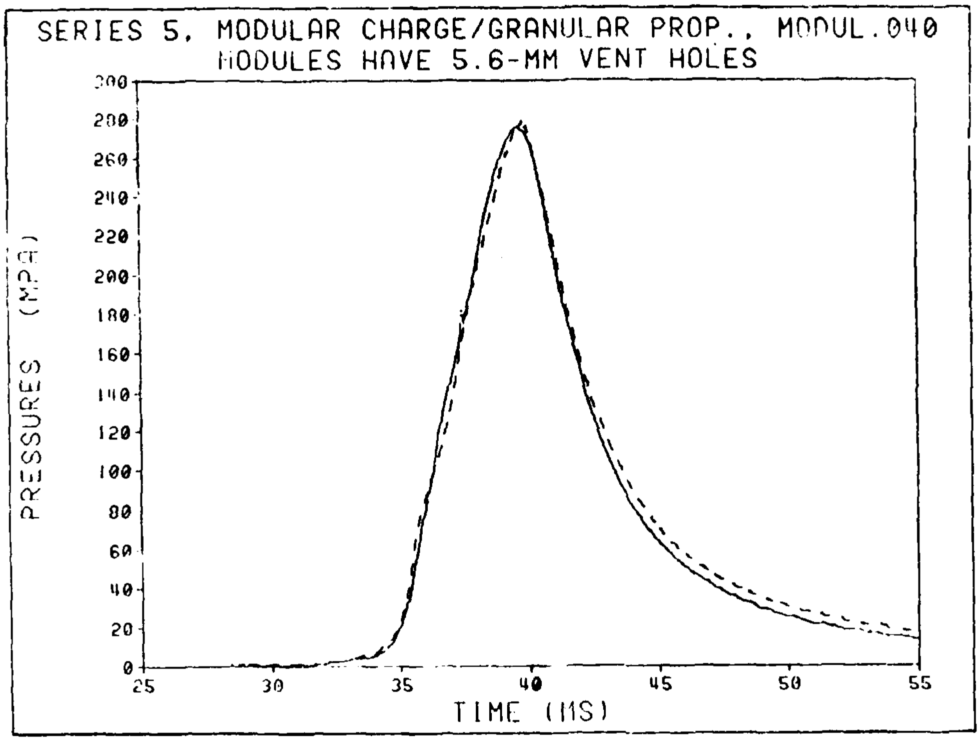

SERIES 5, MODULAR CHARGE/GRANULAR PROP., MODUL.040
MODULES HAVE 5.6-MM VENT HOLES
PRESSURES (MPA)
0
20
40
60
80
100
120
140
160
180
200
220
240
260
280
25
30
35
40
45
50
55
TIME (MS)

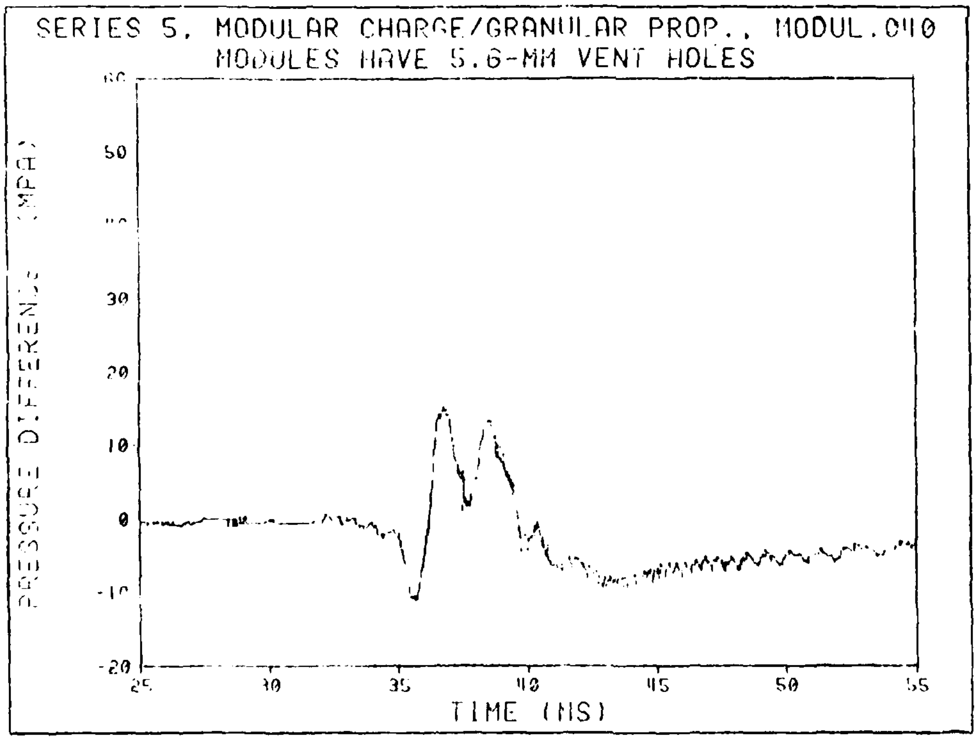

SERIES 5, MODULAR CHARGE/GRANULAR PROP., MODUL.040
MODULES HAVE 5.6-MM VENT HOLES
PRESSURE DIFFERENCE (MPA)
-20
0
10
20
30
50
25
30
35
40
45
50
55
TIME (MS)

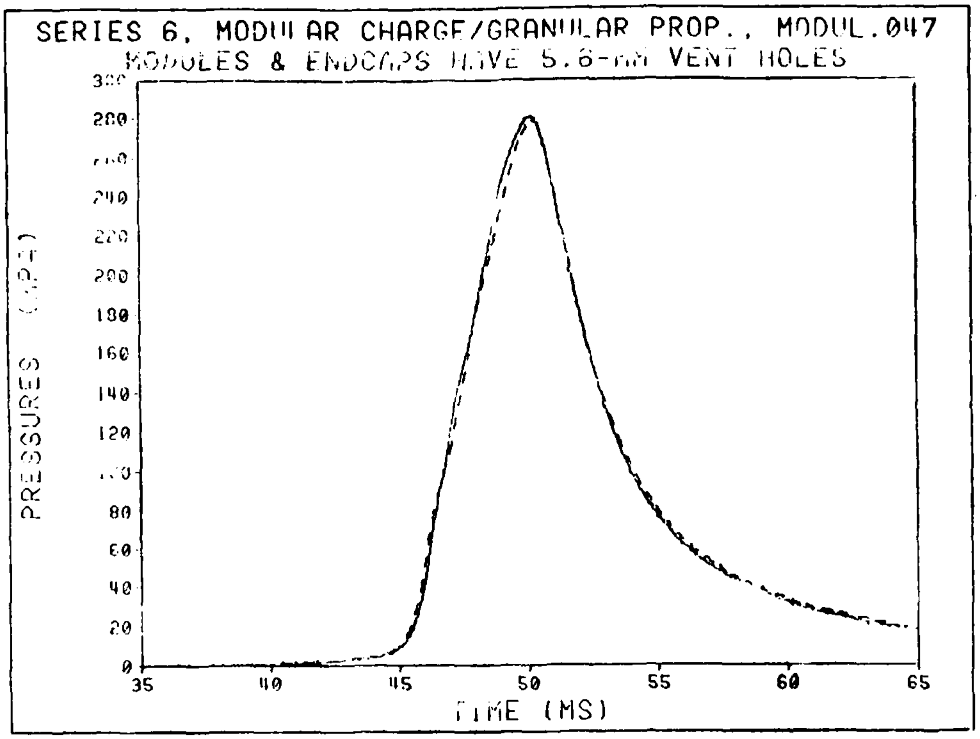
SERIES 6, MODULAR CHARGE/GRANULAR PROP., MODUL.047
MODULES & ENDCAPS HAVE 5.6-MM VENT HOLES
PRESSURES (MPA)
280
240
220
200
180
160
140
120
80
60
40
20
0
35
40
45
50
55
60
65
TIME (MS)

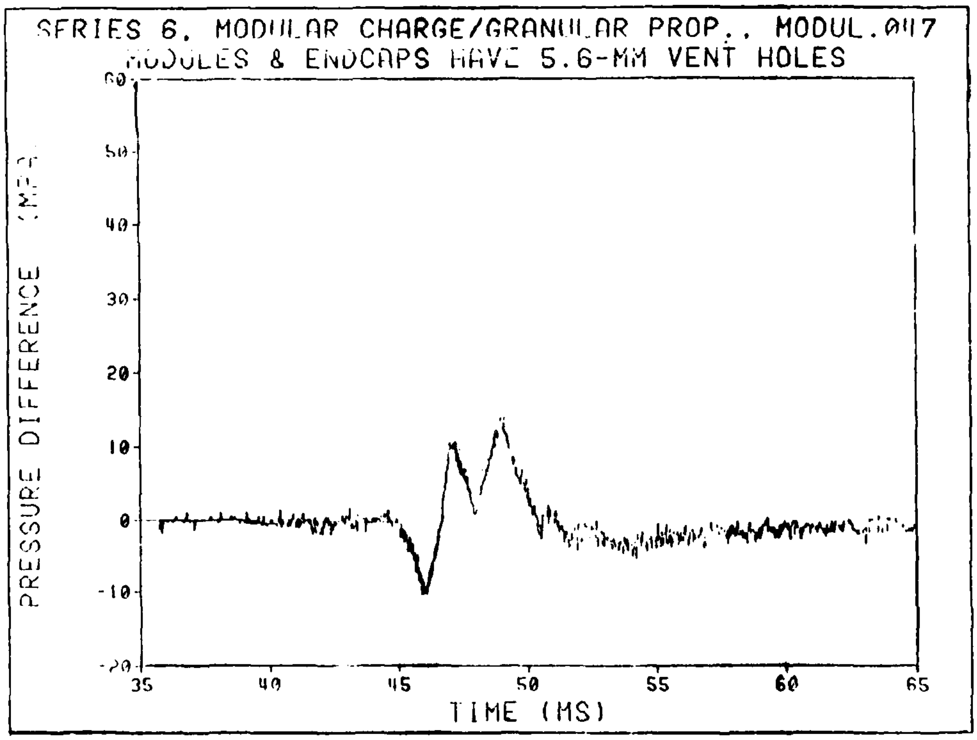
SERIES 6, MODULAR CHARGE/GRANULAR PROP., MODUL.047
MODULES & ENDCAPS HAVE 5.6-MM VENT HOLES
PRESSURE DIFFERENCE (MPA)
60
50
40
30
20
10
0
-10
-20
35
40
45
50
55
60
65
TIME (MS)

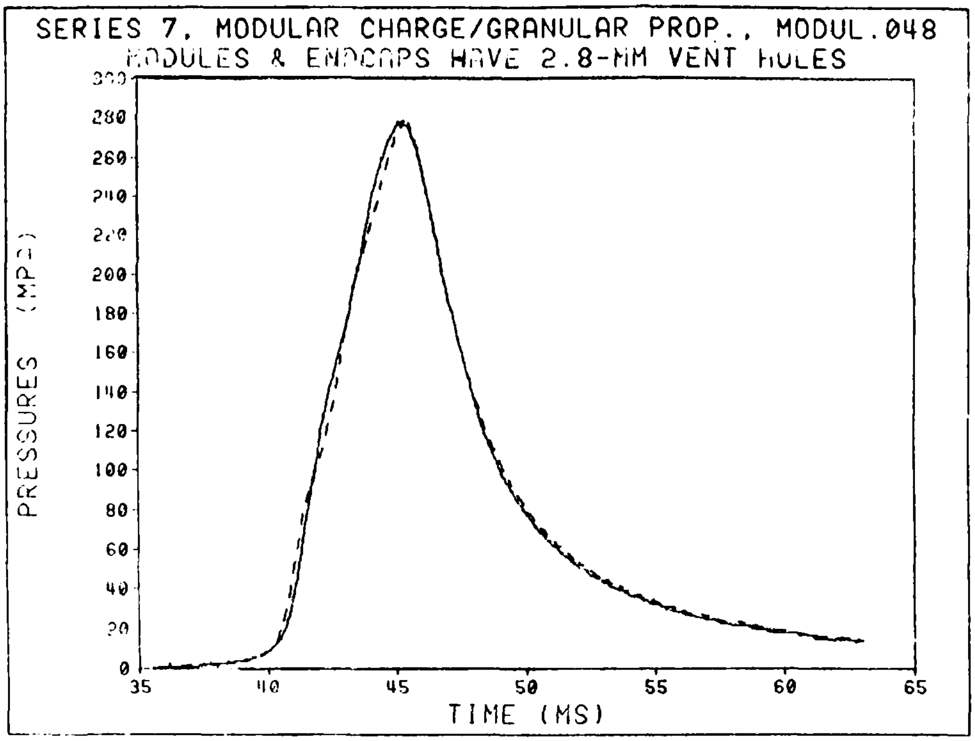
SERIES 7, MODULAR CHARGE/GRANULAR PROP., MODUL.048
MODULES & ENDCAPS HAVE 2.8-MM VENT HOLES
PRESSURES (MPA)
TIME (MS)
0
20
40
60
80
100
120
140
160
180
200
220
240
260
280
300
35
40
45
50
55
60
65

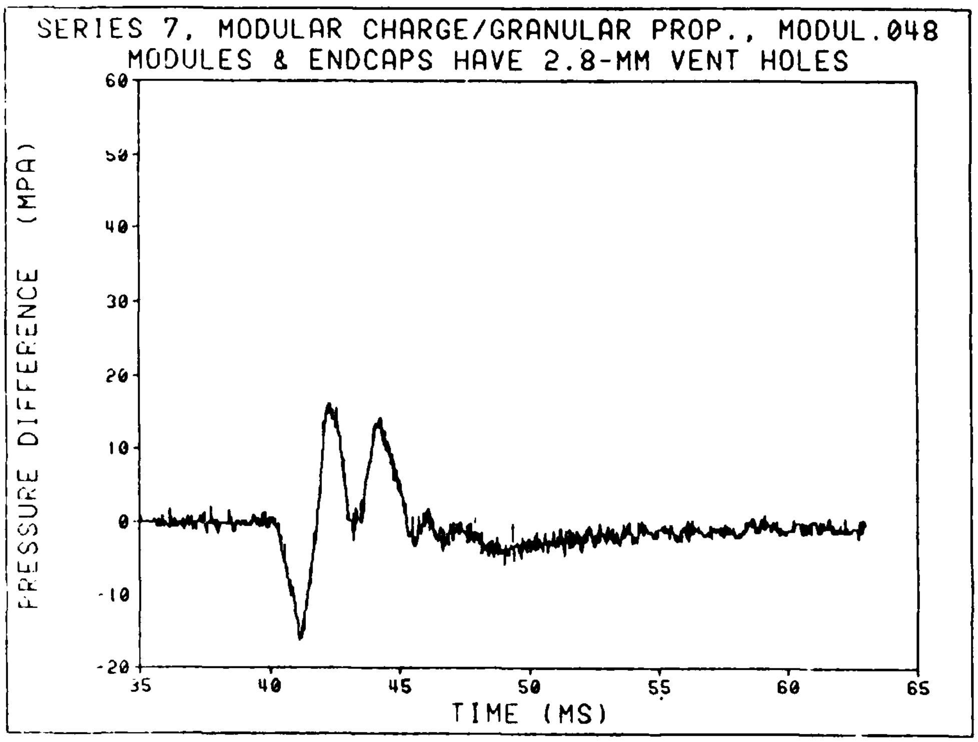
SERIES 7, MODULAR CHARGE/GRANULAR PROP., MODUL.048
MODULES & ENDCAPS HAVE 2.8-MM VENT HOLES
PRESSURE DIFFERENCE (MPA)
TIME (MS)
-20
-10
0
10
20
30
40
50
60
35
40
45
50
55
60
65

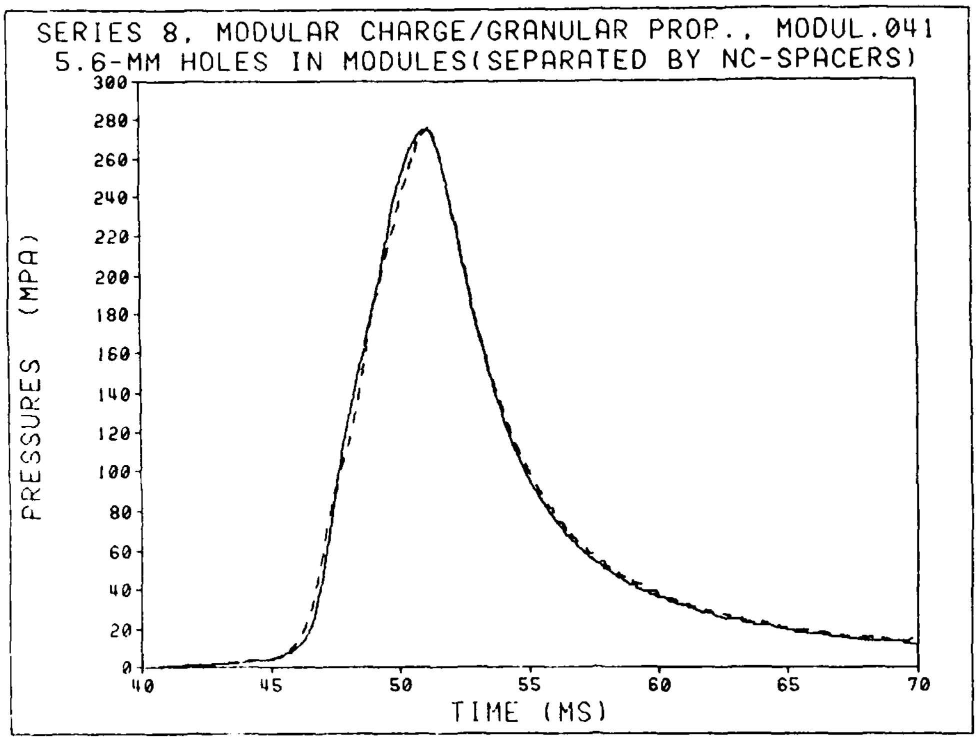
SERIES 8, MODULAR CHARGE/GRANULAR PROP., MODUL.041
5.6-MM HOLES IN MODULES(SEPARATED BY NC-SPACERS)
PRESSURES (MPA)
TIME (MS)

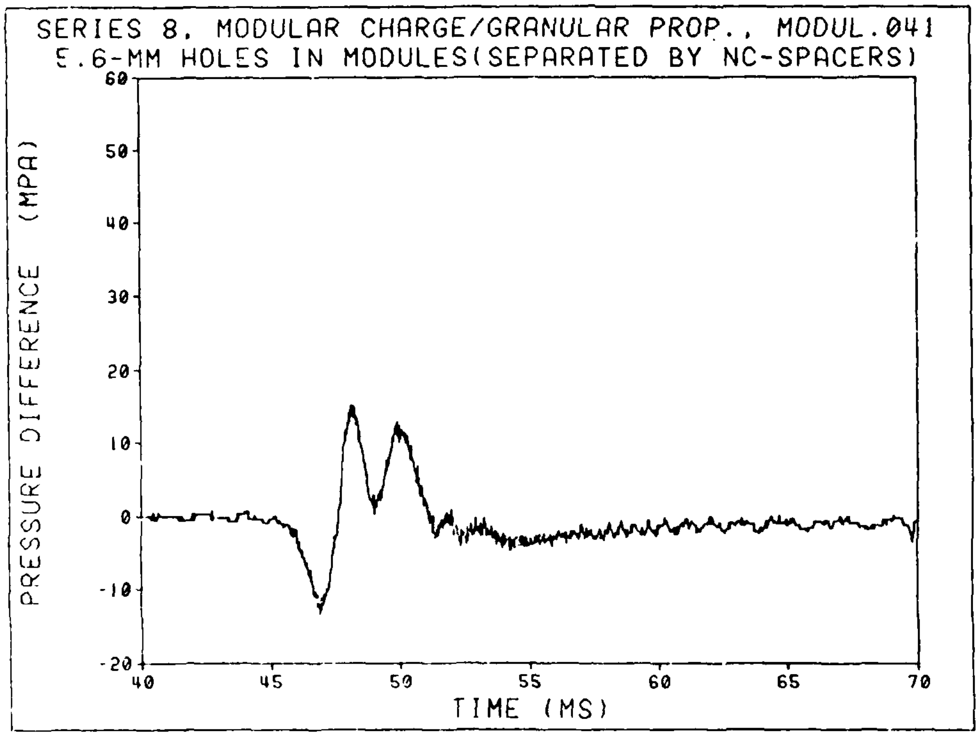
SERIES 8, MODULAR CHARGE/GRANULAR PROP., MODUL.041
5.6-MM HOLES IN MODULES(SEPARATED BY NC-SPACERS)
PRESSURE DIFFERENCE (MPA)
TIME (MS)

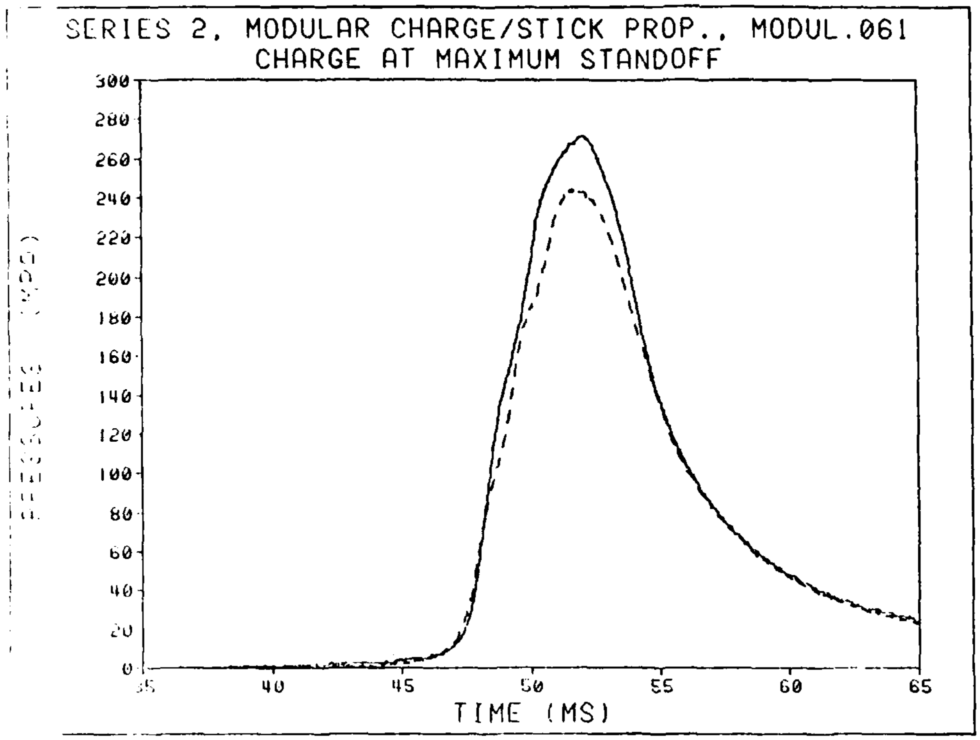
SERIES 2, MODULAR CHARGE/STICK PROP., MODUL.061
CHARGE AT MAXIMUM STANDOFF
300
280
260
240
220
200
180
160
140
120
100
80
60
40
20
0
40
45
50
55
60
65
TIME (MS)

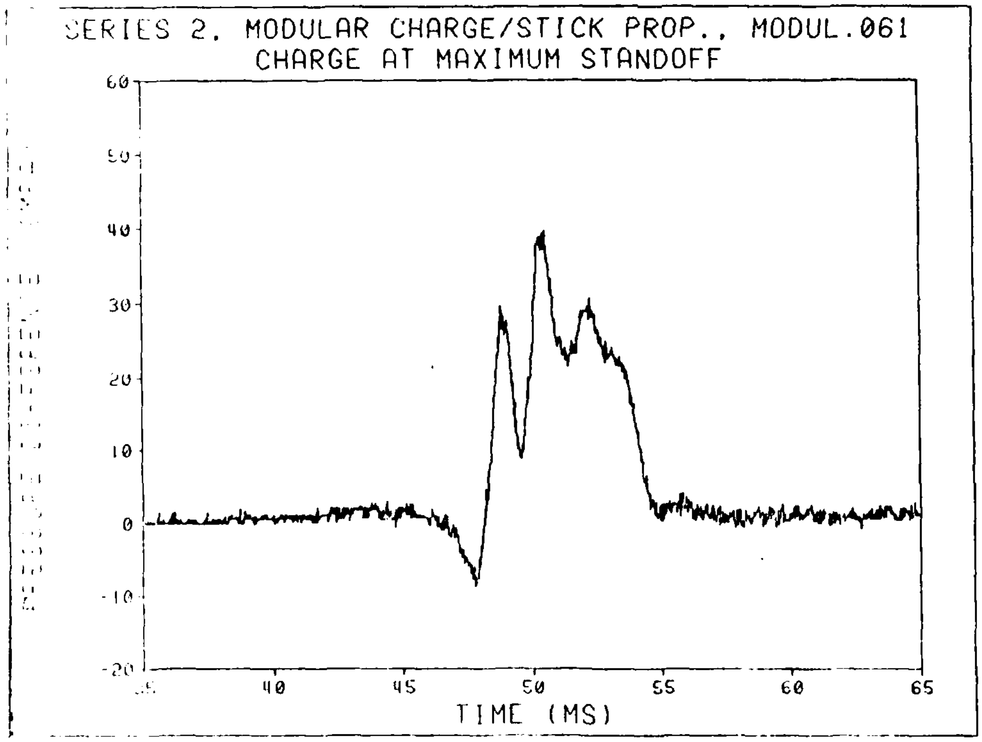
SERIES 2, MODULAR CHARGE/STICK PROP., MODUL.061
CHARGE AT MAXIMUM STANDOFF
60
50
40
30
20
10
0
-10
-20
40
45
50
55
60
65
TIME (MS)

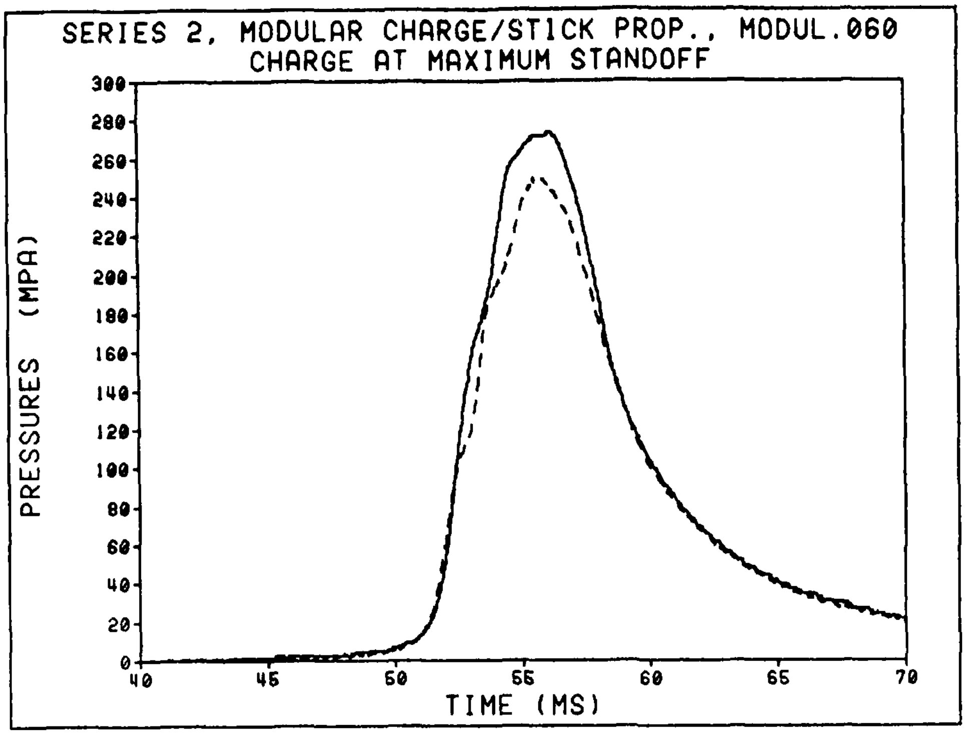
SERIES 2, MODULAR CHARGE/STICK PROP., MODUL.060
CHARGE AT MAXIMUM STANDOFF
PRESSURES (MPA)
TIME (MS)
0
20
40
60
80
100
120
140
160
180
200
220
240
260
280
300
40
45
50
55
60
65
70

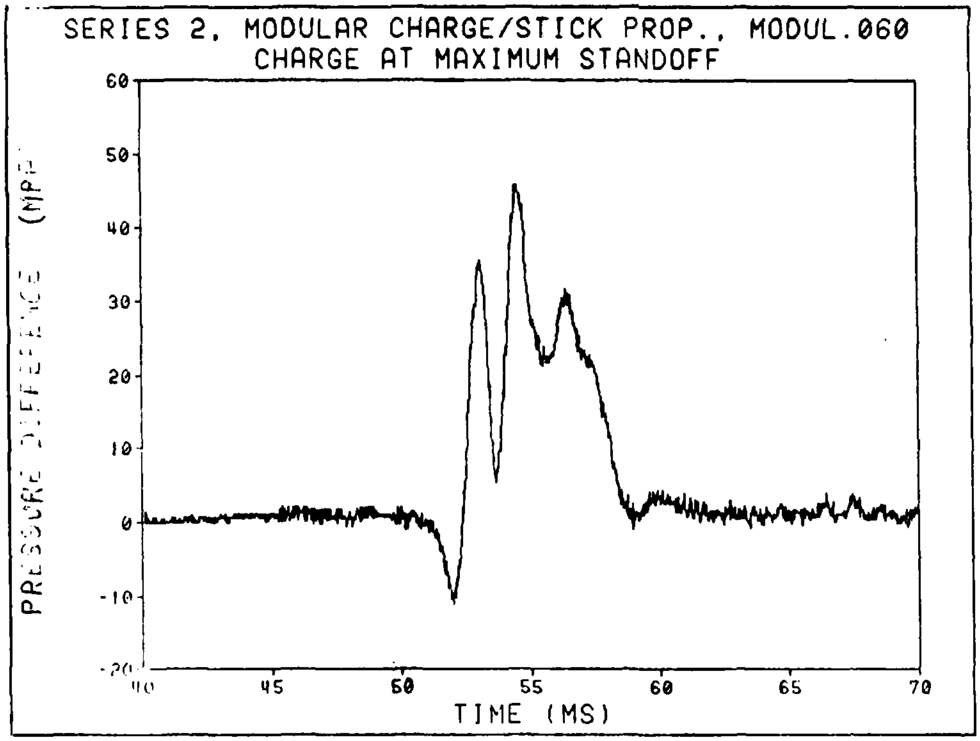
SERIES 2, MODULAR CHARGE/STICK PROP., MODUL.060
CHARGE AT MAXIMUM STANDOFF
TIME (MS)
60
50
40
30
20
10
0
-10
45
50
55
60
65
70

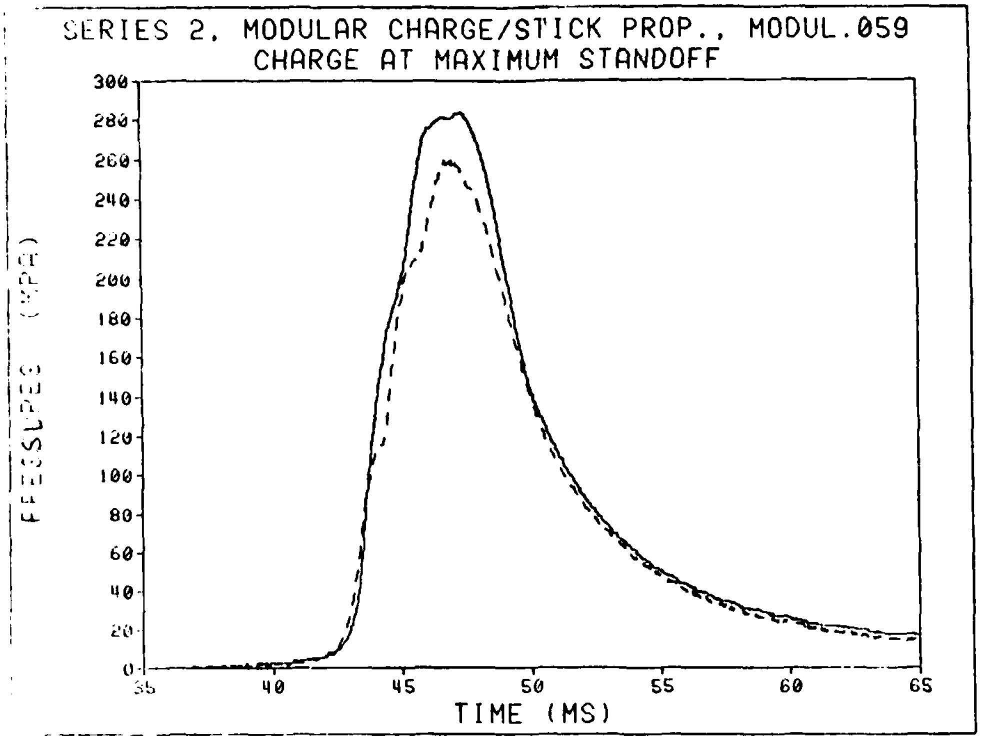
SERIES 2, MODULAR CHARGE/STICK PROP., MODUL.059
CHARGE AT MAXIMUM STANDOFF
PRESSURES (MPA)
TIME (MS)

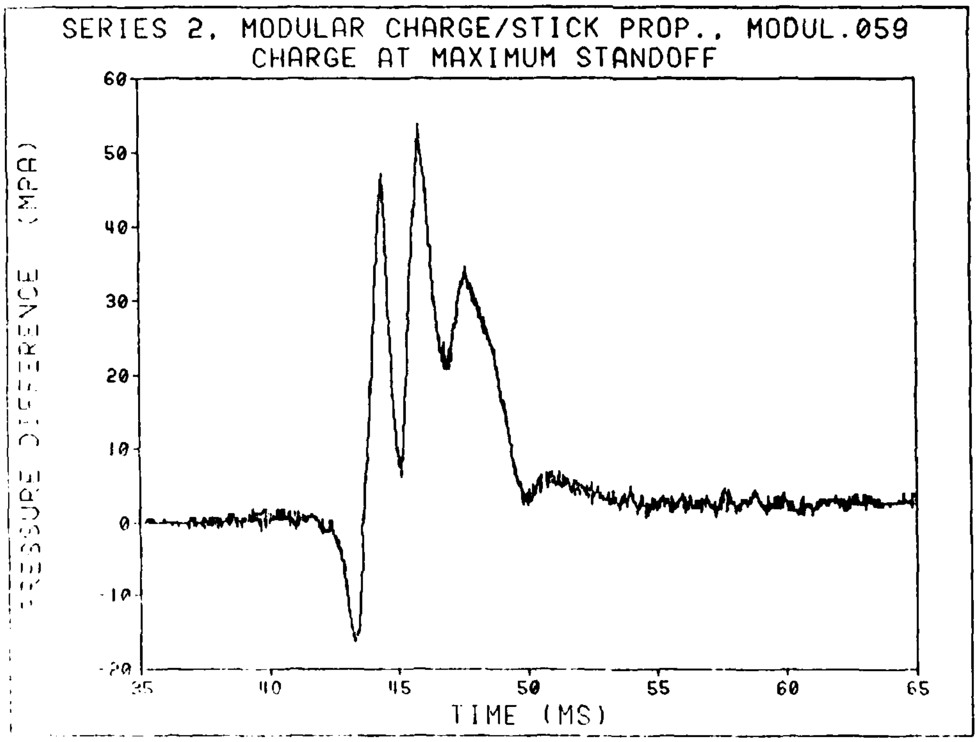
SERIES 2, MODULAR CHARGE/STICK PROP., MODUL.059
CHARGE AT MAXIMUM STANDOFF
PRESSURE DIFFERENCE (MPA)
TIME (MS)

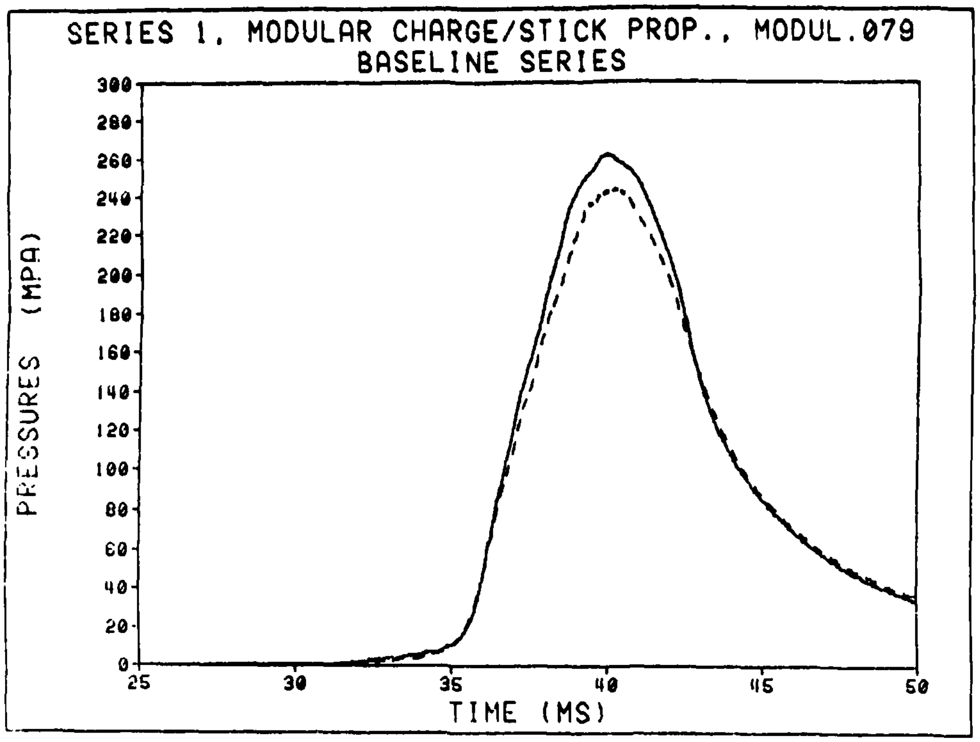

SERIES 1, MODULAR CHARGE/STICK PROP., MODUL.079
BASELINE SERIES
PRESSURES (MPA)
300
280
260
240
220
200
180
160
140
120
100
80
60
40
20
0
25
30
35
40
45
50
TIME (MS)

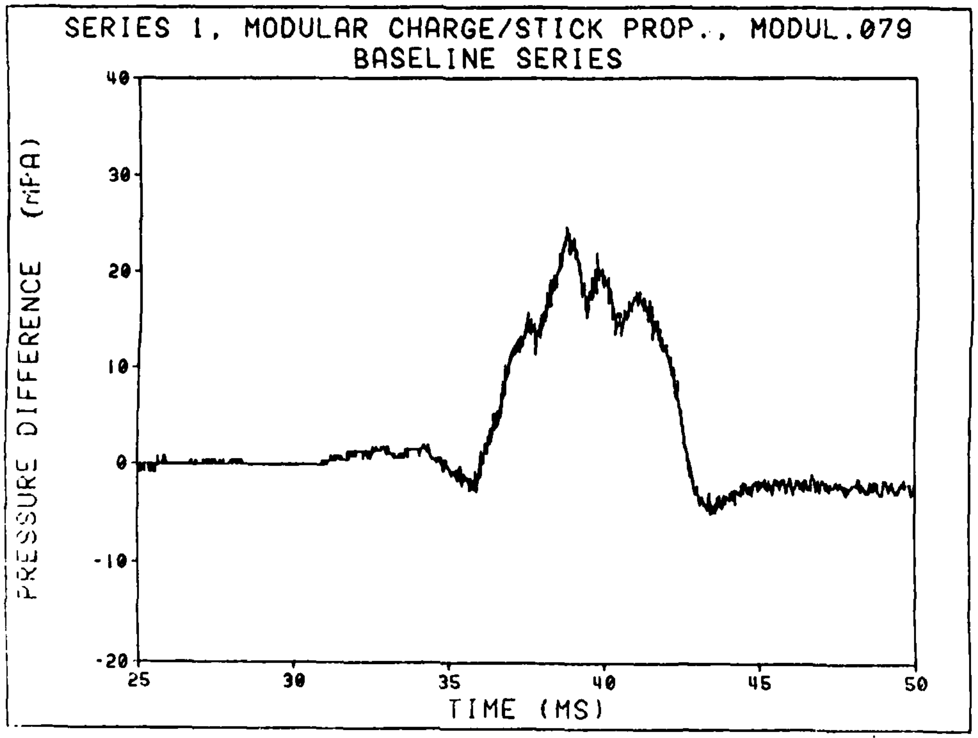

SERIES 1, MODULAR CHARGE/STICK PROP., MODUL.079
BASELINE SERIES
PRESSURE DIFFERENCE (MPA)
40
30
20
10
0
-10
-20
25
30
35
40
45
50
TIME (MS)

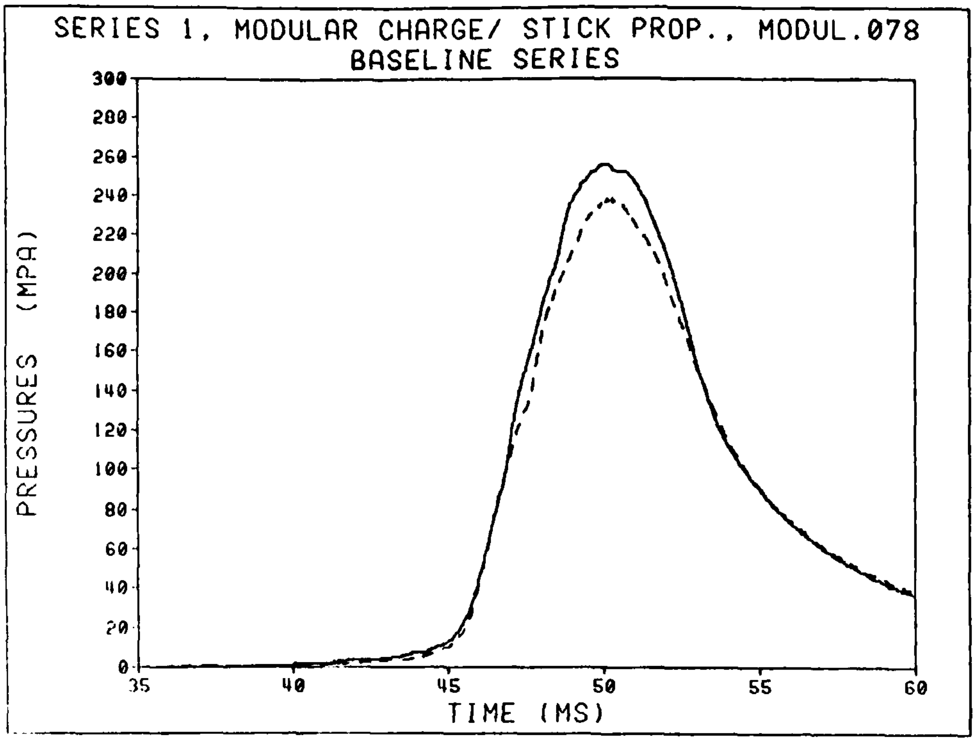
SERIES 1, MODULAR CHARGE/ STICK PROP., MODUL.078
BASELINE SERIES
PRESSURES (MPA)
TIME (MS)
300
280
260
240
220
200
180
160
140
120
100
80
60
40
20
0
35
40
45
50
55
60

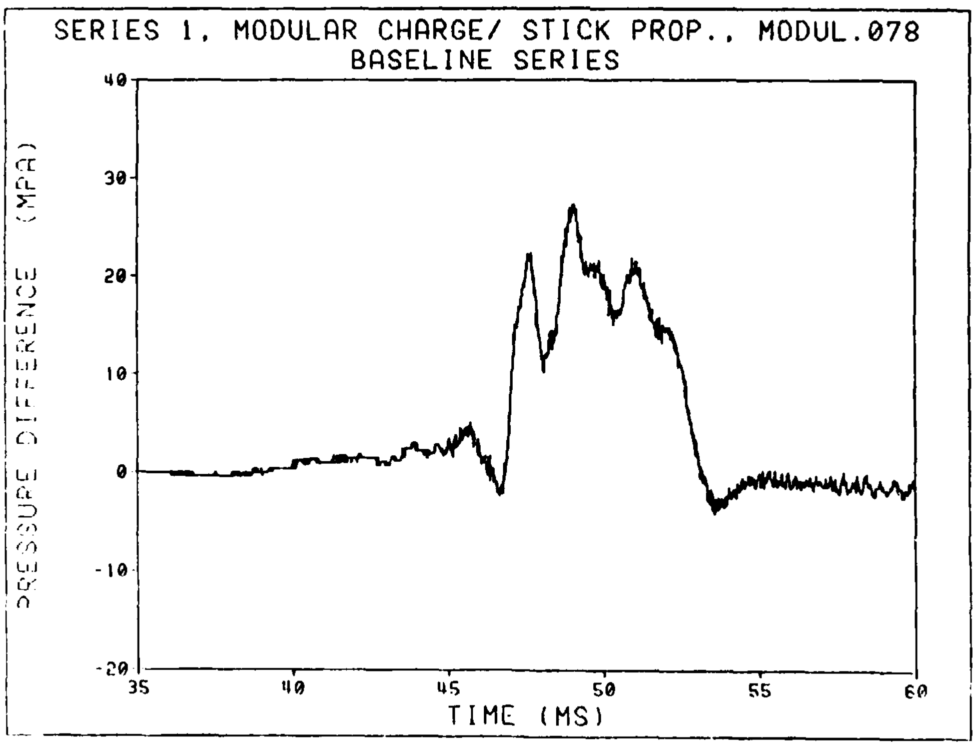
SERIES 1, MODULAR CHARGE/ STICK PROP., MODUL.078
BASELINE SERIES
PRESSURE DIFFERENCE (MPA)
TIME (MS)
40
30
20
10
0
-10
-20
35
40
45
50
55
60

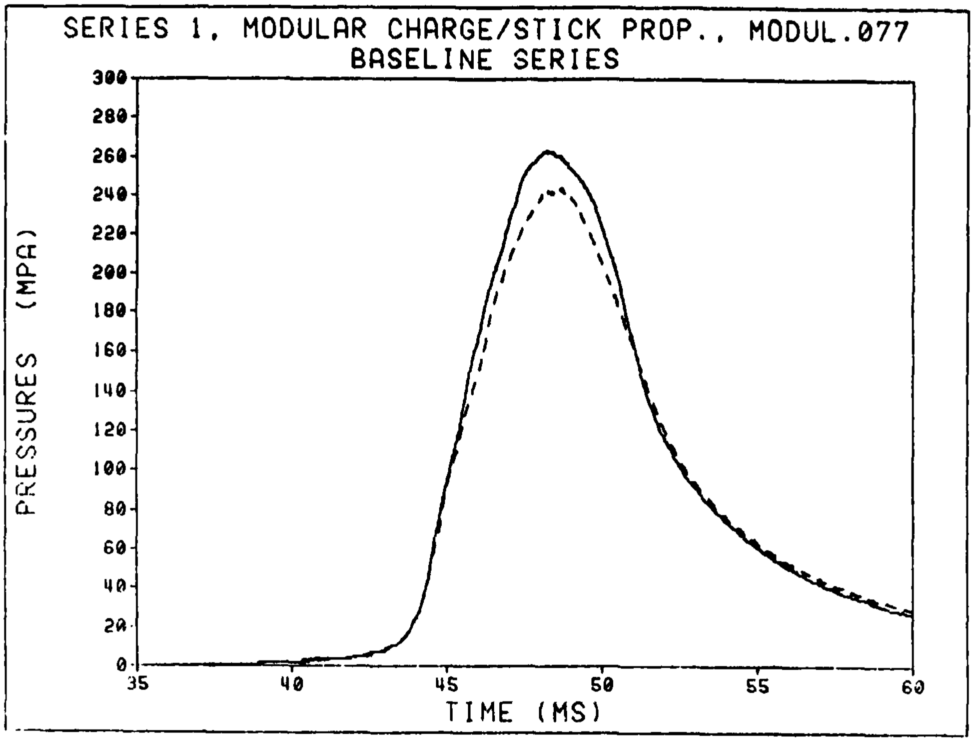
SERIES 1, MODULAR CHARGE/STICK PROP., MODUL.077
BASELINE SERIES
PRESSURES (MPA)
TIME (MS)
300
280
260
240
220
200
180
160
140
120
100
80
60
40
20
0
35
40
45
50
55
60

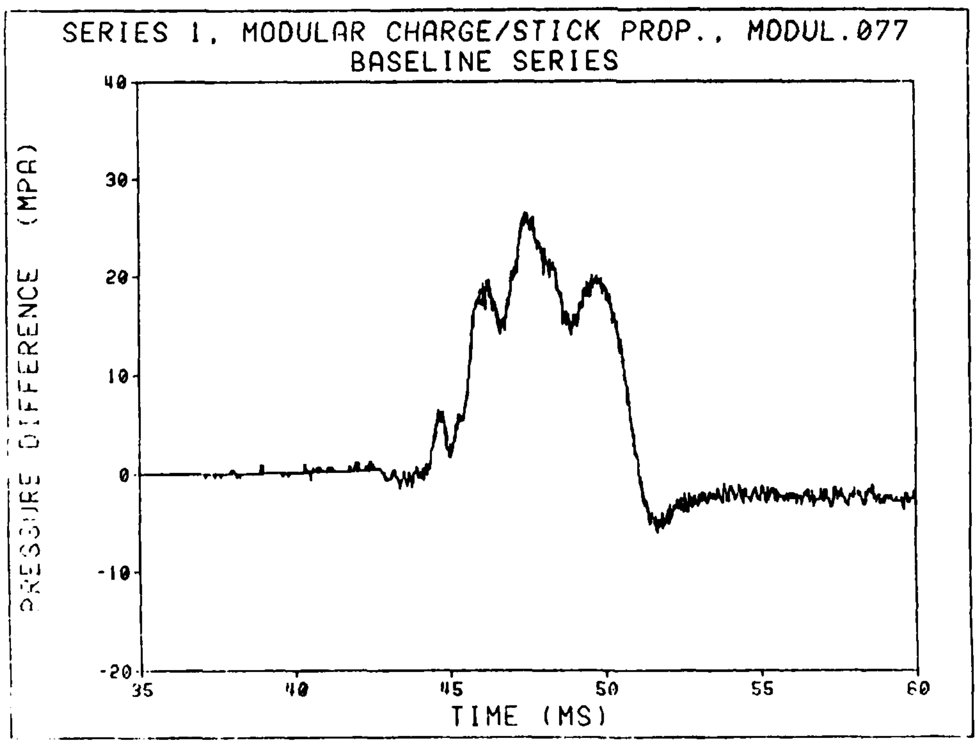
SERIES 1, MODULAR CHARGE/STICK PROP., MODUL.077
BASELINE SERIES
PRESSURE DIFFERENCE (MPA)
TIME (MS)
40
30
20
10
0
-10
-20
35
40
45
50
55
60

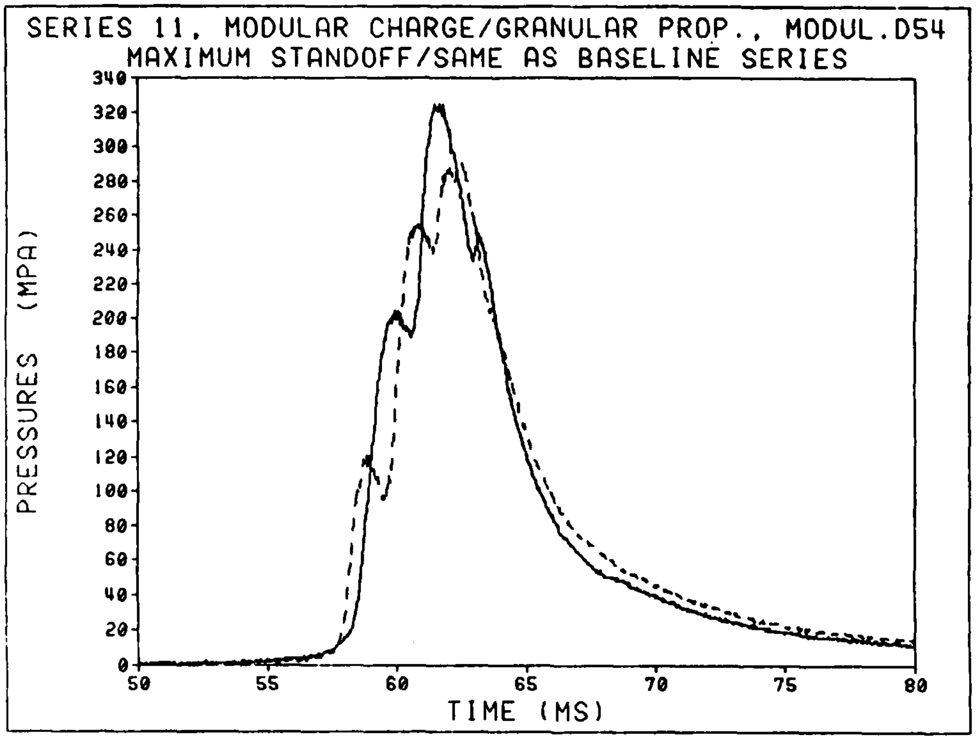
SERIES 11, MODULAR CHARGE/GRANULAR PROP., MODUL.D54
MAXIMUM STANDOFF/SAME AS BASELINE SERIES
PRESSURES (MPA)
TIME (MS)
340
320
300
280
260
240
220
200
180
160
140
120
100
80
60
40
20
0
50
55
60
65
70
75
80

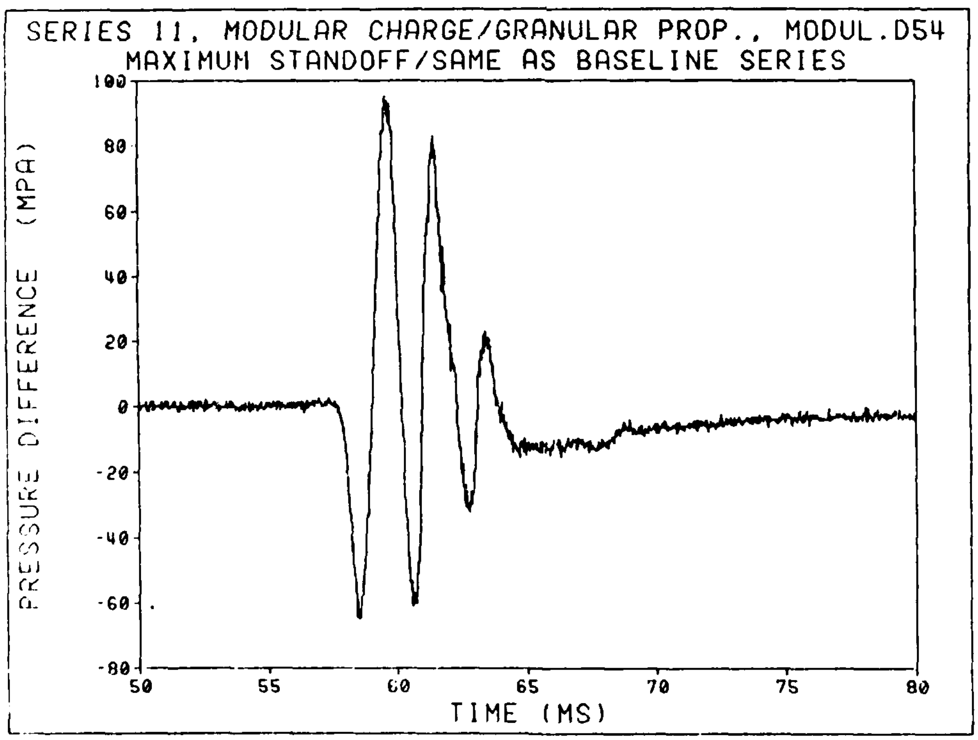
SERIES 11, MODULAR CHARGE/GRANULAR PROP., MODUL.D54
MAXIMUM STANDOFF/SAME AS BASELINE SERIES
PRESSURE DIFFERENCE (MPA)
TIME (MS)
100
80
60
40
20
0
-20
-40
-60
-80
50
55
60
65
70
75
80

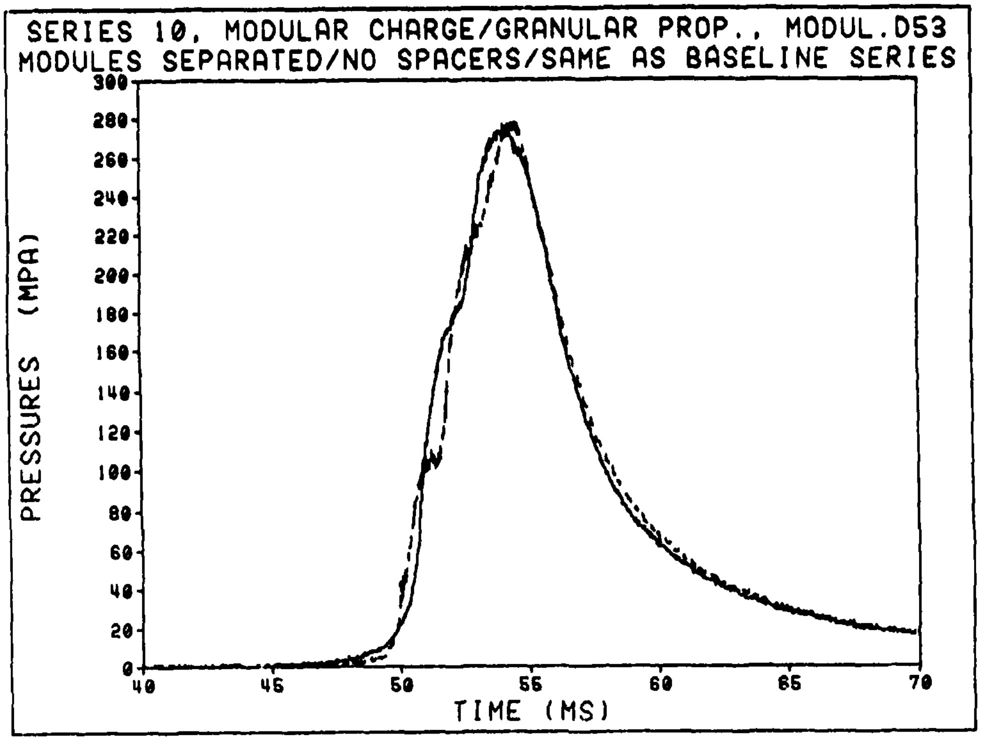
SERIES 10, MODULAR CHARGE/GRANULAR PROP., MODUL.D53
MODULES SEPARATED/NO SPACERS/SAME AS BASELINE SERIES
PRESSURES (MPA)
TIME (MS)
0
20
40
60
80
100
120
140
160
180
200
220
240
260
280
300
40
45
50
55
60
65
70

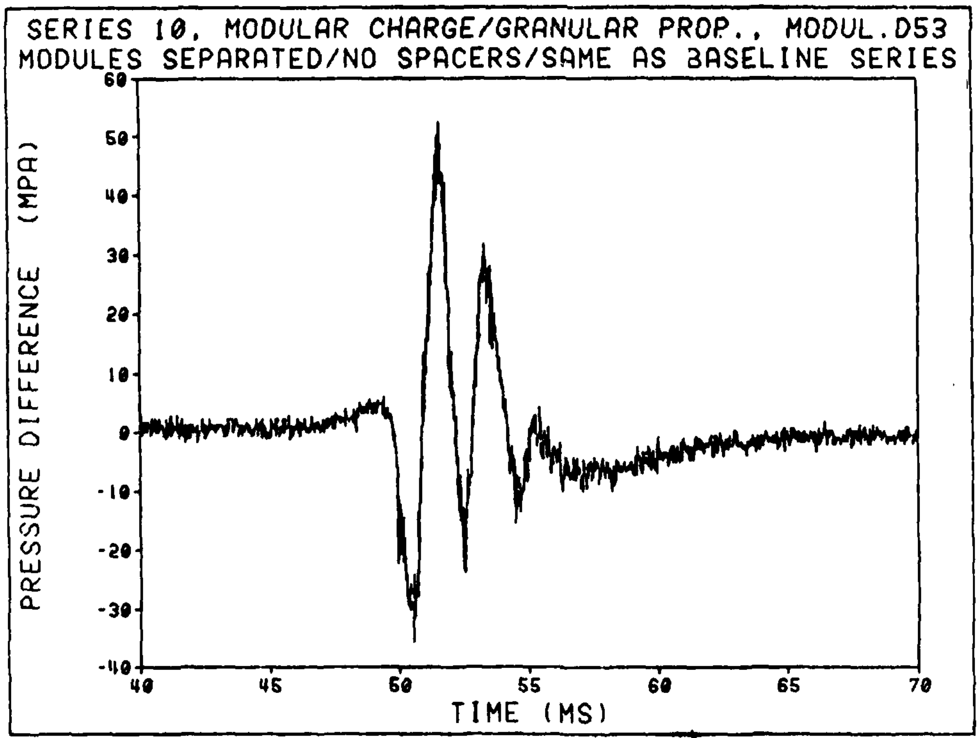
SERIES 10, MODULAR CHARGE/GRANULAR PROP., MODUL.D53
MODULES SEPARATED/NO SPACERS/SAME AS BASELINE SERIES
PRESSURE DIFFERENCE (MPA)
TIME (MS)
-40
-30
-20
-10
0
10
20
30
40
50
60
40
45
50
55
60
65
70

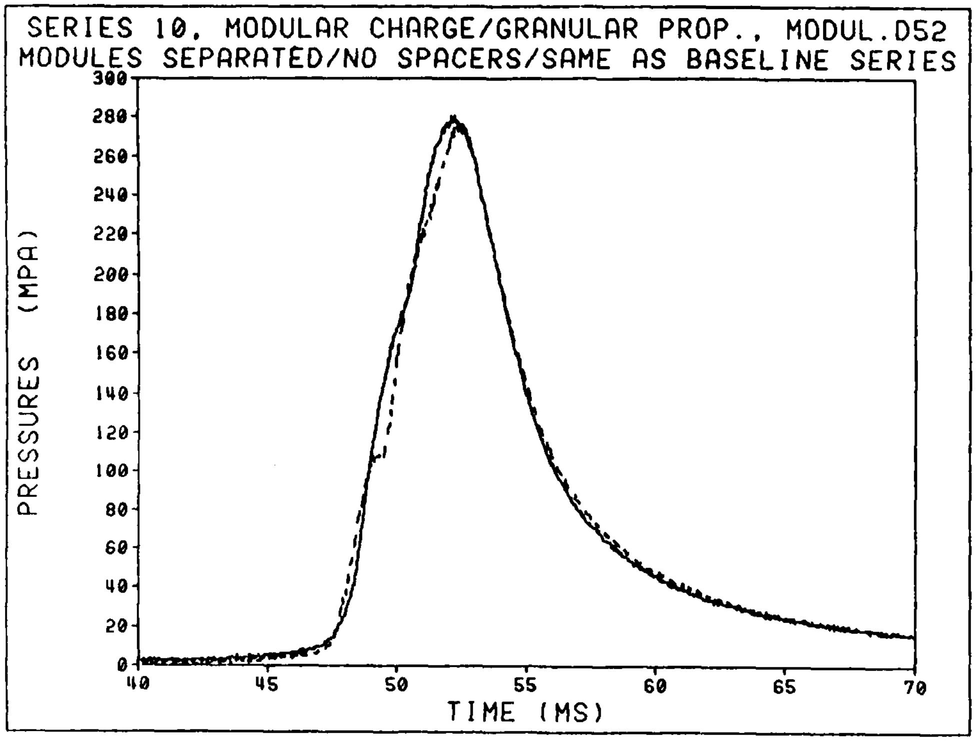
SERIES 10, MODULAR CHARGE/GRANULAR PROP., MODUL.D52
MODULES SEPARATED/NO SPACERS/SAME AS BASELINE SERIES
PRESSURES (MPA)
300
280
260
240
220
200
180
160
140
120
100
80
60
40
20
0
40
45
50
55
60
65
70
TIME (MS)

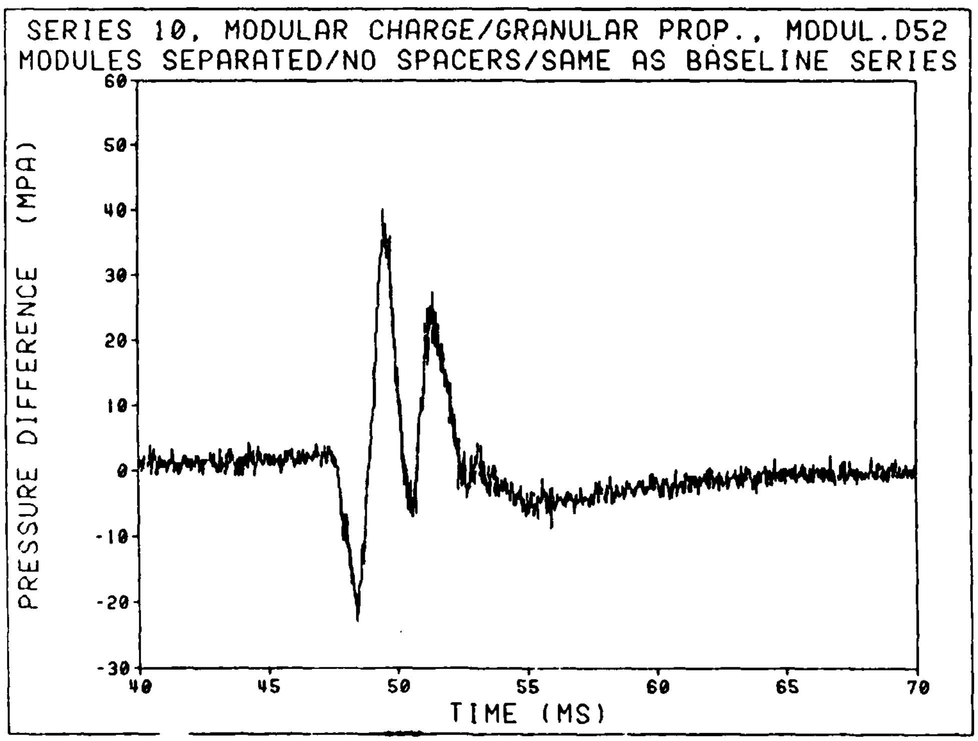
SERIES 10, MODULAR CHARGE/GRANULAR PROP., MODUL.D52
MODULES SEPARATED/NO SPACERS/SAME AS BASELINE SERIES
PRESSURE DIFFERENCE (MPA)
60
50
40
30
20
10
0
-10
-20
-30
40
45
50
55
60
65
70
TIME (MS)

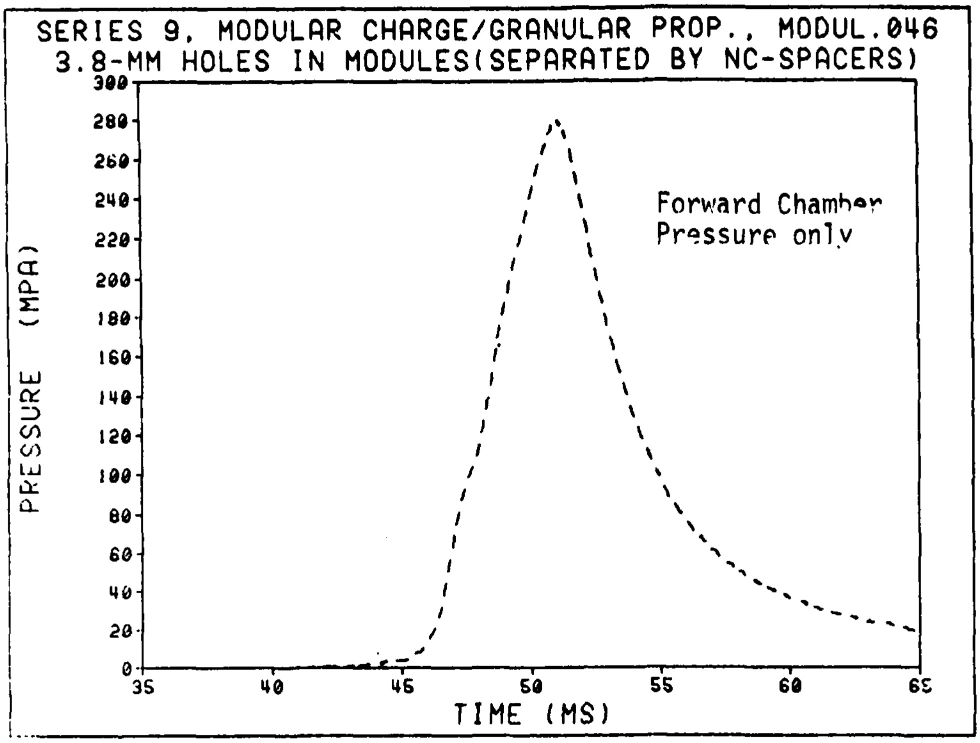

No Spindle Pressure---Therefore no Pressure
Difference could be calculated.

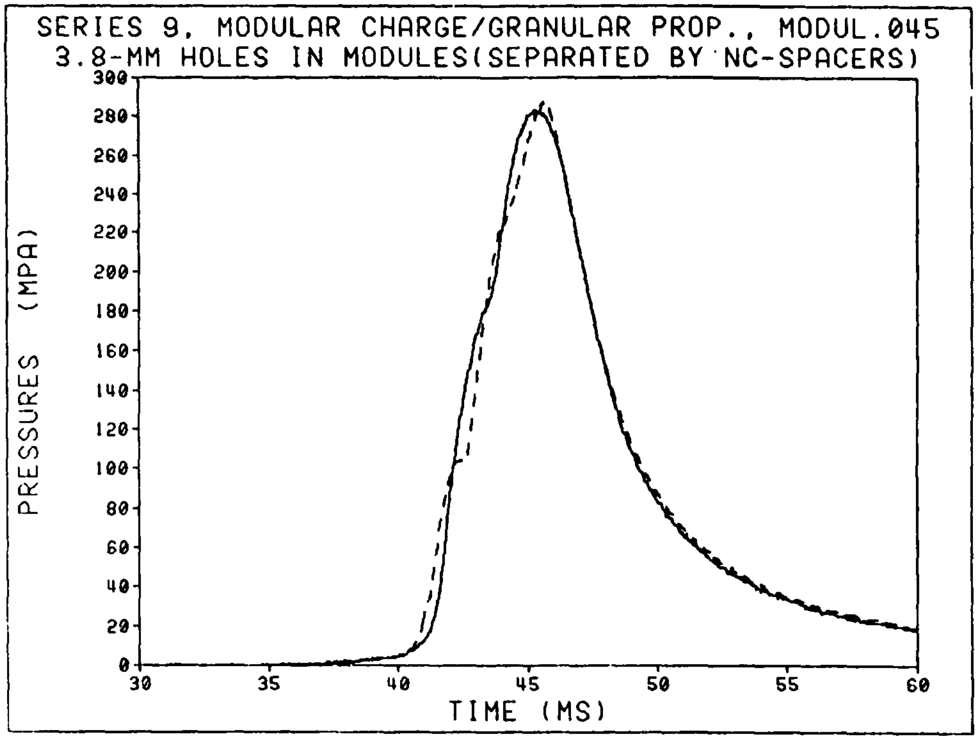
SERIES 9, MODULAR CHARGE/GRANULAR PROP., MODUL.045
3.8-MM HOLES IN MODULES(SEPARATED BY NC-SPACERS)
PRESSURES (MPA)
TIME (MS)
0
20
40
60
80
100
120
140
160
180
200
220
240
260
280
300
30
35
40
45
50
55
60

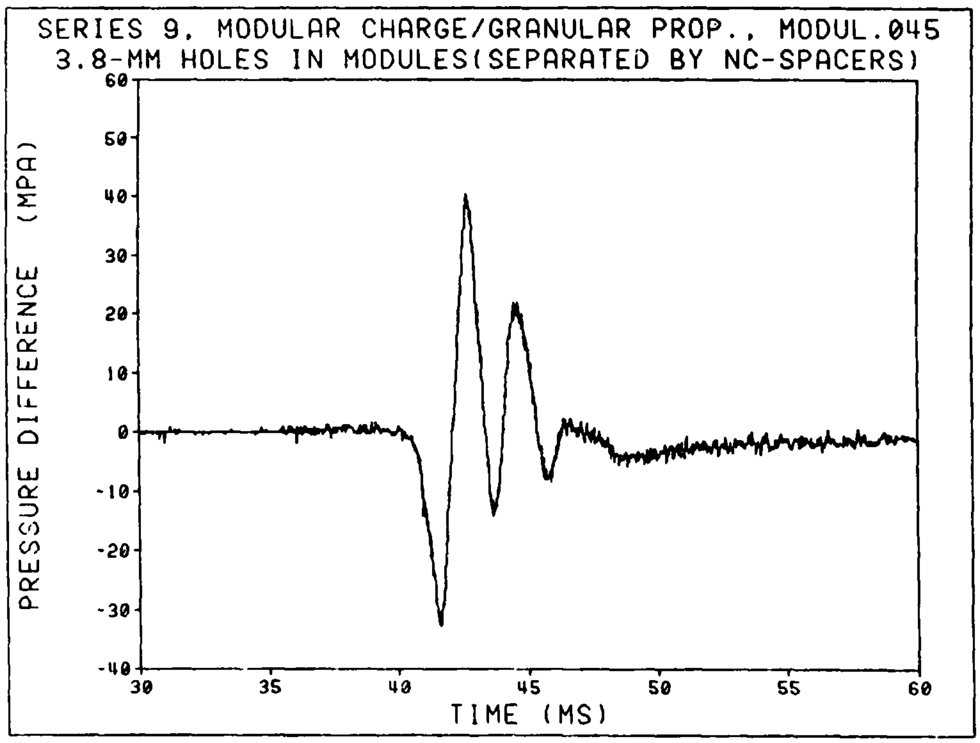
SERIES 9, MODULAR CHARGE/GRANULAR PROP., MODUL.045
3.8-MM HOLES IN MODULES(SEPARATED BY NC-SPACERS)
PRESSURE DIFFERENCE (MPA)
TIME (MS)
-40
-30
-20
-10
0
10
20
30
40
50
60
30
35
40
45
50
55
60

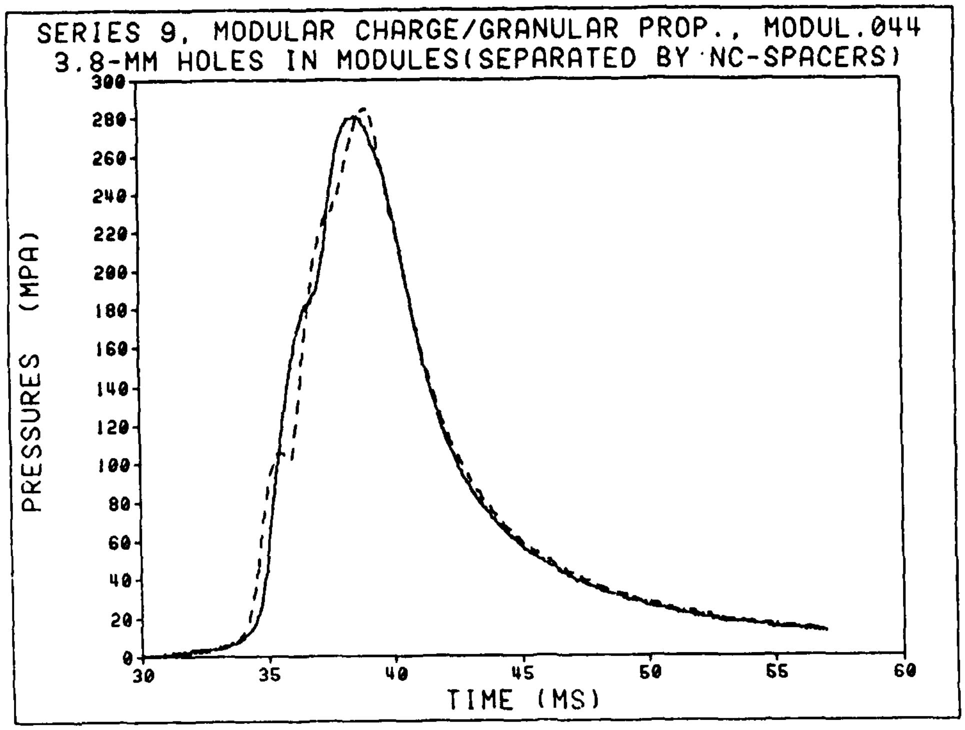
SERIES 9, MODULAR CHARGE/GRANULAR PROP., MODUL.044
3.8-MM HOLES IN MODULES(SEPARATED BY NC-SPACERS)
PRESSURES (MPA)
TIME (MS)

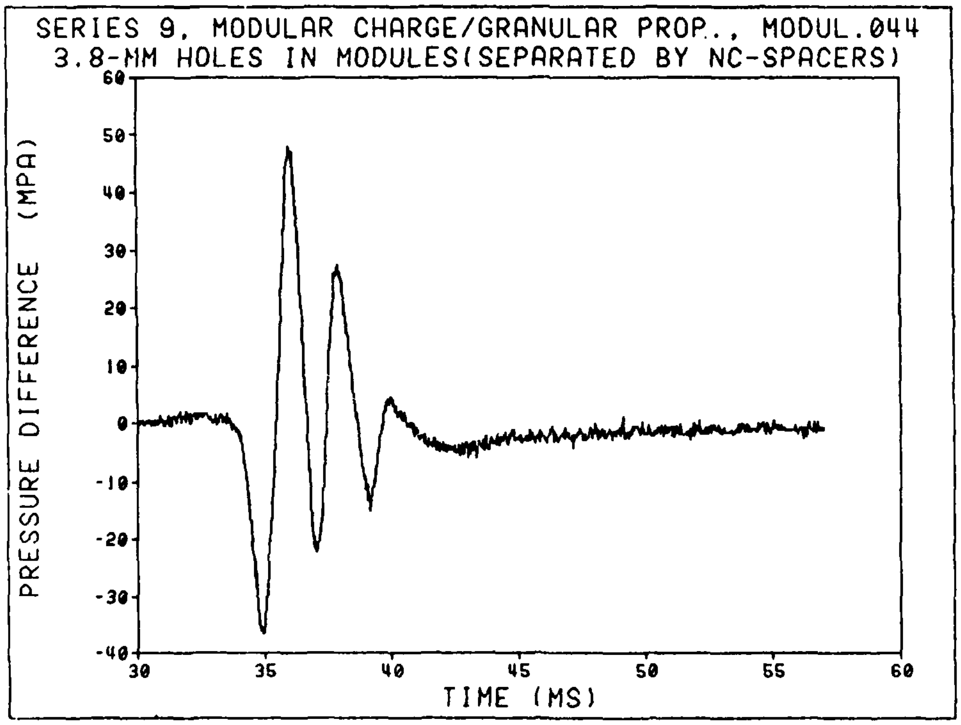
SERIES 9, MODULAR CHARGE/GRANULAR PROP., MODUL.044
3.8-MM HOLES IN MODULES(SEPARATED BY NC-SPACERS)
PRESSURE DIFFERENCE (MPA)
TIME (MS)

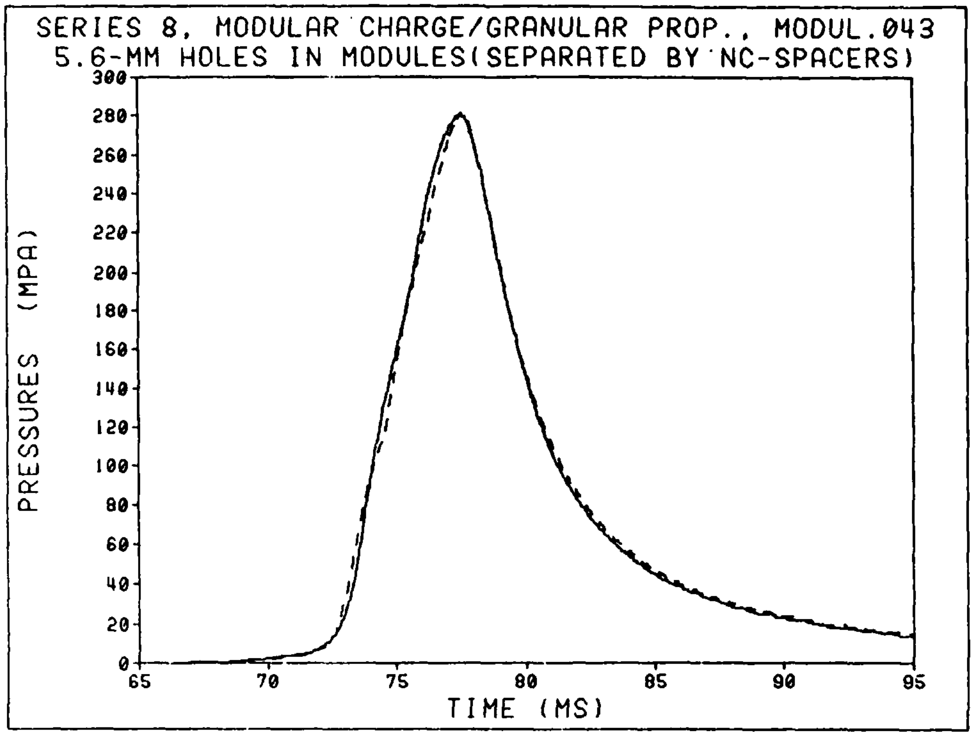
SERIES 8, MODULAR CHARGE/GRANULAR PROP., MODUL.043
5.6-MM HOLES IN MODULES(SEPARATED BY NC-SPACERS)
PRESSURES (MPA)
300
280
260
240
220
200
180
160
140
120
100
80
60
40
20
0
65
70
75
80
85
90
95
TIME (MS)

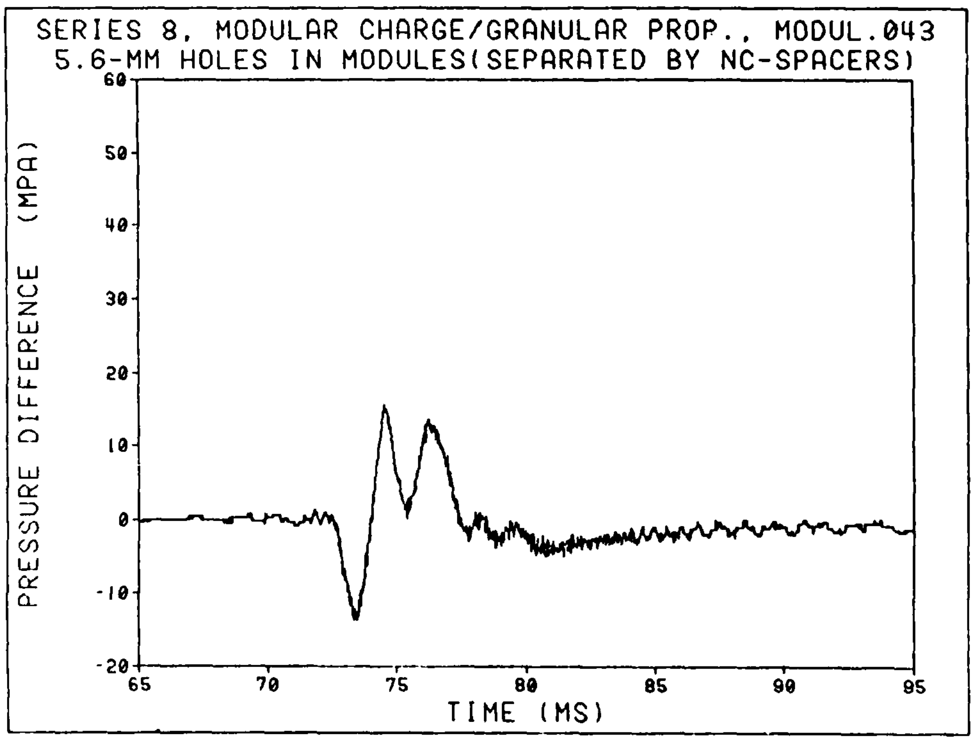
SERIES 8, MODULAR CHARGE/GRANULAR PROP., MODUL.043
5.6-MM HOLES IN MODULES(SEPARATED BY NC-SPACERS)
PRESSURE DIFFERENCE (MPA)
60
50
40
30
20
10
0
-10
-20
65
70
75
80
85
90
95
TIME (MS)

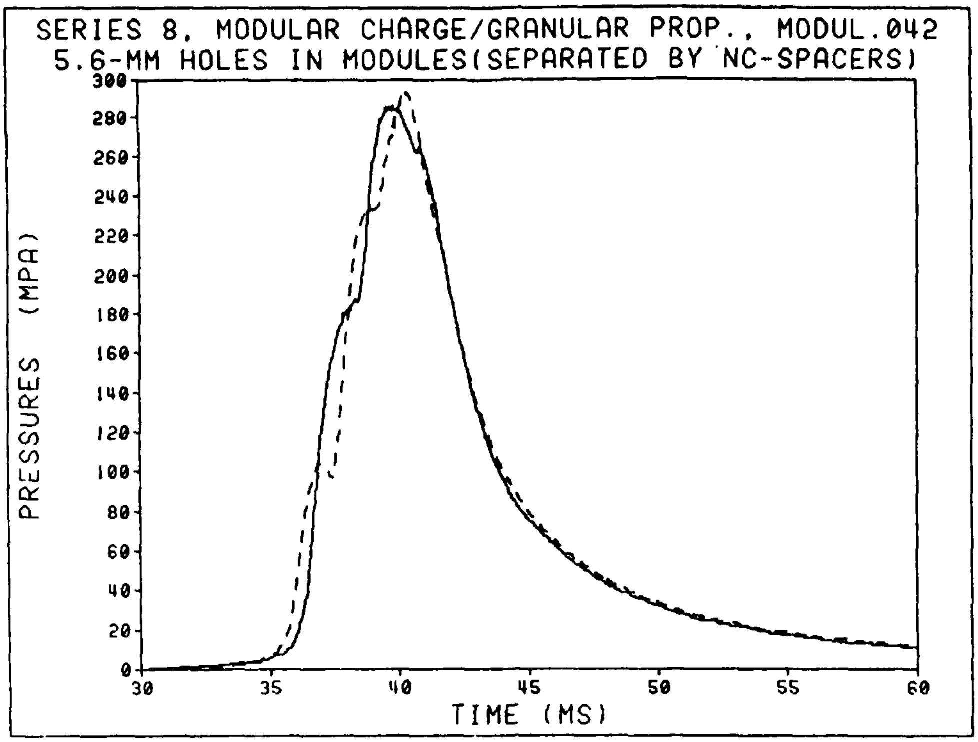
SERIES 8, MODULAR CHARGE/GRANULAR PROP., MODUL.042
5.6-MM HOLES IN MODULES(SEPARATED BY NC-SPACERS)
PRESSURES (MPA)
300
280
260
240
220
200
180
160
140
120
100
80
60
40
20
0
30
35
40
45
50
55
60
TIME (MS)

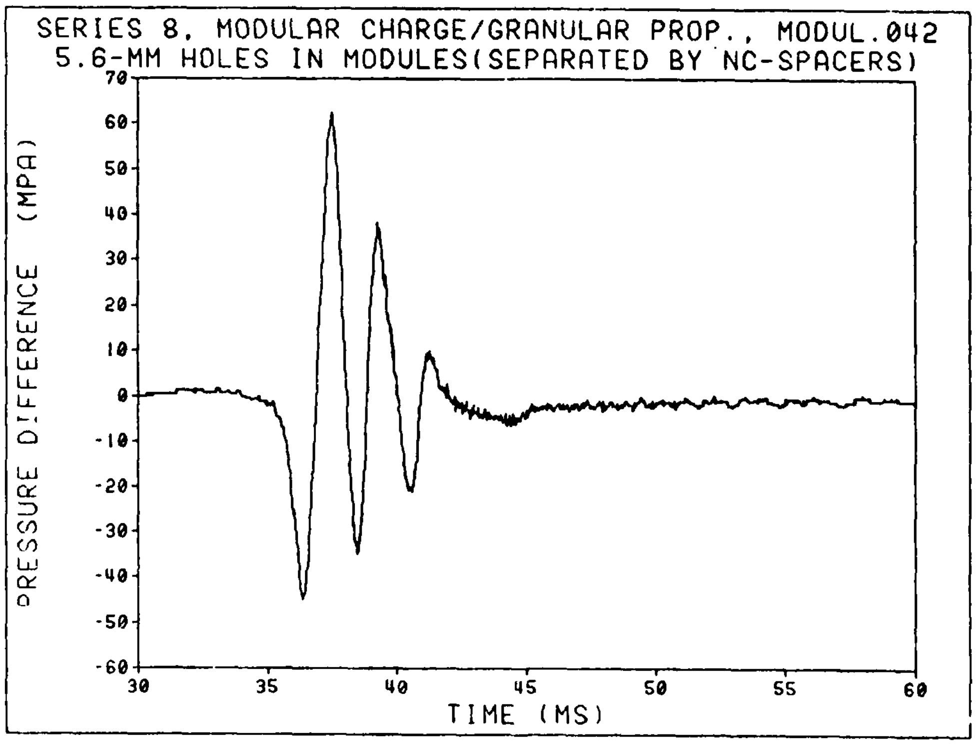
SERIES 8, MODULAR CHARGE/GRANULAR PROP., MODUL.042
5.6-MM HOLES IN MODULES(SEPARATED BY NC-SPACERS)
PRESSURE DIFFERENCE (MPA)
70
60
50
40
30
20
10
0
-10
-20
-30
-40
-50
-60
30
35
40
45
50
55
60
TIME (MS)

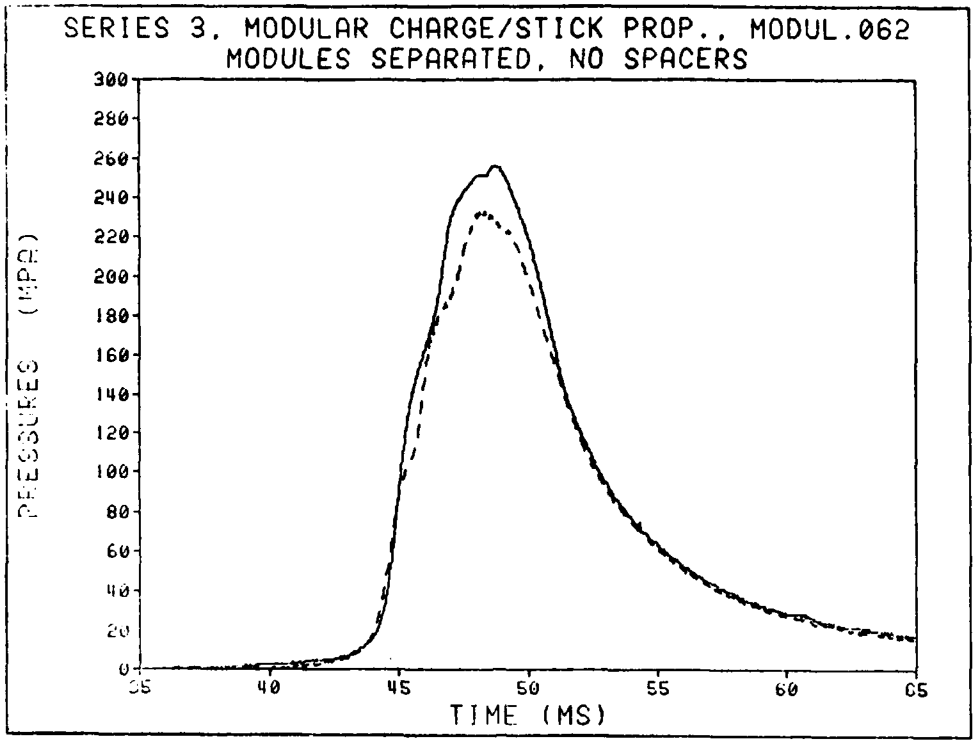
SERIES 3, MODULAR CHARGE/STICK PROP., MODUL.062
MODULES SEPARATED, NO SPACERS
PRESSURES (MPA)
TIME (MS)

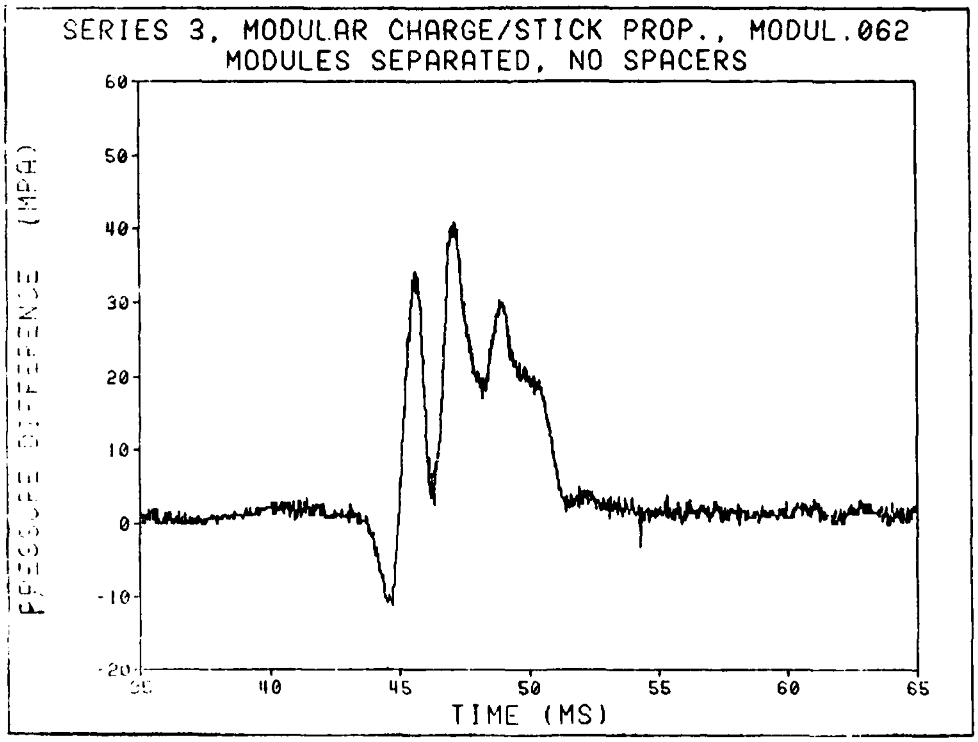
SERIES 3, MODULAR CHARGE/STICK PROP., MODUL.062
MODULES SEPARATED, NO SPACERS
PRESSURE DIFFERENCE (MPA)
TIME (MS)

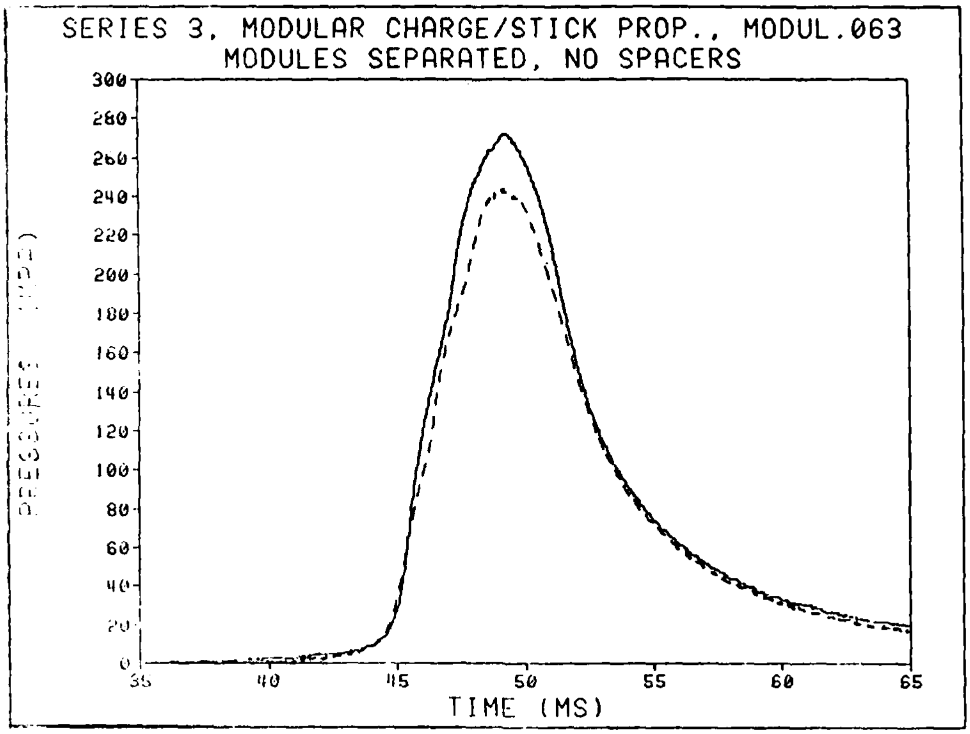
SERIES 3, MODULAR CHARGE/STICK PROP., MODUL.063
MODULES SEPARATED, NO SPACERS
PRESSURES (MPA)
TIME (MS)

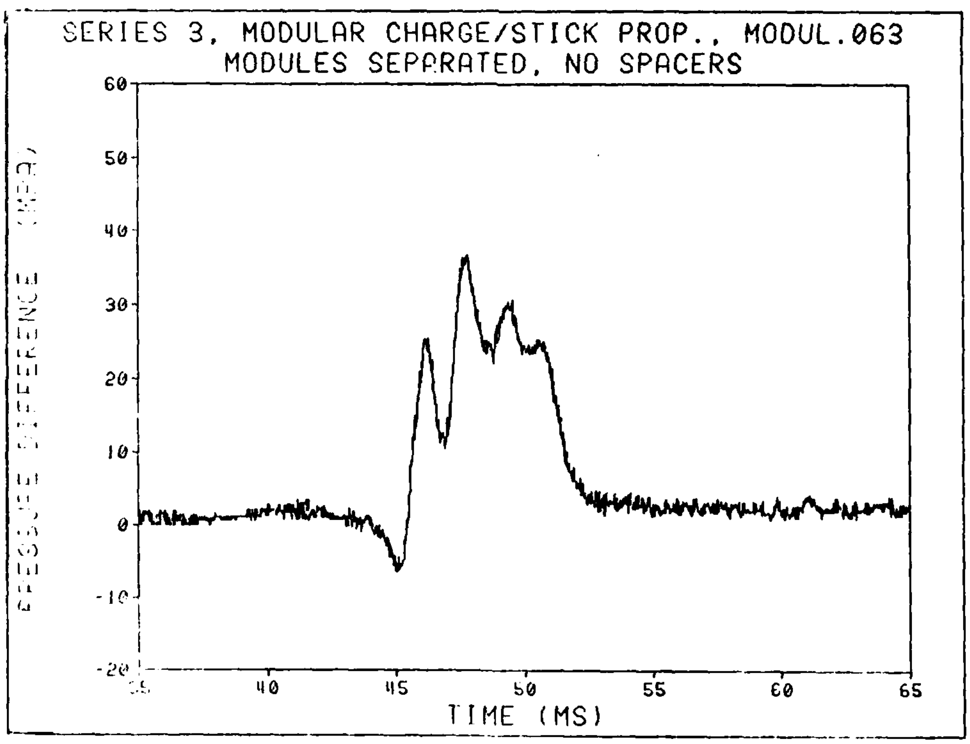
SERIES 3, MODULAR CHARGE/STICK PROP., MODUL.063
MODULES SEPARATED, NO SPACERS
PRESSURE DIFFERENCE (MPA)
TIME (MS)

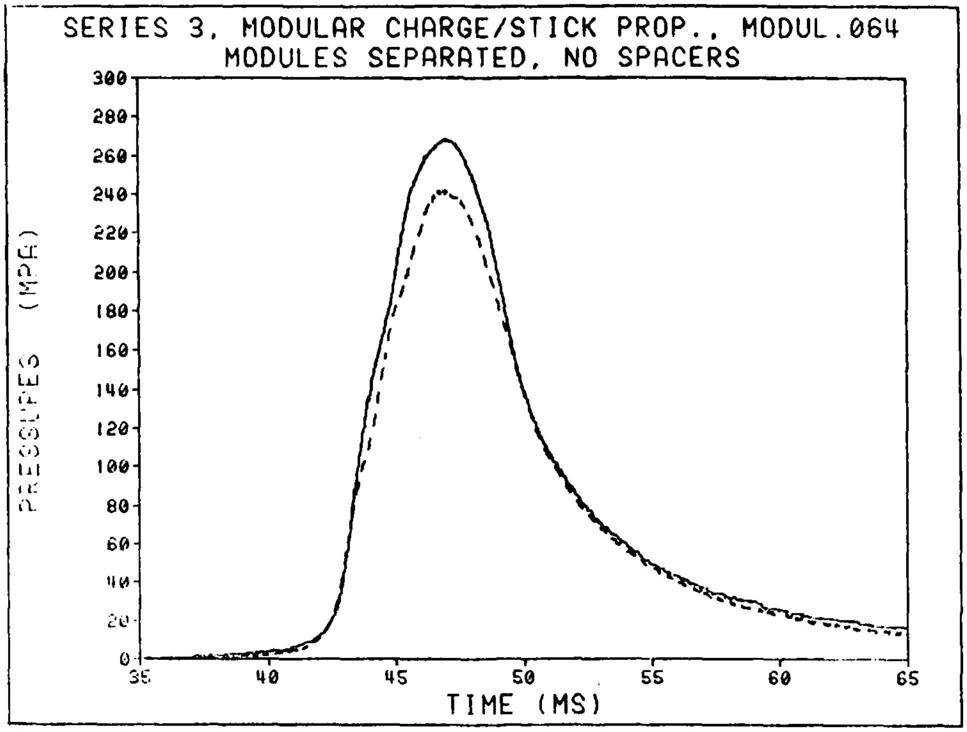
SERIES 3, MODULAR CHARGE/STICK PROP., MODUL.064
MODULES SEPARATED, NO SPACERS
PRESSURES (MPA)
TIME (MS)

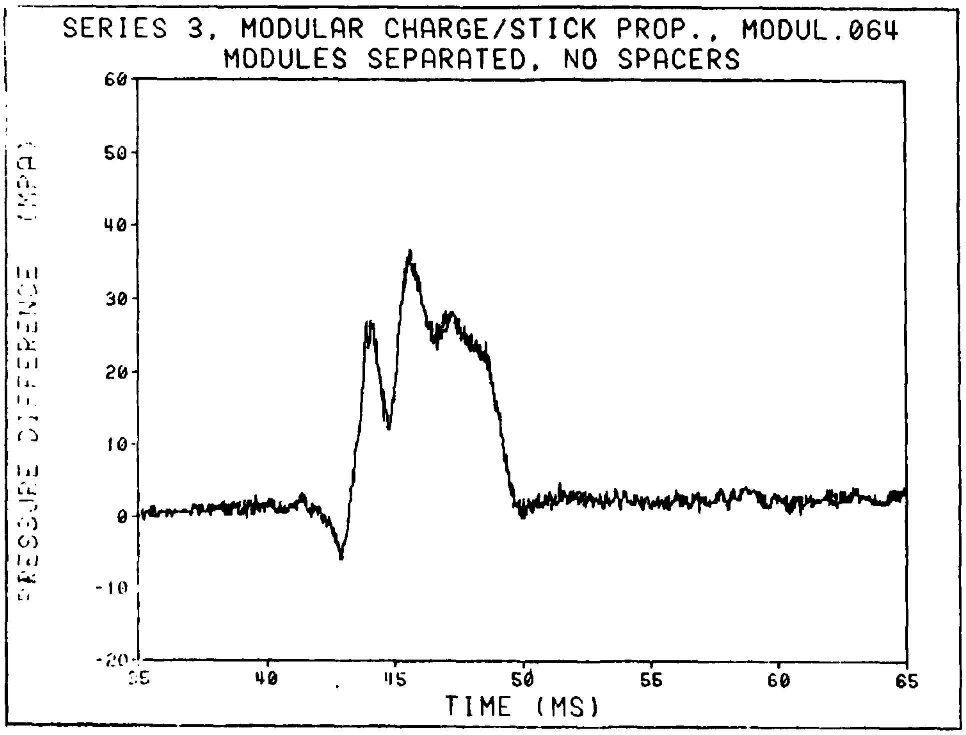
SERIES 3, MODULAR CHARGE/STICK PROP., MODUL.064
MODULES SEPARATED, NO SPACERS
PRESSURE DIFFERENCE (MPA)
TIME (MS)

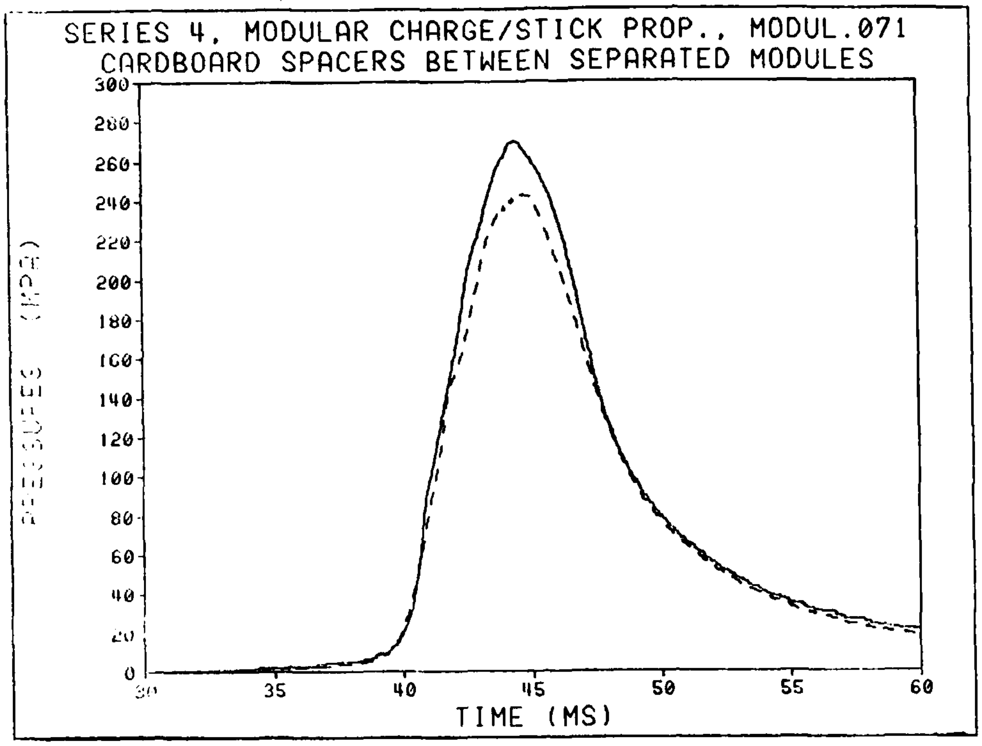
SERIES 4, MODULAR CHARGE/STICK PROP., MODUL.071
CARDBOARD SPACERS BETWEEN SEPARATED MODULES
PRESSURES (MPa)
TIME (MS)
0
20
40
60
80
100
120
140
160
180
200
220
240
260
280
300
30
35
40
45
50
55
60

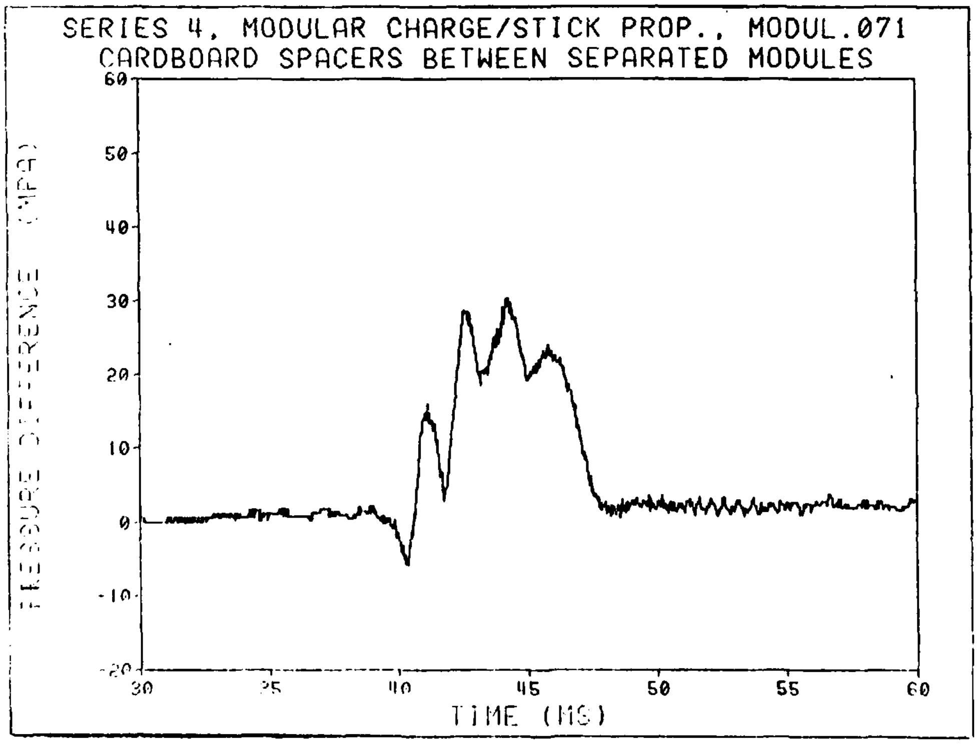
SERIES 4, MODULAR CHARGE/STICK PROP., MODUL.071
CARDBOARD SPACERS BETWEEN SEPARATED MODULES
PRESSURE DIFFERENCE (MPa)
TIME (MS)
-20
-10
0
10
20
30
40
50
60
30
35
40
45
50
55
60

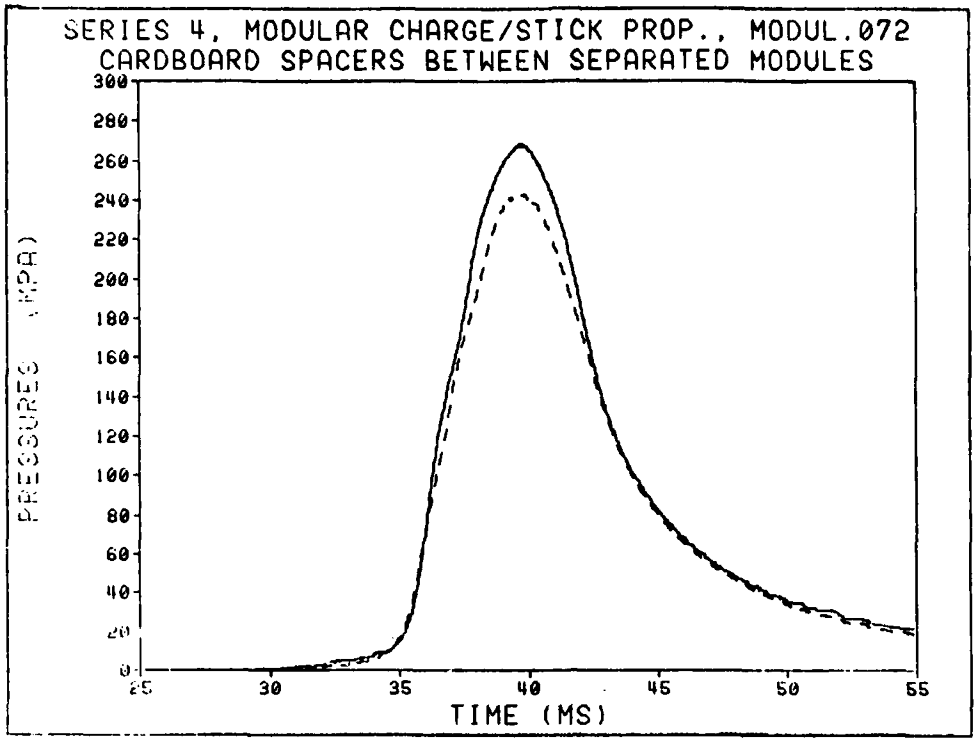
SERIES 4, MODULAR CHARGE/STICK PROP., MODUL.072
CARDBOARD SPACERS BETWEEN SEPARATED MODULES
PRESSURES (MPA)
TIME (MS)

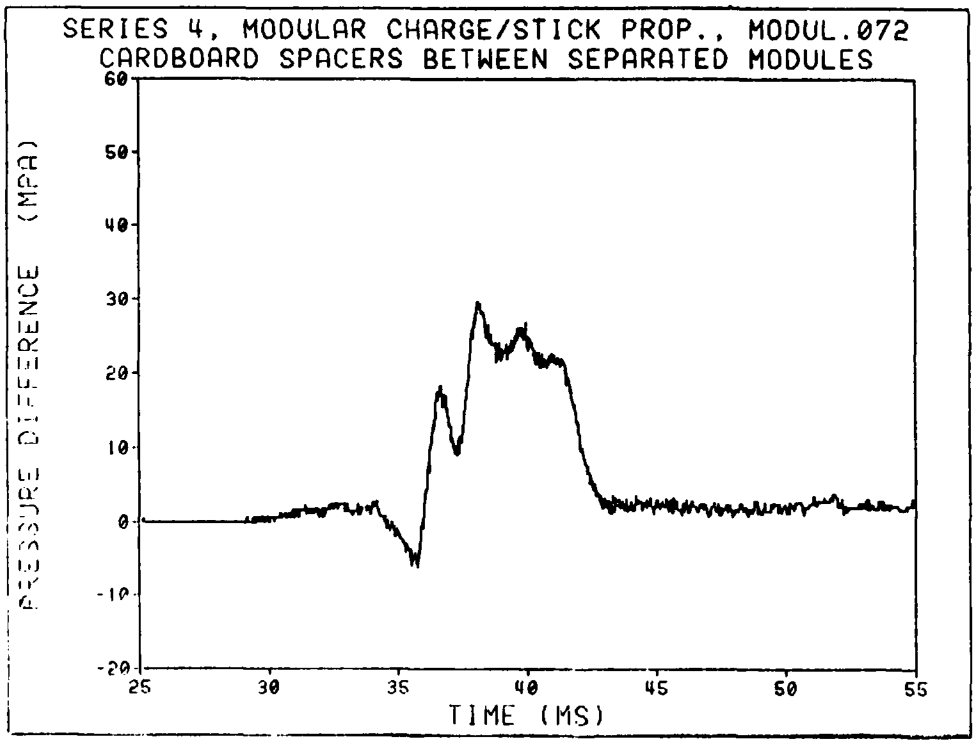
SERIES 4, MODULAR CHARGE/STICK PROP., MODUL.072
CARDBOARD SPACERS BETWEEN SEPARATED MODULES
PRESSURE DIFFERENCE (MPA)
TIME (MS)

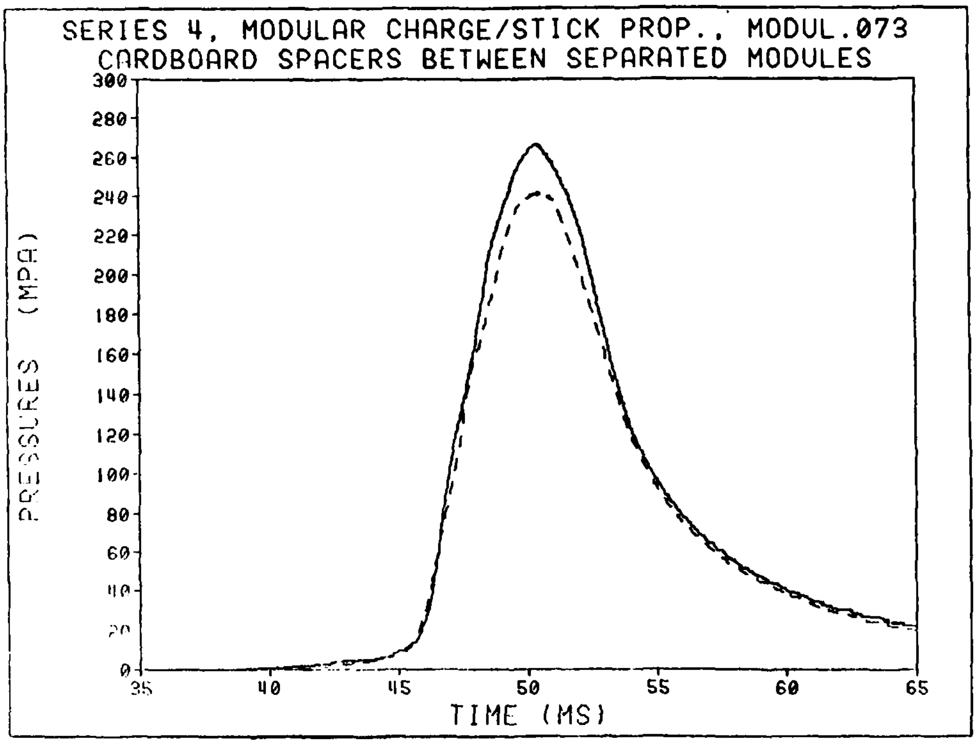
SERIES 4, MODULAR CHARGE/STICK PROP., MODUL.073
CARDBOARD SPACERS BETWEEN SEPARATED MODULES
PRESSURES (MPA)
TIME (MS)

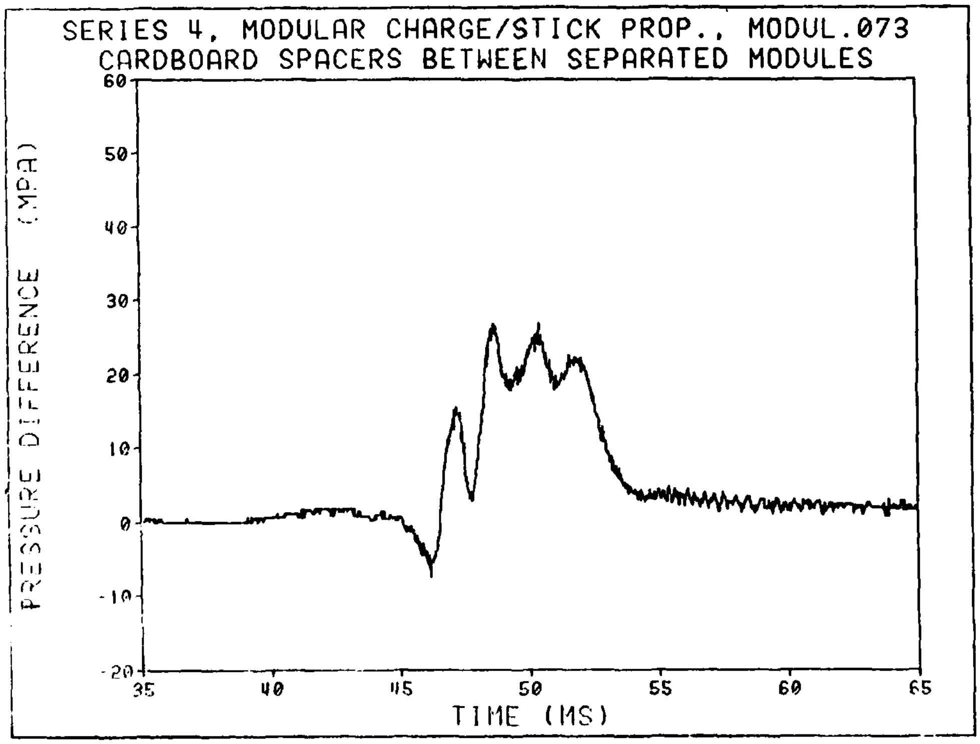
SERIES 4, MODULAR CHARGE/STICK PROP., MODUL.073
CARDBOARD SPACERS BETWEEN SEPARATED MODULES
PRESSURE DIFFERENCE (MPA)
TIME (MS)

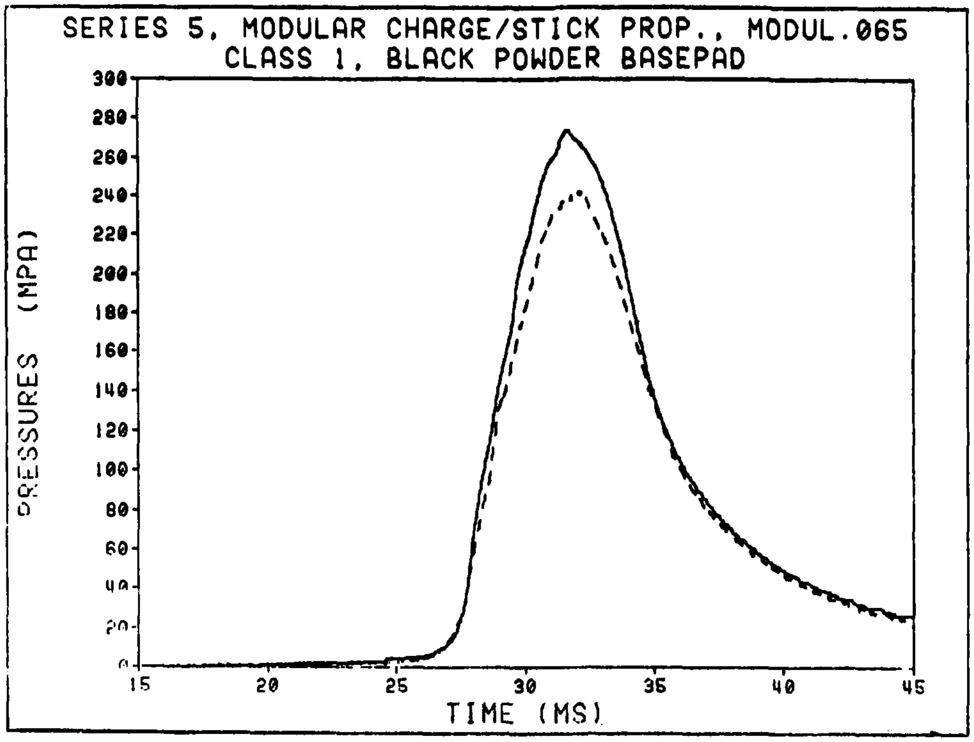
SERIES 5, MODULAR CHARGE/STICK PROP., MODUL.065
CLASS 1, BLACK POWDER BASEPAD
PRESSURES (MPA)
TIME (MS)

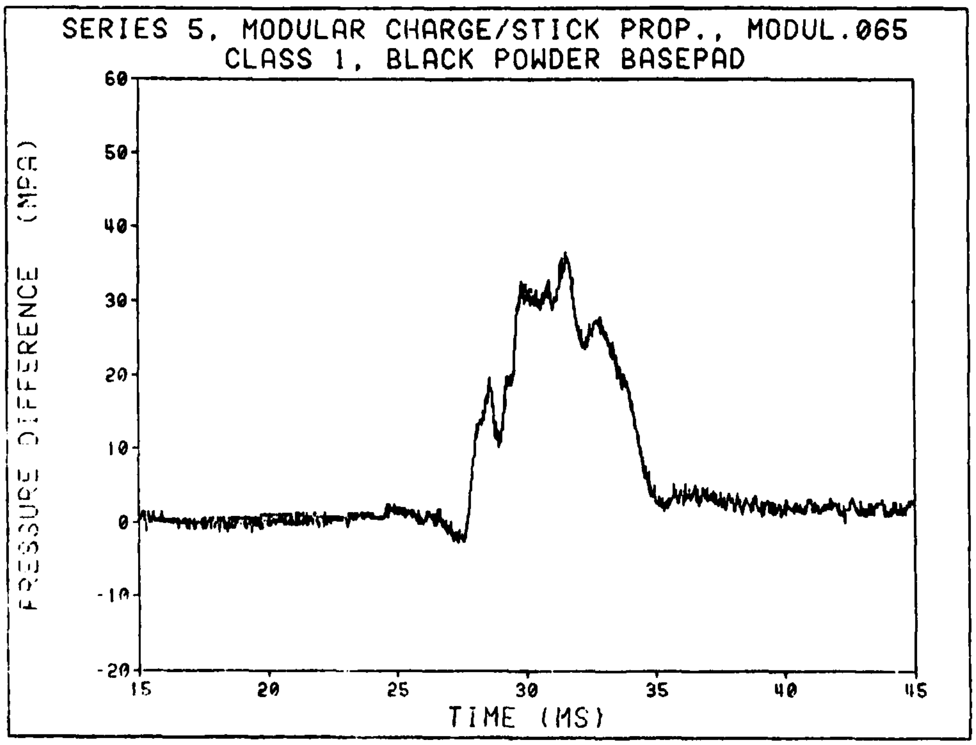
SERIES 5, MODULAR CHARGE/STICK PROP., MODUL.065
CLASS 1, BLACK POWDER BASEPAD
PRESSURE DIFFERENCE (MPA)
TIME (MS)

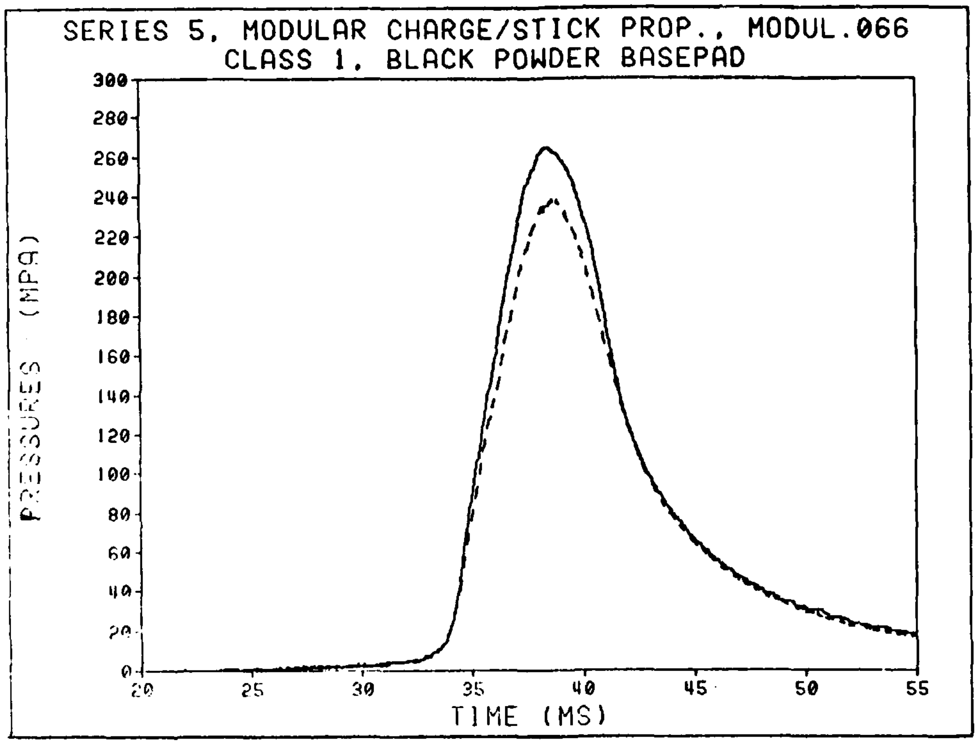
SERIES 5, MODULAR CHARGE/STICK PROP., MODUL.066
CLASS 1, BLACK POWDER BASEPAD
PRESSURES (MPA)
TIME (MS)

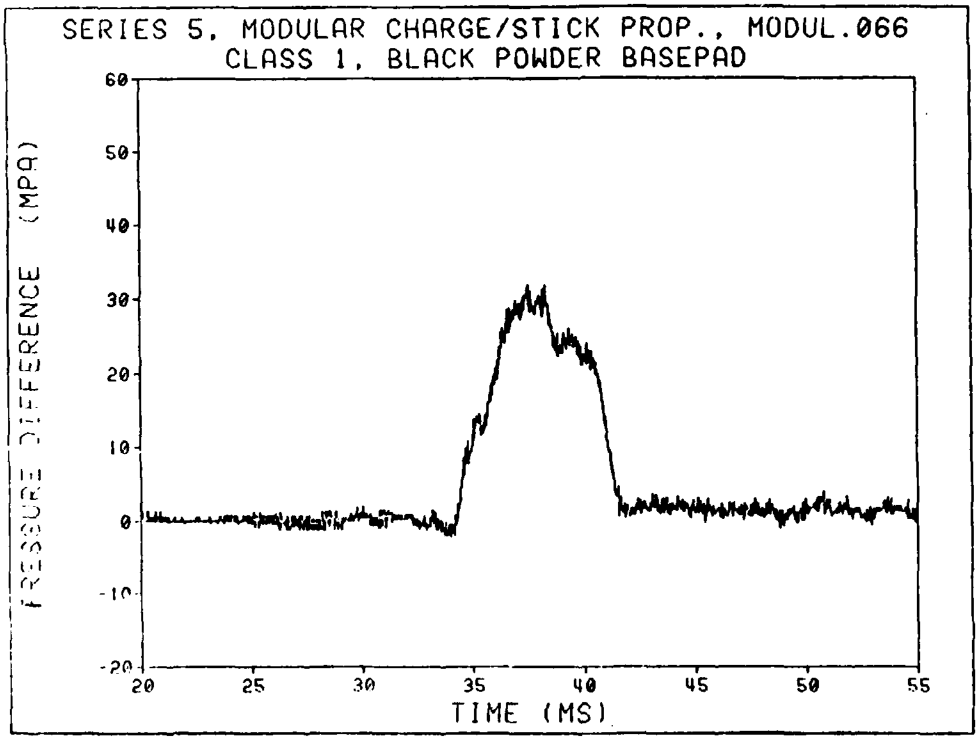
SERIES 5, MODULAR CHARGE/STICK PROP., MODUL.066
CLASS 1, BLACK POWDER BASEPAD
PRESSURE DIFFERENCE (MPA)
TIME (MS)

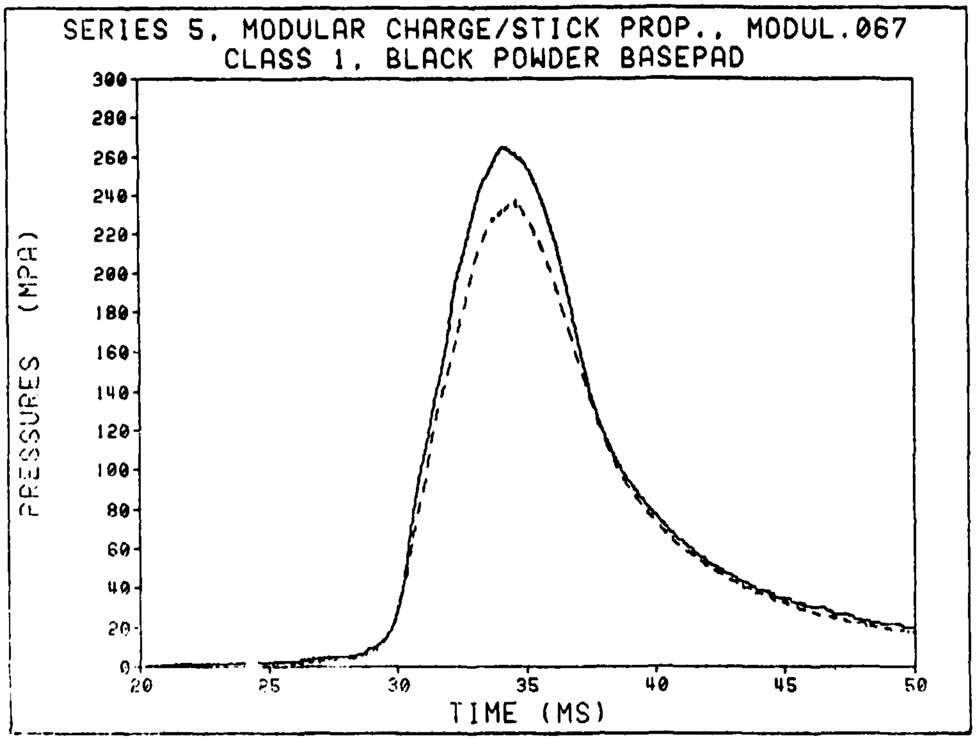

SERIES 5, MODULAR CHARGE/STICK PROP., MODUL.067
CLASS 1, BLACK POWDER BASEPAD
PRESSURES (MPA)
TIME (MS)

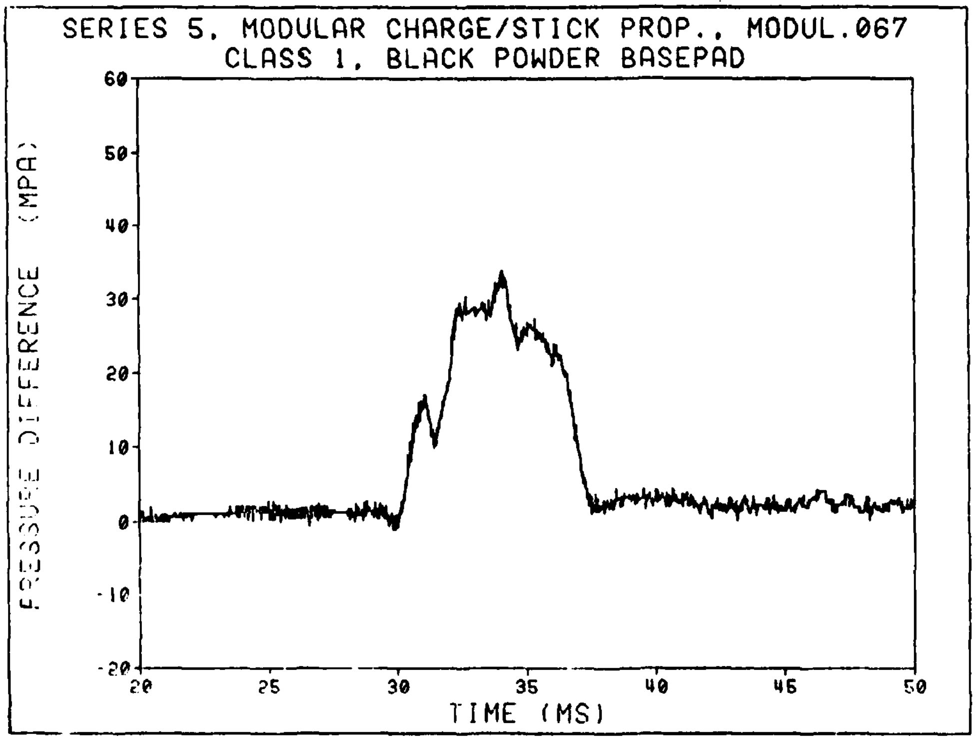

SERIES 5, MODULAR CHARGE/STICK PROP., MODUL.067
CLASS 1, BLACK POWDER BASEPAD
PRESSURE DIFFERENCE (MPA)
TIME (MS)

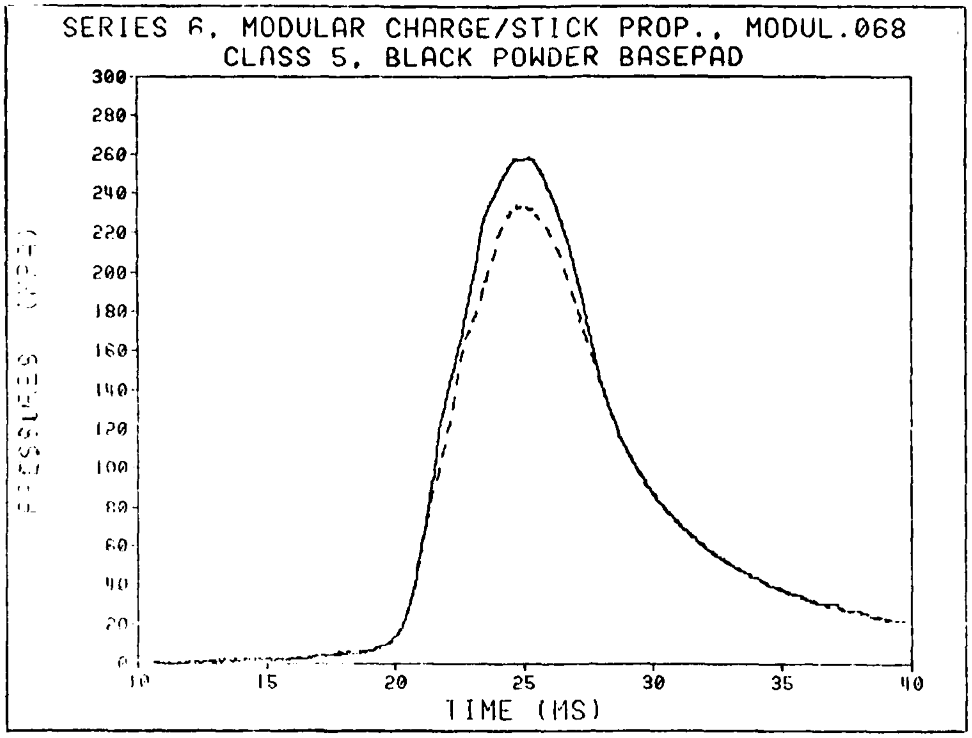
SERIES 6, MODULAR CHARGE/STICK PROP., MODUL.068
CLASS 5, BLACK POWDER BASEPAD
PRESSURES (MPA)
TIME (MS)

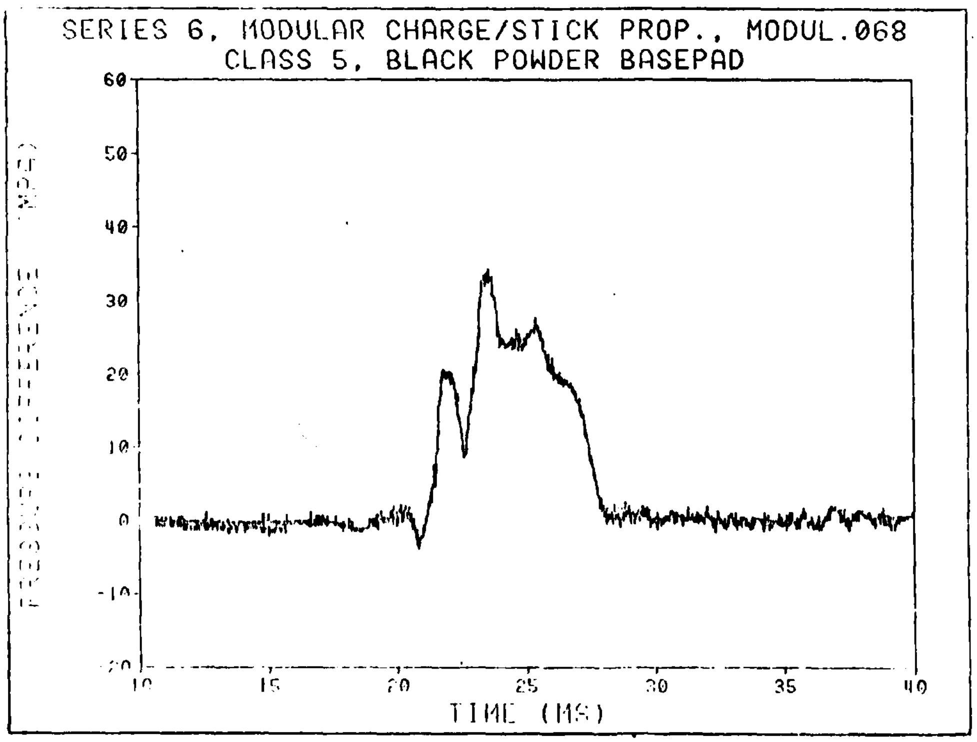
SERIES 6, MODULAR CHARGE/STICK PROP., MODUL.068
CLASS 5, BLACK POWDER BASEPAD
PRESSURE DIFFERENCE (MPA)
TIME (MS)

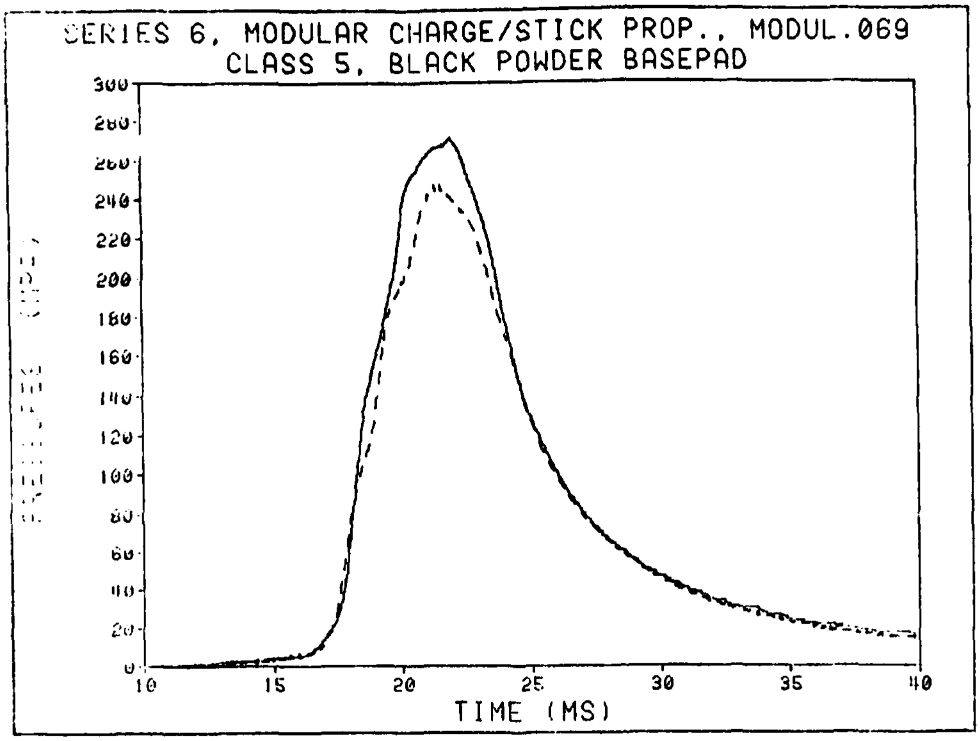
SERIES 6, MODULAR CHARGE/STICK PROP., MODUL.069
CLASS 5, BLACK POWDER BASEPAD
TIME (MS)

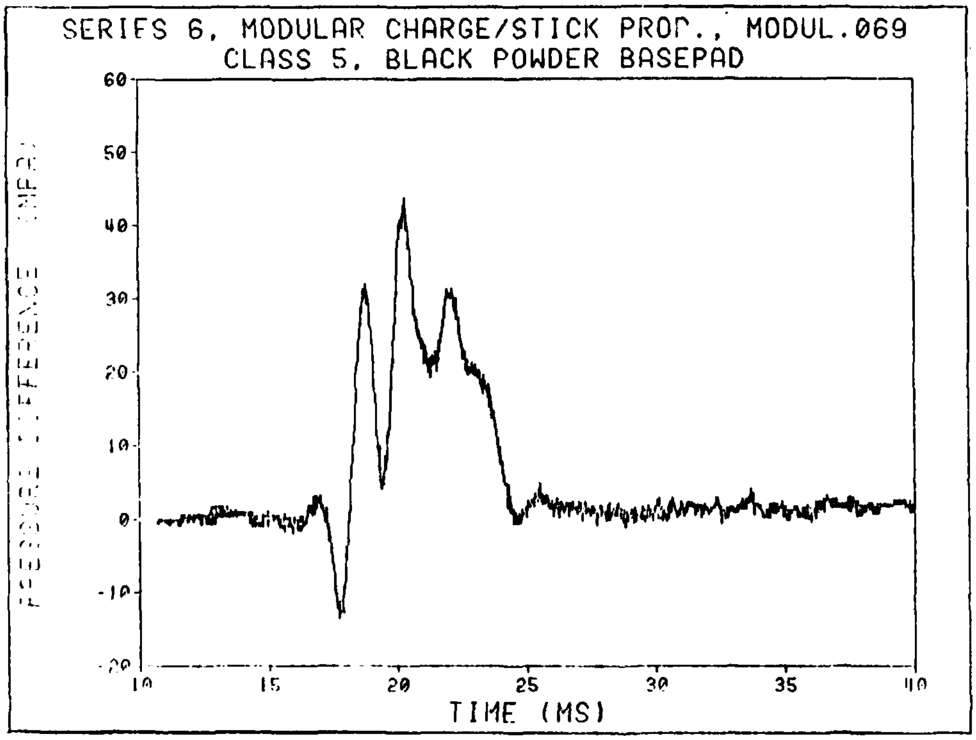
SERIES 6, MODULAR CHARGE/STICK PROP., MODUL.069
CLASS 5, BLACK POWDER BASEPAD
TIME (MS)

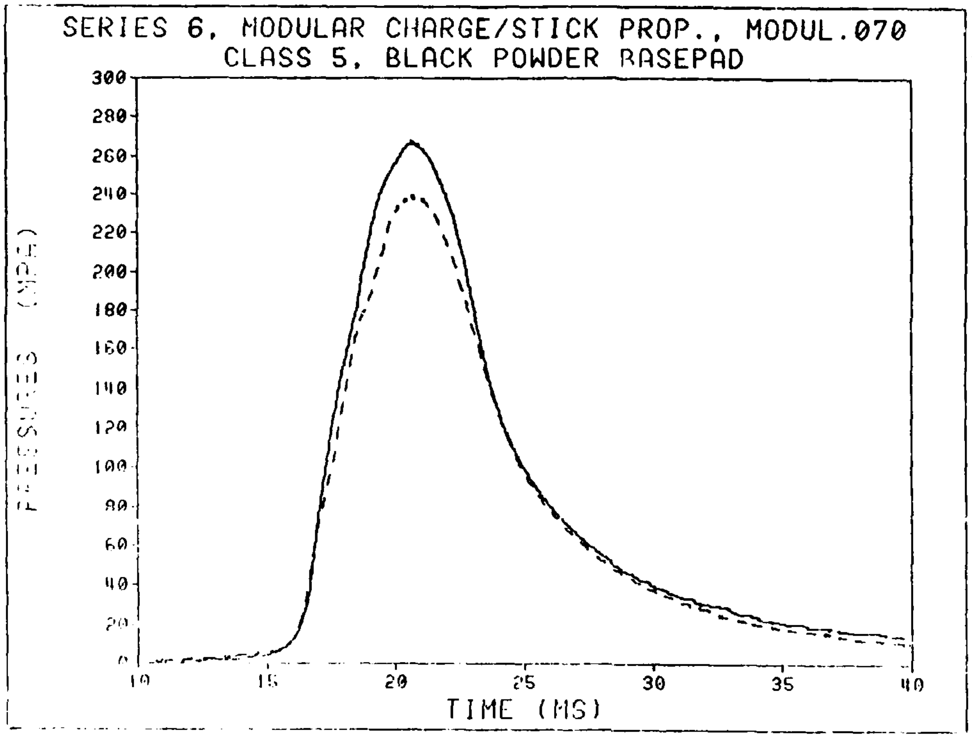
SERIES 6, MODULAR CHARGE/STICK PROP., MODUL.070
CLASS 5, BLACK POWDER BASEPAD
PRESSURES (MPA)
TIME (MS)

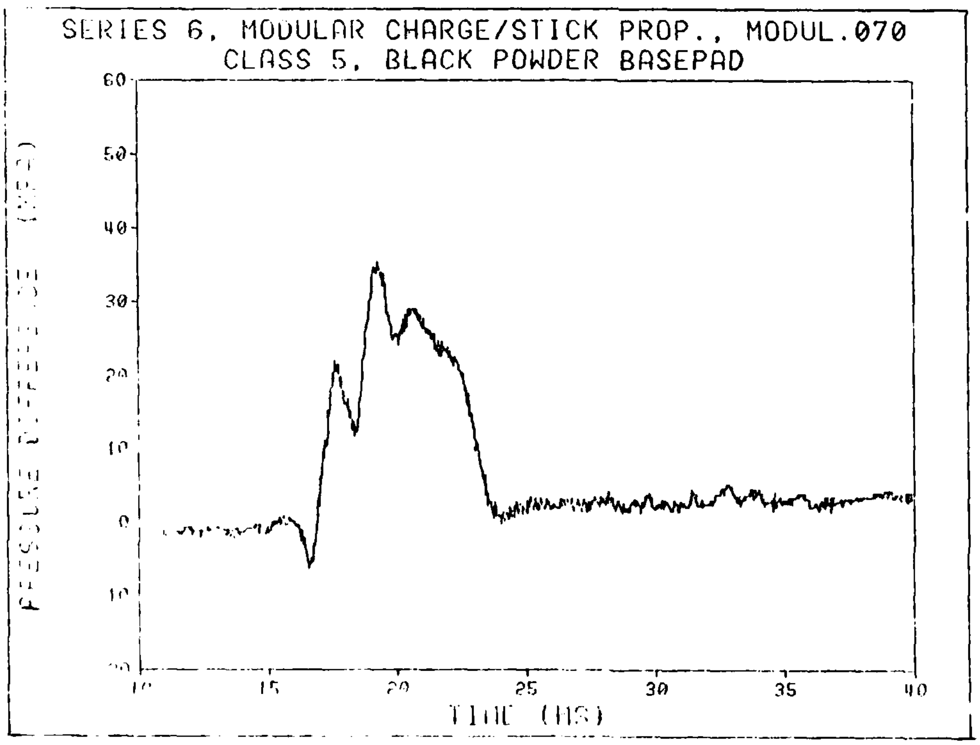
SERIES 6, MODULAR CHARGE/STICK PROP., MODUL.070
CLASS 5, BLACK POWDER BASEPAD
TIME (MS)

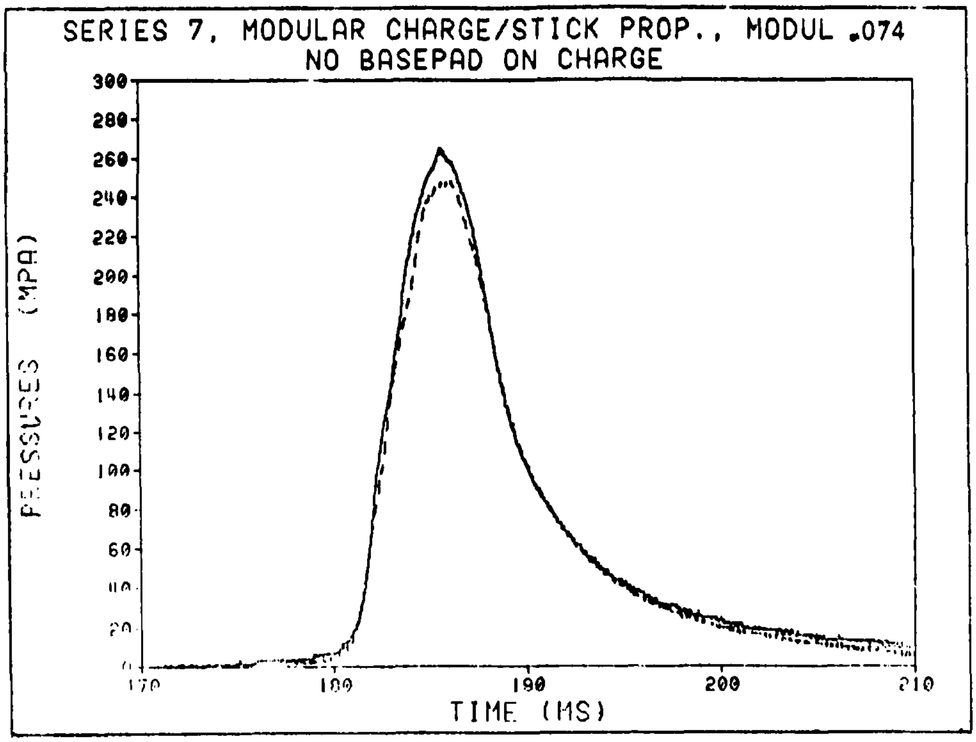
SERIES 7, MODULAR CHARGE/STICK PROP., MODUL .074
NO BASEPAD ON CHARGE
PRESSURES (MPA)
TIME (MS)

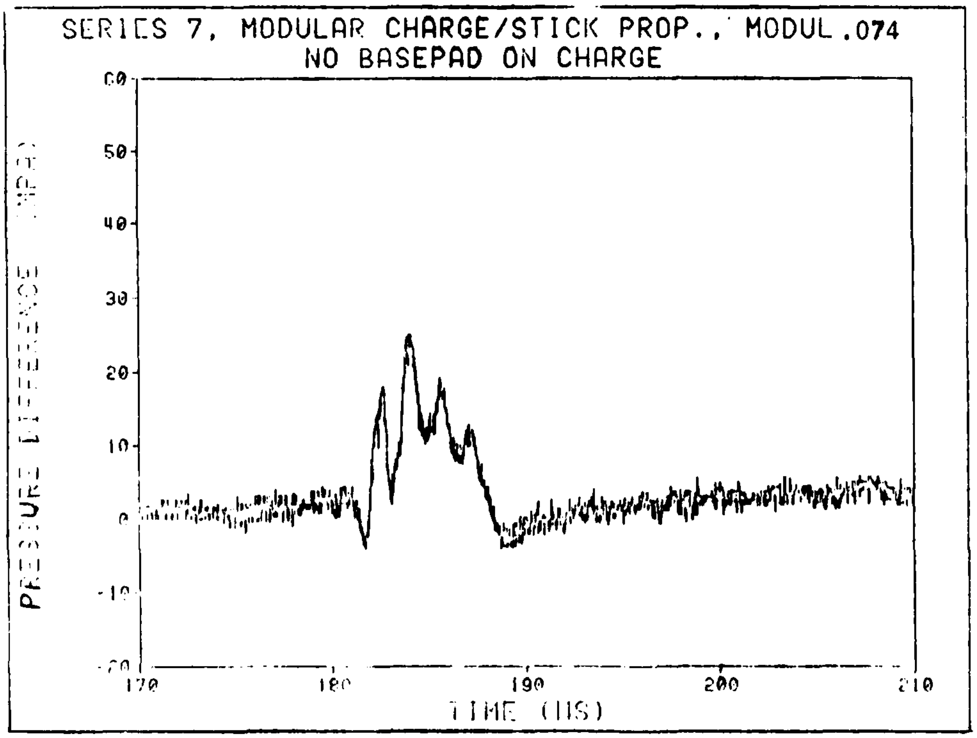
SERIES 7, MODULAR CHARGE/STICK PROP., MODUL .074
NO BASEPAD ON CHARGE
PRESSURE DIFFERENCE (MPA)
TIME (MS)

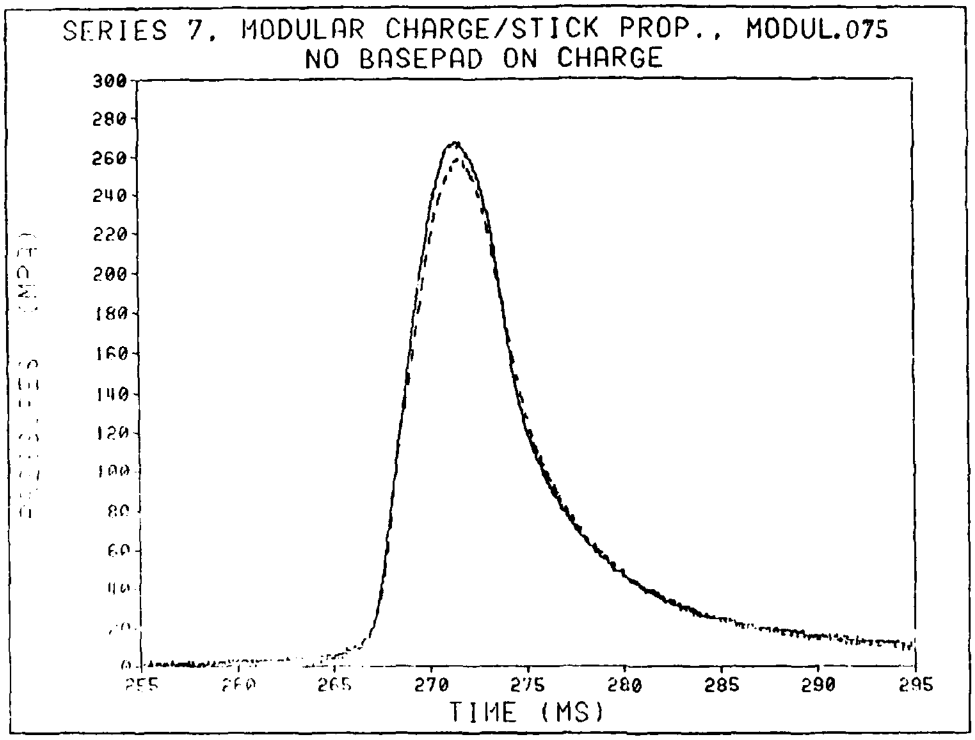
SERIES 7, MODULAR CHARGE/STICK PROP., MODUL.075
NO BASEPAD ON CHARGE
300
280
260
240
220
200
180
160
140
120
100
270
275
280
285
290
295
TIME (MS)

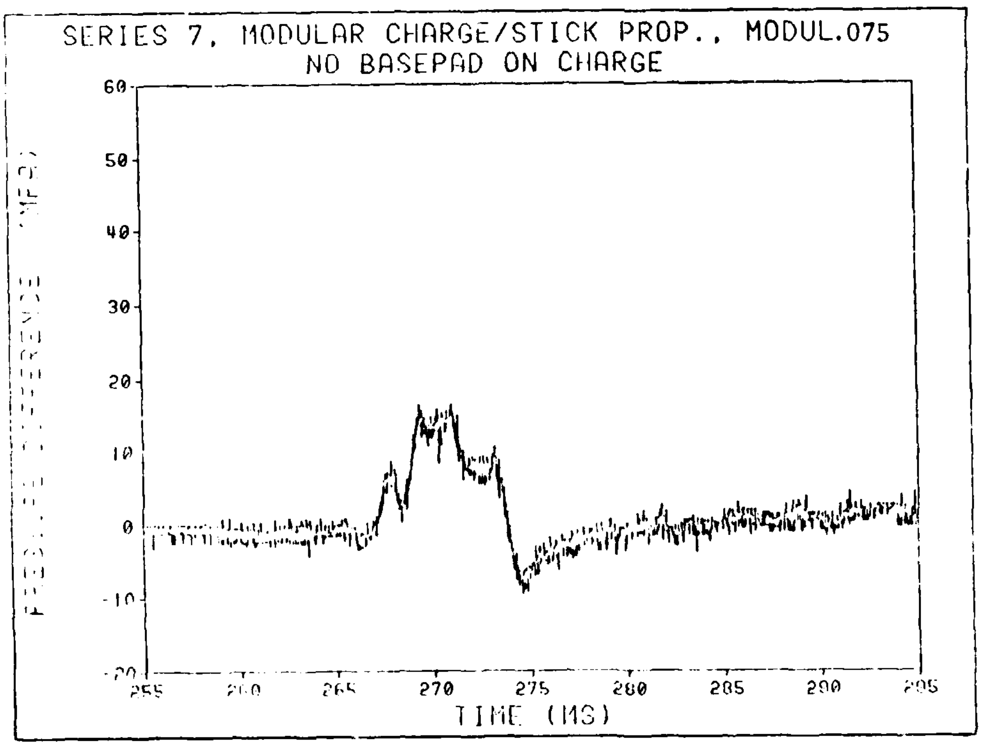
SERIES 7, MODULAR CHARGE/STICK PROP., MODUL.075
NO BASEPAD ON CHARGE
60
50
40
30
20
10
0
270
275
280
285
290
TIME (MS)

AD-A152 654 MULTIZONE MODULAR ARTILLERY PROPELLING CHARGE STUDIES (U) ARMY BALLISTIC RESEARCH LAB ABERDEEN PROVING GROUND MD C R RUTH ET AL. FEB 85 BRL-TR-2636 SBI-AD-F300 597 2/2

UNCLASSIFIED F/G 19/6 NL

END

FILMED

DTIC

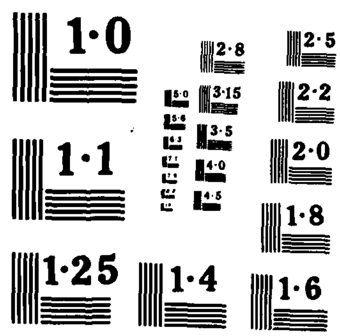
1·0
2·8
2·5
3·15
2·2
3·5
1·1
4·0
2·0
4·5
1·8
1·25
1·4
1·6

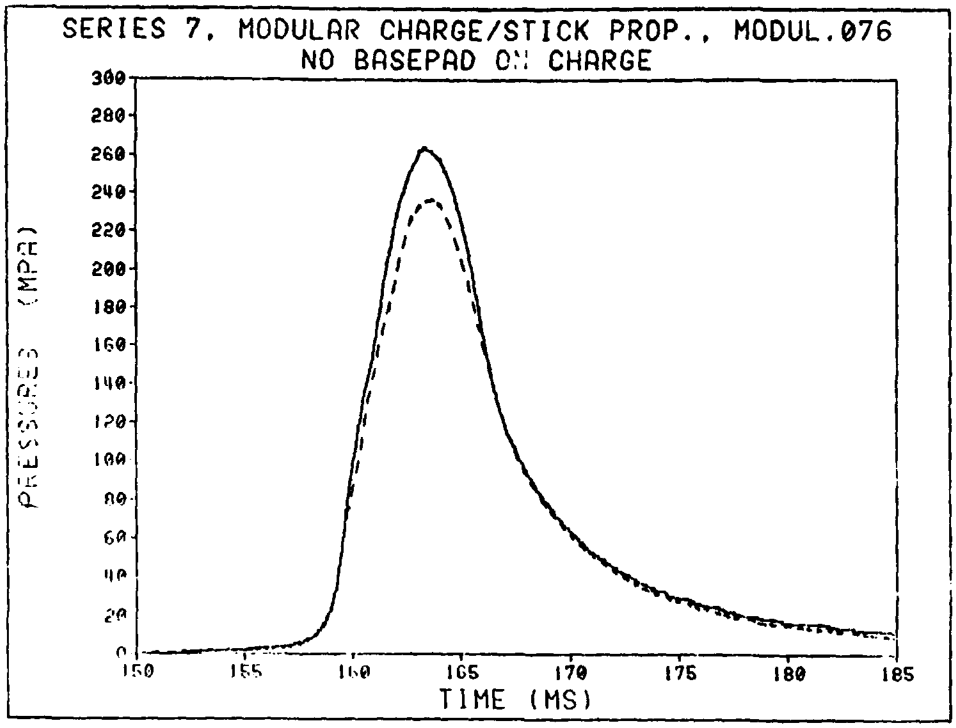
SERIES 7, MODULAR CHARGE/STICK PROP., MODUL.076
NO BASEPAD ON CHARGE
PRESSURES (MPA)
TIME (MS)
0
20
40
60
80
100
120
140
160
180
200
220
240
260
280
300
150
155
160
165
170
175
180
185

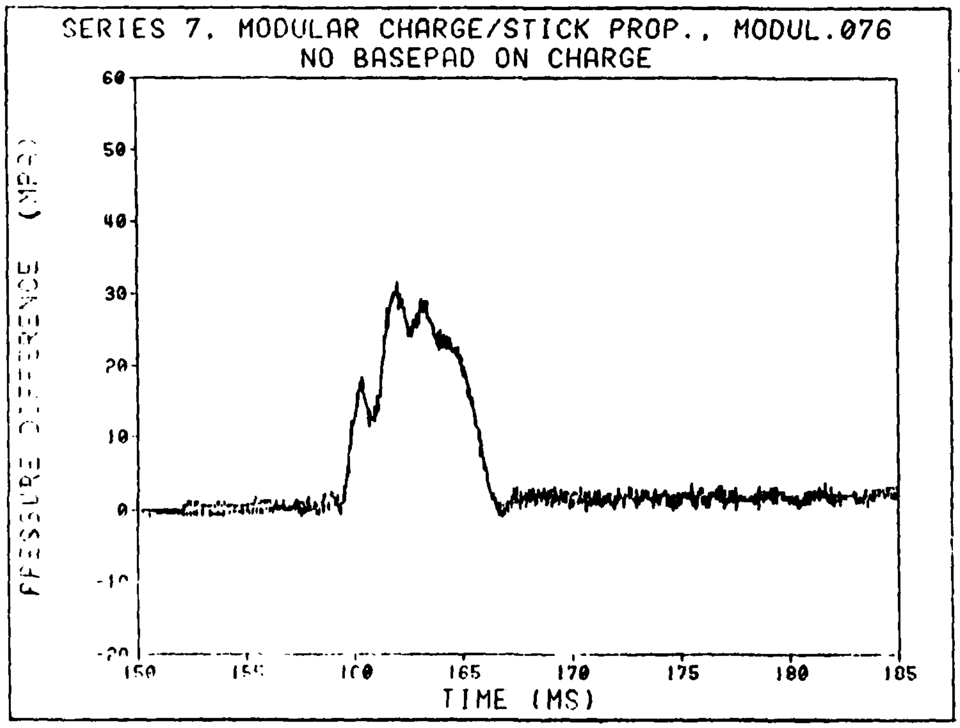
SERIES 7, MODULAR CHARGE/STICK PROP., MODUL.076
NO BASEPAD ON CHARGE
PRESSURE DIFFERENCE (MPA)
TIME (MS)
-20
-10
0
10
20
30
40
50
60
150
155
160
165
170
175
180
185

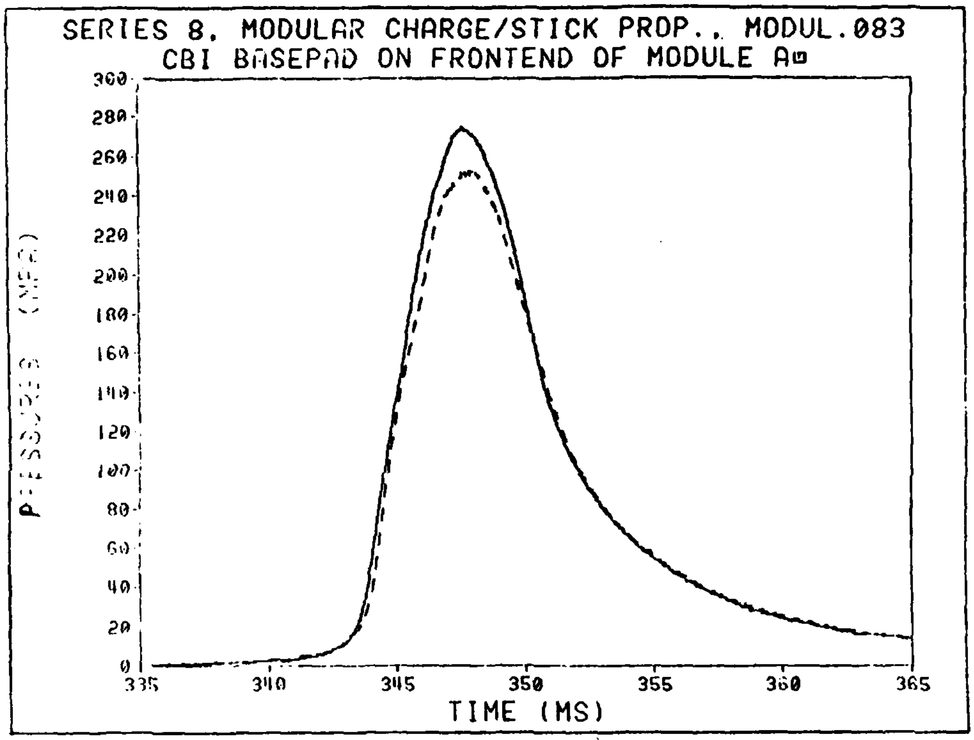
SERIES 8, MODULAR CHARGE/STICK PROP., MODUL.083
CBI BASEPAD ON FRONTEND OF MODULE A
PRESSURE (MPA)
TIME (MS)
0
20
40
60
80
100
120
140
160
180
200
220
240
260
280
300
335
340
345
350
355
360
365

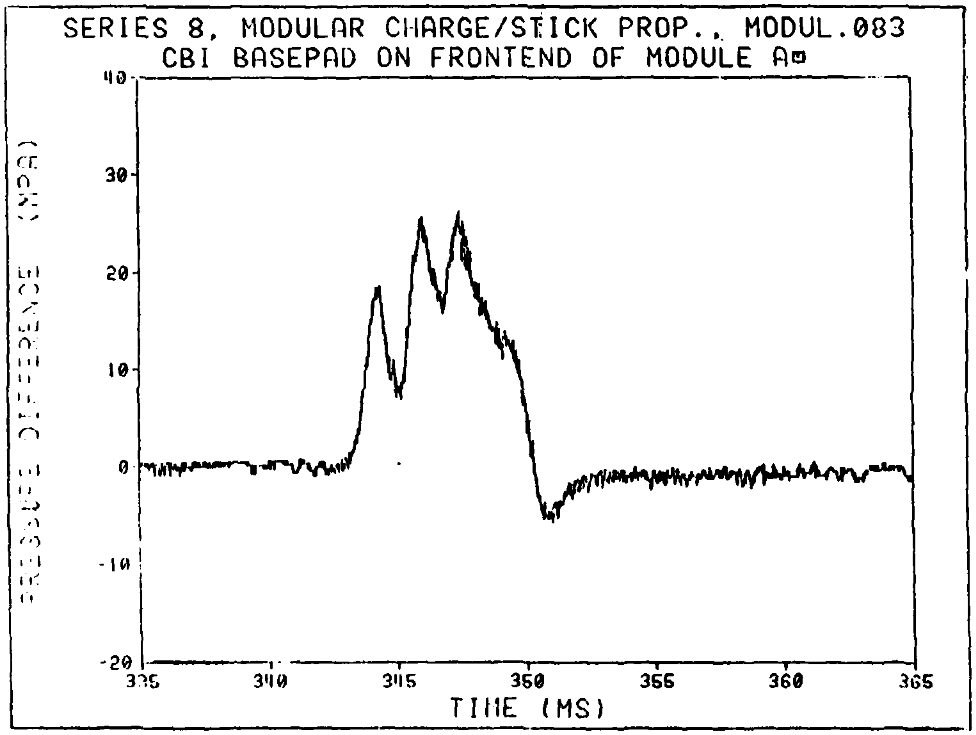
SERIES 8, MODULAR CHARGE/STICK PROP., MODUL.083
CBI BASEPAD ON FRONTEND OF MODULE A
PRESSURE DIFFERENCE (MPA)
TIME (MS)
-20
-10
0
10
20
30
40
335
340
345
350
355
360
365

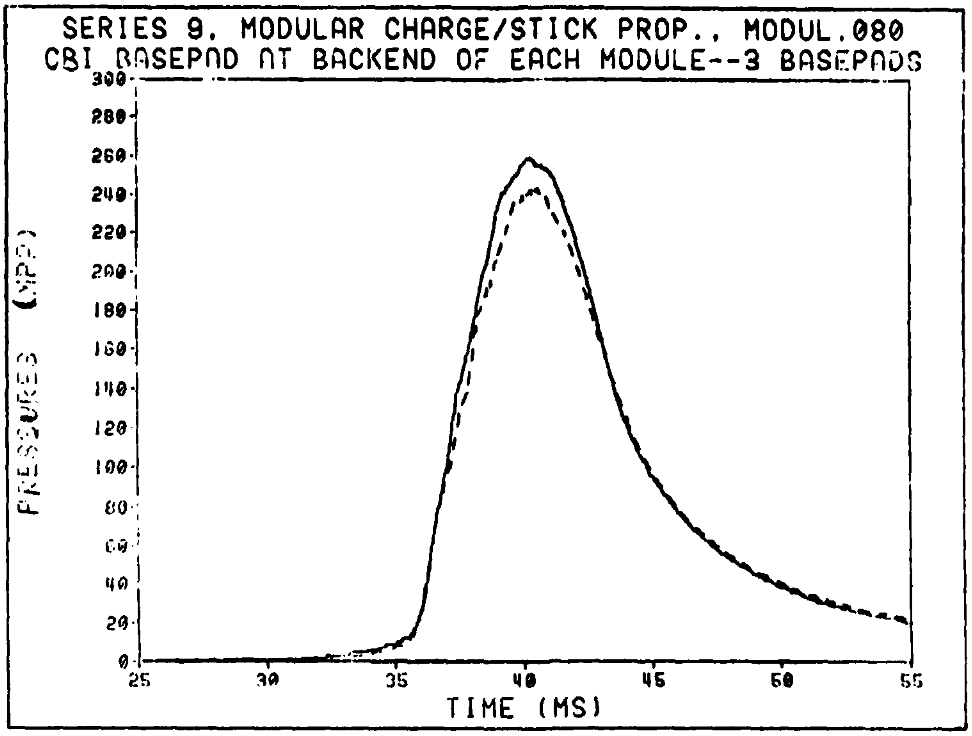
SERIES 9, MODULAR CHARGE/STICK PROP., MODUL.080
CBI BASEPAD AT BACKEND OF EACH MODULE--3 BASEPADS
PRESSURES (MPA)
TIME (MS)
0
20
40
60
80
100
120
140
160
180
200
220
240
260
280
300
25
30
35
40
45
50
55

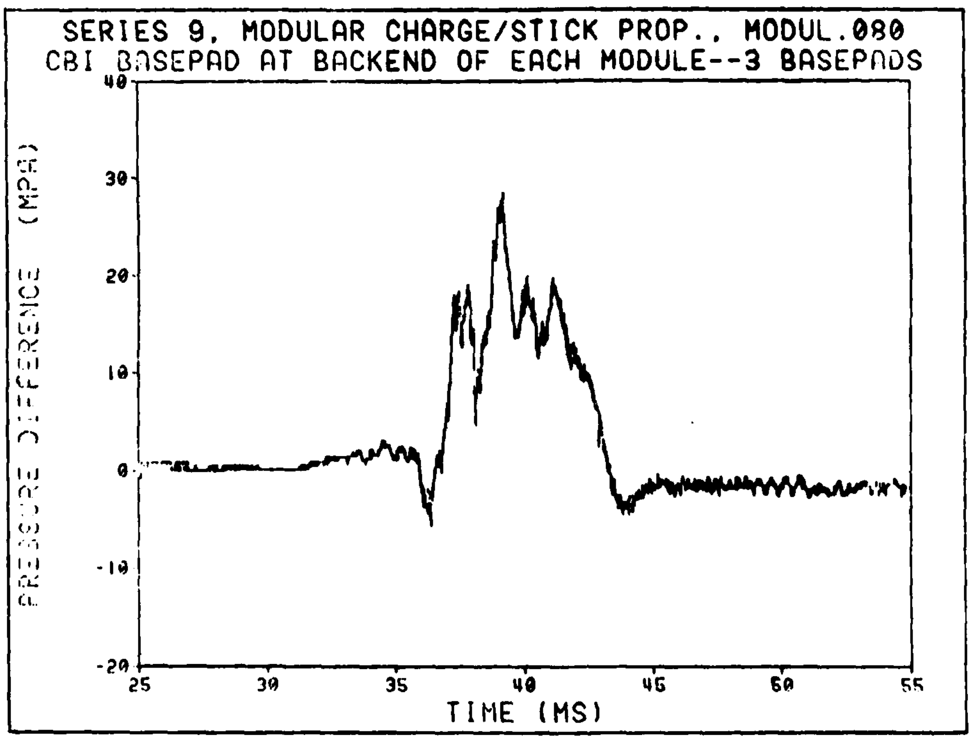
SERIES 9, MODULAR CHARGE/STICK PROP., MODUL.080
CBI BASEPAD AT BACKEND OF EACH MODULE--3 BASEPADS
PRESSURE DIFFERENCE (MPA)
TIME (MS)
-20
-10
0
10
20
30
40
25
30
35
40
45
50
55

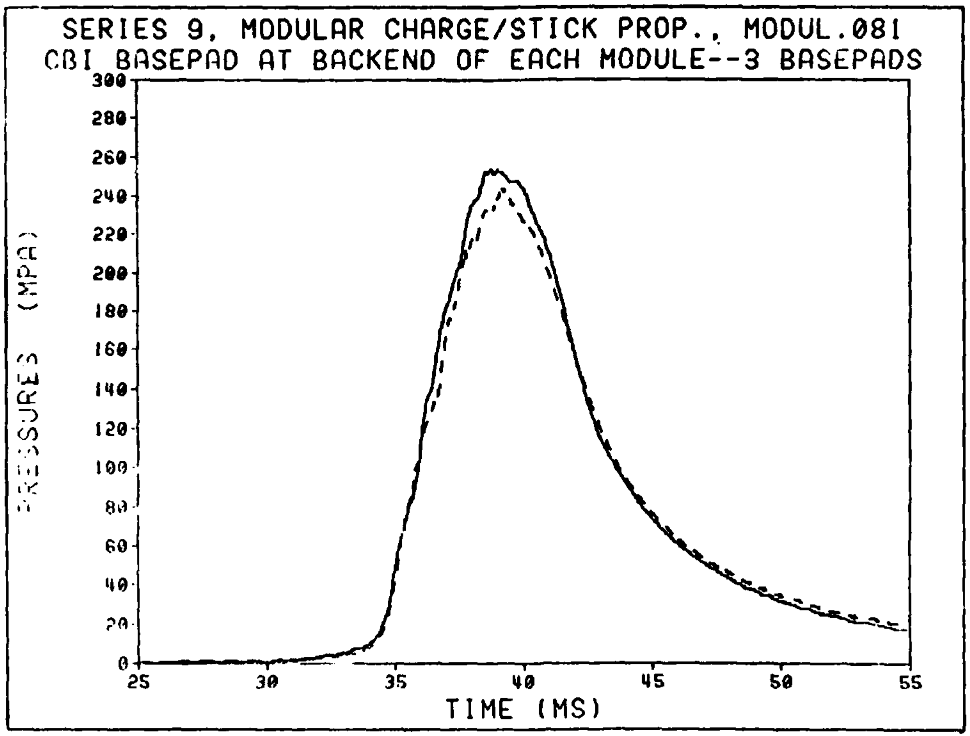
SERIES 9, MODULAR CHARGE/STICK PROP., MODUL.081
CBI BASEPAD AT BACKEND OF EACH MODULE--3 BASEPADS
PRESSURES (MPA)
TIME (MS)

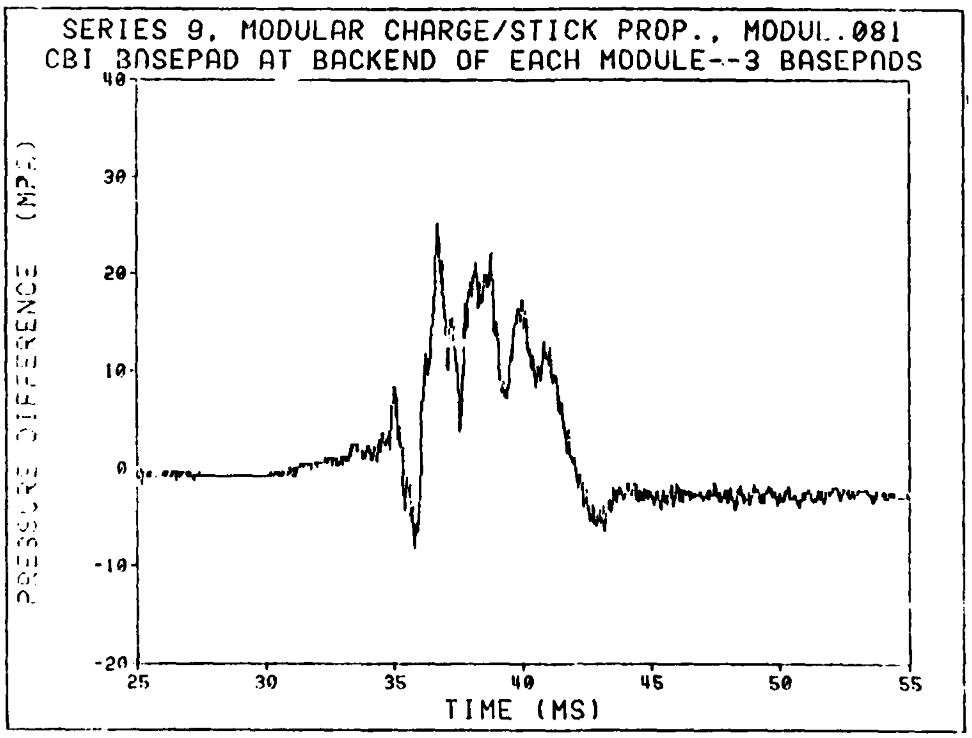
SERIES 9, MODULAR CHARGE/STICK PROP., MODUL.081
CBI BASEPAD AT BACKEND OF EACH MODULE--3 BASEPADS
PRESSURE DIFFERENCE (MPA)
TIME (MS)

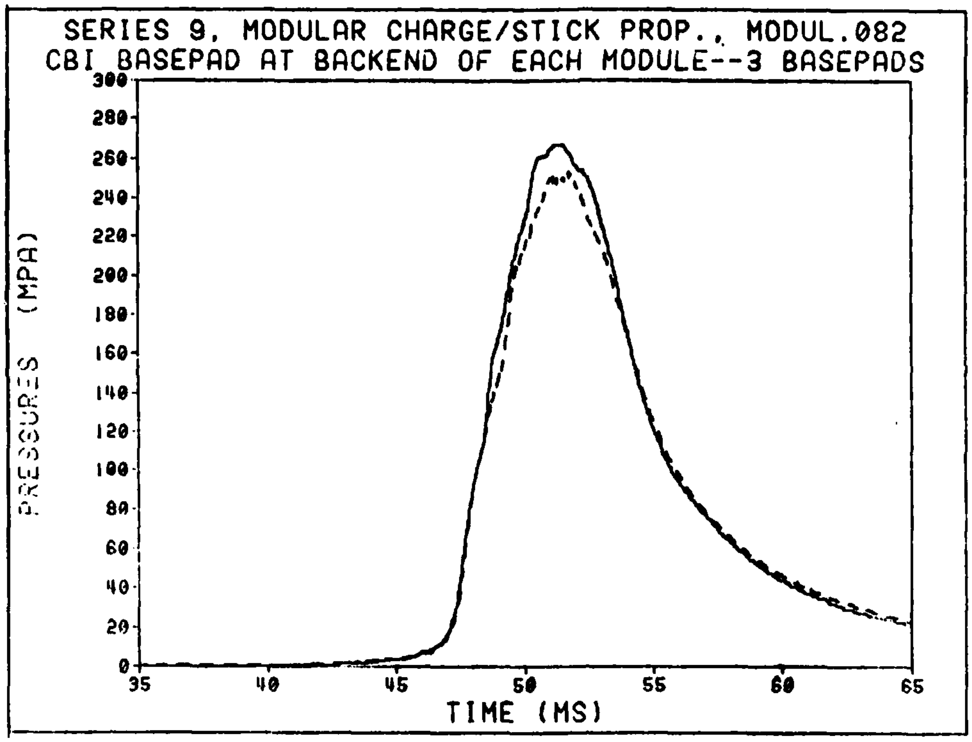

SERIES 9, MODULAR CHARGE/STICK PROP., MODUL.082
CBI BASEPAD AT BACKEND OF EACH MODULE--3 BASEPADS
PRESSURES (MPA)
TIME (MS)

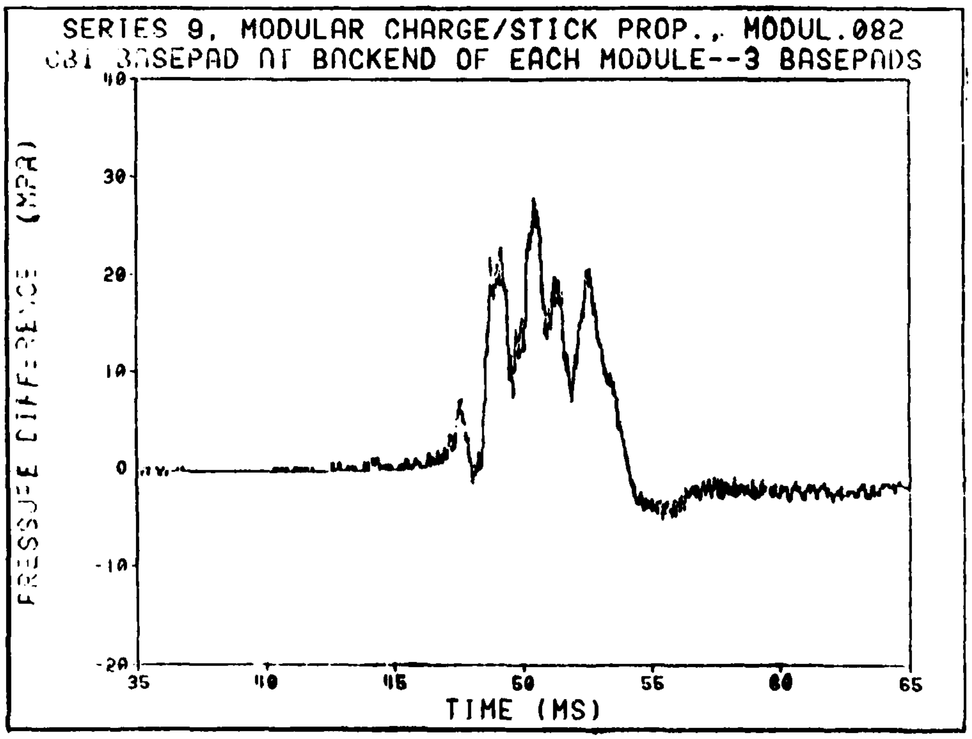

SERIES 9, MODULAR CHARGE/STICK PROP., MODUL.082
CBI BASEPAD AT BACKEND OF EACH MODULE--3 BASEPADS
PRESSURE DIFFERENCE (MPA)
TIME (MS)

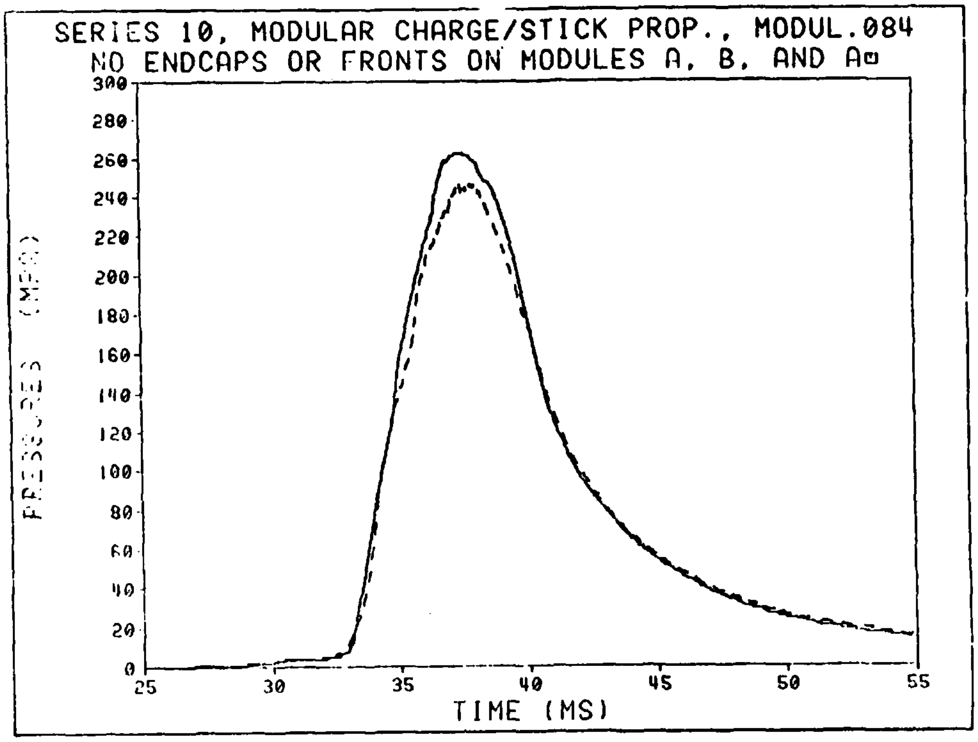

SERIES 10, MODULAR CHARGE/STICK PROP., MODUL.084
NO ENDCAPS OR FRONTS ON MODULES A, B, AND A
PRESSURES (MPA)
300
280
260
240
220
200
180
160
140
120
100
80
60
40
20
0
25
30
35
40
45
50
55
TIME (MS)

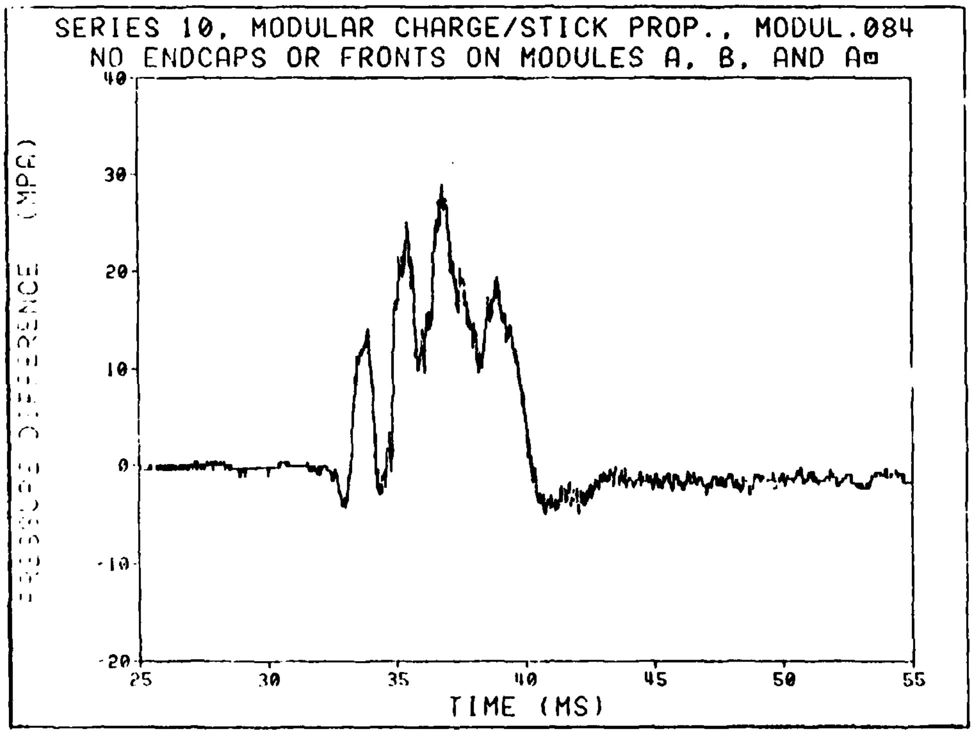

SERIES 10, MODULAR CHARGE/STICK PROP., MODUL.084
NO ENDCAPS OR FRONTS ON MODULES A, B, AND A
PRESSURE DIFFERENCE (MPA)
40
30
20
10
0
-10
-20
25
30
35
40
45
50
55
TIME (MS)

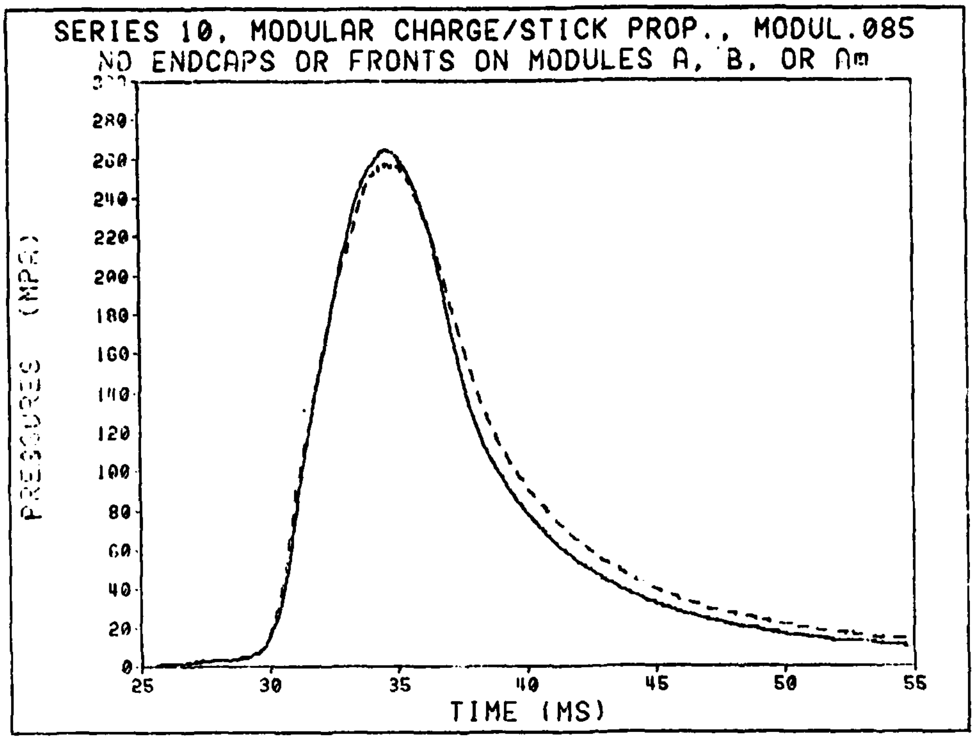
SERIES 10, MODULAR CHARGE/STICK PROP., MODUL.085
NO ENDCAPS OR FRONTS ON MODULES A, B, OR Am
PRESSURES (MPA)
TIME (MS)

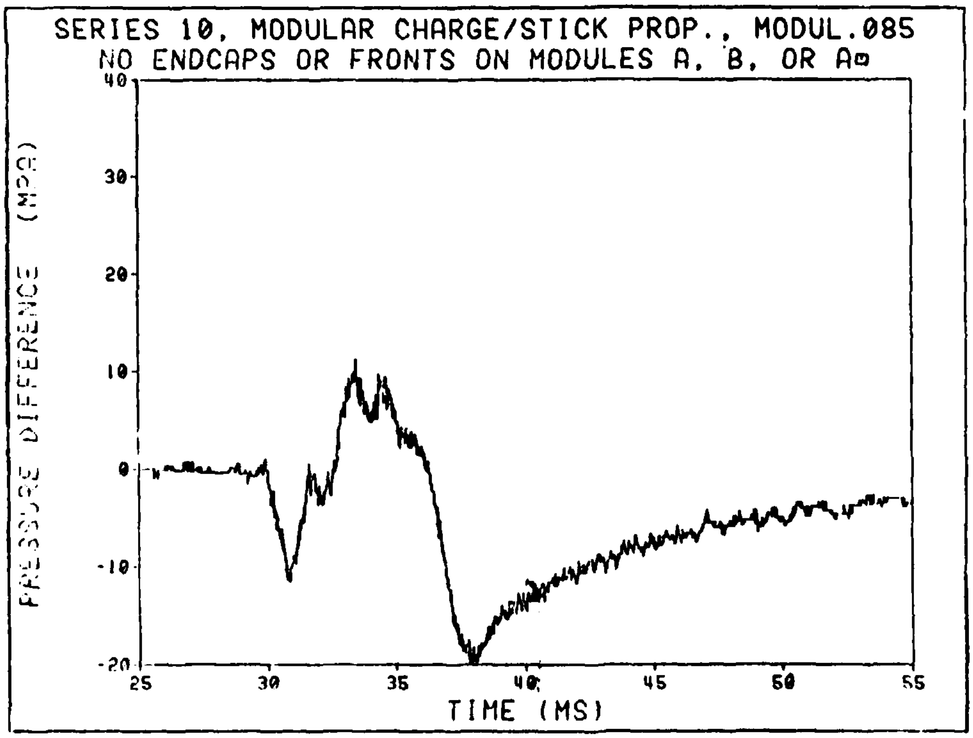
SERIES 10, MODULAR CHARGE/STICK PROP., MODUL.085
NO ENDCAPS OR FRONTS ON MODULES A, B, OR Am
PRESSURE DIFFERENCE (MPA)
TIME (MS)

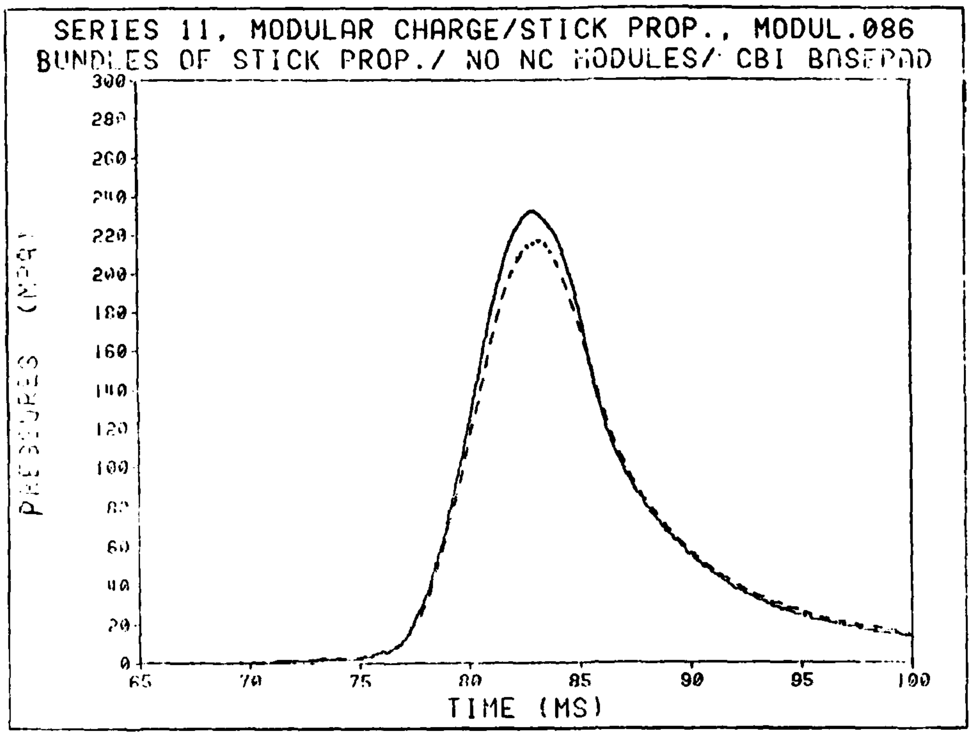
SERIES 11, MODULAR CHARGE/STICK PROP., MODUL.086
BUNDLES OF STICK PROP./ NO NC MODULES/ CBI BASEPAD
TIME (MS)
PRESSURES (MPA)

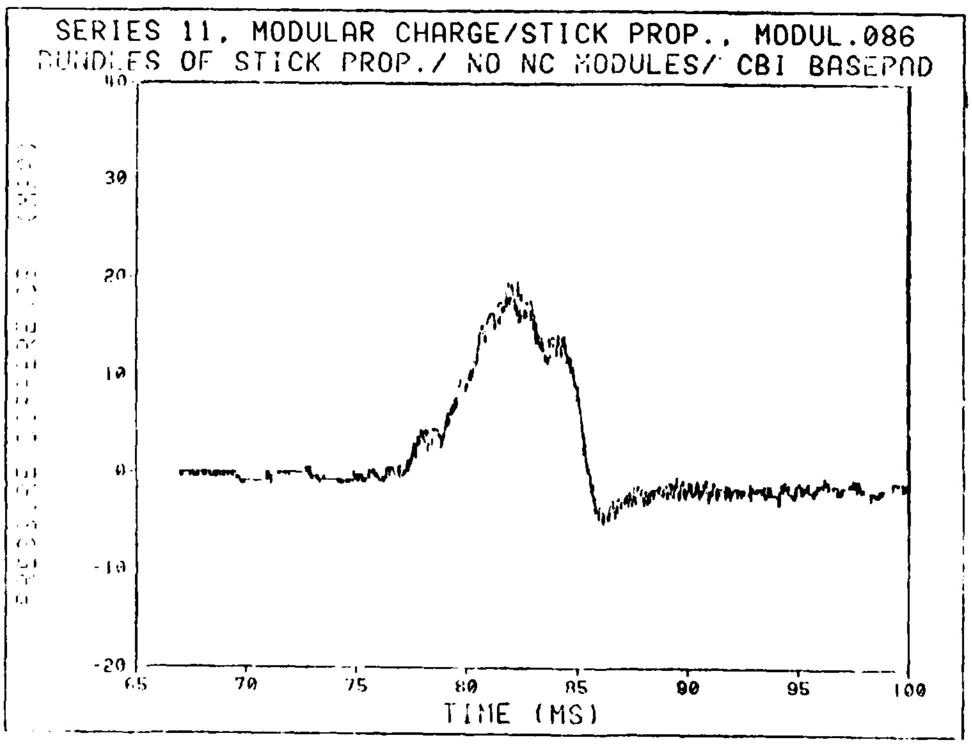
SERIES 11, MODULAR CHARGE/STICK PROP., MODUL.086
BUNDLES OF STICK PROP./ NO NC MODULES/ CBI BASEPAD
TIME (MS)

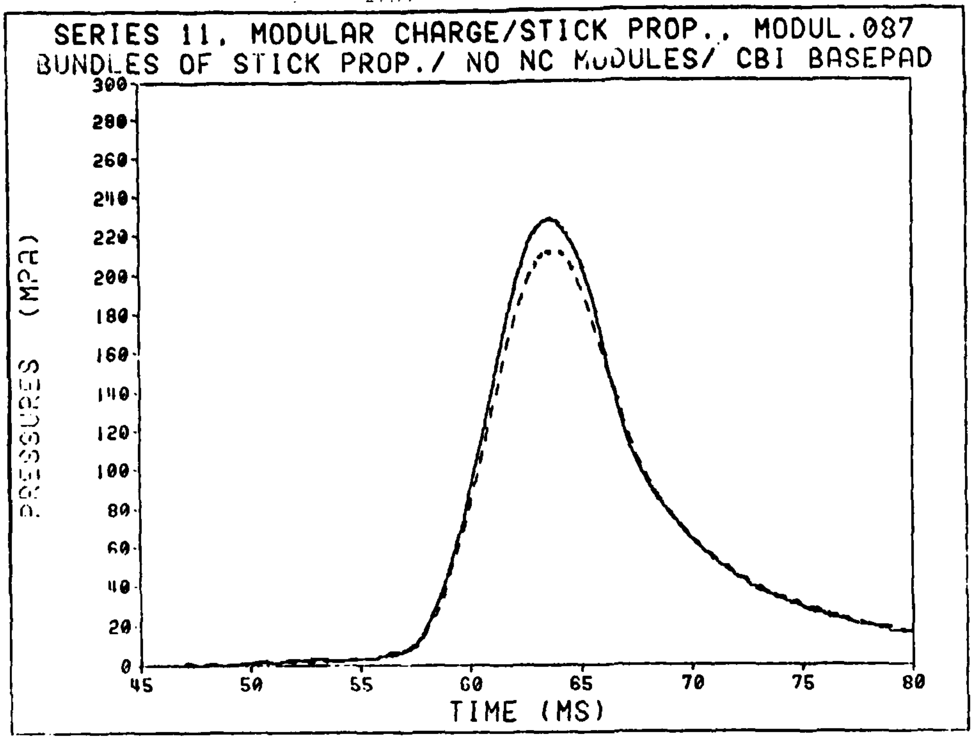
SERIES 11, MODULAR CHARGE/STICK PROP., MODUL.087
BUNDLES OF STICK PROP./ NO NC MODULES/ CBI BASEPAD
PRESSURES (MPA)
TIME (MS)

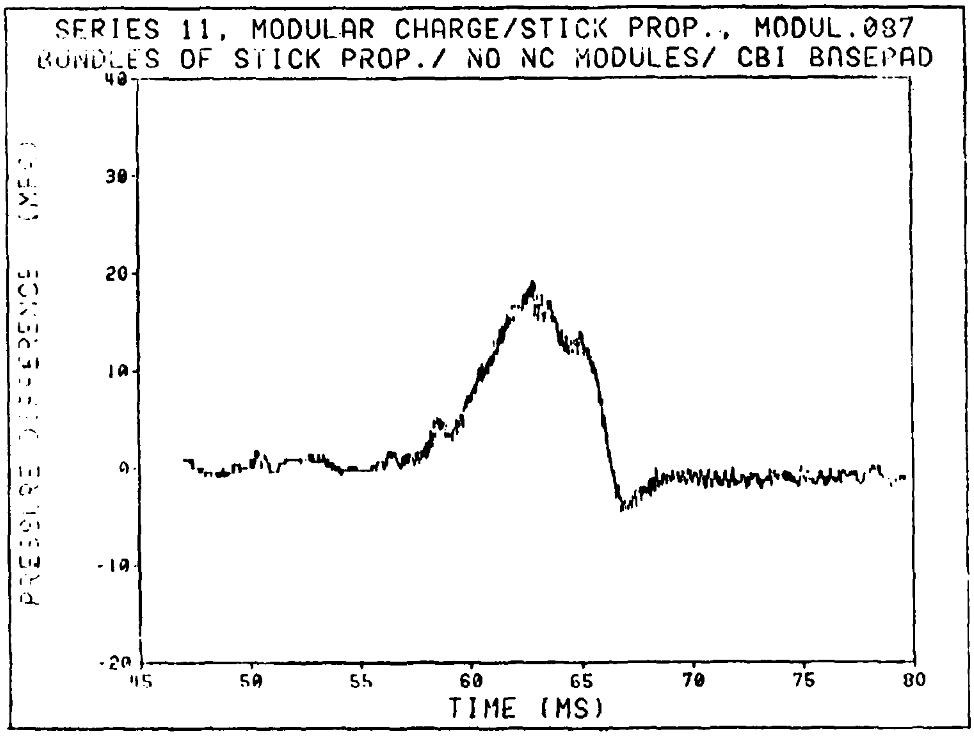
SERIES 11, MODULAR CHARGE/STICK PROP., MODUL.087
BUNDLES OF STICK PROP./ NO NC MODULES/ CBI BASEPAD
PRESSURE DIFFERENCE (MPA)
TIME (MS)

DISTRIBUTION LIST

No. Of Copies	Organization
12	Administrator Defense Technical Info Center ATTN: DTIC-DDA Cameron Station Alexandria, VA 22314
1	Office of the Under Secretary of Defense Research & Engineering ATTN: R. Thorkildsen Washington, DC 20301
1	HQDA/SAUS-OR, D. Hardison Washington, DC 20301
1	HQDA/DAMA-ZA Washington, DC 20310
1	HQDA, DAMA-CSM, E. Lippi Washington, DC 20310
1	HQDA/SARDA Washington, DC 20310
1	Commandant US Army War College ATTN: Library-FF229 Carlisle Barracks, PA 17013
1	Commander Ballistic Missile Defense Advanced Technology Center PO Box 1500 Huntsville, AL 35807
1	Chairman DOD Explosives Safety Board Room 856-C Hoffman Bldg. 1 2461 Eisenhower Avenue Alexandria, VA 22331
1	Commander US Army Materiel Command ATTN: AMCDRA-ST 5001 Eisenhower Avenue Alexandria, VA 22333
1	HQ DAMA-ART-M Washington, DC 20310
13	Commander Armament R&D Center, US Army AMCCOM ATTN: SMCAR-TSS SMCAR-TDC D. Gyorog SMCAR-LCA J. Lannon A. Beardell D. Downs S. Einstein L. Schlosberg S. Westley S. Bernstein P. Kemmey C. Heyman A. Bracuti Dover, NJ 07801
8	Commander Armament R&D Center, US Army AMCCOM ATTN: SMCAR-SCA, L. Stiefel B. Brodman SMCAR-LCB-I, D. Spring SMCAR-LCE, R. Walker SMCAR-LCU-CT, E. Barrieres R. Davitt SMCAR-LCU-CV C. Mandala SMCAR-LCM-E, S. Kaplowitz Dover, NJ 07801

DISTRIBUTION LIST

No. Of Copies	Organization
1	Commander Armament R&D Center, US Army AMCCOM ATTN: SMCAR-QAR, J. Rutkowski Dover, NJ 07801
5	Project Manager Cannon Artillery Weapons System, ATTN: AMCPM-CW, F. Menke AMCPM-CWW H. Noble AMCPM-CWS M. Fisette AMCPM-CWA R. DeKleine H. Hassmann Dover, NJ 07801
2	Project Manager Munitions Production Base Modernization and Expansion ATTN: AMCPM-PBM, A. Siklosi SARPM-PBM-E, L. Laibson Dover, NJ 07801
3	Project Manager Tank Main Armament System ATTN: AMCPM-TMA, K. Russell AMCPM-TMA-105 AMCPM-TMA-120 Dover, NJ 07801
3	Commander Armament R&D Center, US Army AMCCOM ATTN: SMCAR-LCW-A, M. Salisbury SMCAR-LCS SMCAR-LC, J. Frasier Dover, NJ 07801
5	Commander US Army Armament Munitions and Chemical Command ATTN: SMCAR-ES -L AMSMC-LC, L. Ambrosini AMSMC-IRC, G. Cowan AMSMC-LEM, W. Fortune R. Zastrow Rock Island, IL 61299
1	Commander Benet Weapons Laboratory ATTN: SARWV-RD, R. Thierry Watervliet, NY 12189
1	Director US Army AMCCOM Armament R&D Center Benet Weapons Laboratory ATTN: SMCAR-LCB-TL Watervliet, NY 12189
1	Commander US Army Aviation Research and Development Command ATTN: AMSAV-E 4300 Goodfellow Blvd. St. Louis, MO 63120
1	Commander US Army TSARCOM 4300 Goodfellow Blvd St. Louis, MO 63120.
1	Director US Army Air Mobility Research And Development Laboratory Ames Research Center Moffett Field, CA 94035
1	Commander US Army Communications-Electronics Command ATTN: AMSEL-ED Fort Monmouth, NJ 07703

DISTRIBUTION LIST

No. Of Copies	Organization
1	Commander US Army Electronics Research and Development Command Technical Support Activity ATTN: DELSD-L Fort Monmouth, NJ 07703-5301
1	Commander US Army Harry Diamond Lab. ATTN: DELHD-TI 2800 Powder Mill Road Adelphi, MD 20783
	Commander US Army Missile Command ATTN: AMSMI-R Redstone Arsenal, AL 35898
1	Commander US Army Natick Research and Development Command ATTN: AMDNA-DT, D. Sieling Natick, MA 01762
1	Commander US Army Tank Automotive Command ATTN: AMSTA-TSL Warren, MI 48090
1	US Army Tank Automotive Command ATTN: AMSTA-CG Warren, MI 48090
1	Project Manager Improved TOW Vehicle ATTN: AMCPM-ITV US Army Tank Automotive Research & Development Command Warren, MI 48090
1	Project Manager Fighting Vehicle Systems ATTN: AMCPM-FVS Warren, MI 48090
2	Program Manager M1 Tank System ATTN: AMCPM-GMC-SA, J. Roossien Warren, MI 48090
1	Director US Army TRADOC Systems Analysis Activity ATTN: ATAA-SL, Tech Lib White Sands Missile Range NM 88002
1	Project Manager M-60 Tank Development ATTN: AMCPM-M60TD Warren, MI 48090
1	Commander US Army Training & Doctrine Command ATTN: ATCD-MA/ MAJ Williams Fort Monroe, VA 23651
2	Commander US Army Materials and Mechanics Research Center ATTN: AMXMR-ATL Tech Library Watertown, MA 02172
1	Commander US Army Research Office ATTN: Tech Library P. O. Box 12211 Research Triangle Park, NC 27709-2211
1	Commander US Army Belvoir R&D Center ATTN: STRBE-WC Fort Belvoir, VA 22060

DISTRIBUTION LIST

No. Of Copies	Organization
1	Commander US Army Logistics Mgmt Ctr Defense Logistics Studies Fort Lee, VA 23801
1	Commandant US Army Infantry School ATTN: ATSH-CD-CSO-OR Fort Benning, GA 31905
1	President US Army Armor & Engineer Board ATTN: STEBB-AD-S Fort Knox, KY 40121
1	Commandant US Army Aviation School ATTN: Aviation Agency Fort Rucker, AL 36360
1	Commandant US Army Command and General Staff College Fort Leavenworth, KS 66027
1	Commandant US Army Special Warfare School ATTN: Rev & Tng Lit Div Fort Bragg, NC 28307
1	President US Army Artillery Board Ft. Sill, OK 73503
1	Commander US Army Foreign Science & Technology Center ATTN: AMXST-MC-3 Federal Office Building 220 Seventh Street, NE Charlottesville, VA 22901
2	Commandant US Army Field Artillery School ATTN: ATSF-CO-MW, B. Willis Ft. Sill, OK 73503
3	Commandant US Army Armor School ATTN: ATZK-CD-MS/ M. Falkovitch Armor Agency Fort Knox, KY 40121
1	Commander US Army Missile Command ATTN: AMSMI-YDL Redstone Arsenal, AL 35898
1	Office of Naval Research ATTN: Code 473, R. S. Miller 800 N. Quincy Street Arlington, VA 22217
1	Commander Naval Sea Systems Command ATTN: SEA-62R2, R. Beauregard National Center, Bldg. 2 Room 6E08 Washington, DC 20362
1	Commander Naval Air Systems Command ATTN: NAIR-954-Tech Lib Washington, DC 20360
1	Strategic Systems Project Office Dept. of the Navy Rm. 901 ATTN: J. F. Kincaid Washington, D.C. 20360

DISTRIBUTION LIST

No. Of Copies	Organization
1	Assistant Secretary of the Navy (R,E, and S) ATTN: R. Reichenbach Room 5E787 Pentagon Bldg. Washington, DC 20350
1	Naval Research Lab Tech Library Washington, DC 20375
5	Commander Naval Surface Weapons Center ATTN: Code G33, J. L. East W. Burrell J. Johndrow Code G23, D. McClure Code DX-21 Tech Lib Dahlgren, VA 22448
2	Commander US Naval Surface Weapons Center ATTN: J. P. Consaga C. Gotzmer Indian Head, MD 20640
4	Commander Naval Surface Weapons Center ATTN: S. Jacobs/Code 240 Code 730 K. Kim/Code R-13 R. Bernecker Silver Spring, MD 20910
2	Commanding Officer Naval Underwater Systems Center Energy Conversion Dept. ATTN: CODE 5B331, R. S. Lazar Tech Lib Newport, RI 02840
4	Commander Naval Weapons Center ATTN: Code 388, R. L. Derr C. F. Price T. Boggs Info. Sci. Div. China Lake, CA 93555
2	Superintendent Naval Postgraduate School Dept. of Mechanical Engineering ATTN: A.E. Fuhs Code 1424 Library Monterey, CA 93940
6	Commander Naval Ordnance Station ATTN: P. L. Stang J. Birkett S. Mitchell C. Christensen D. Brooks Tech Library Indian Head, MD 20640
1	AFSC/SDOA Andrews AFB Andrews AFB, MD 20334
1	Program Manager AFOSR Directorate of Aerospace Sciences ATTN: L. H. Caveny Bolling AFB Washington, DC 20332
5	AFRPL (DYSC) ATTN: D. George J. N. Levine Tech Library D. Thrasher N. Vander Hyde Edwards AFB, CA 93523

DISTRIBUTION LIST

No. Of Copies	Organization
1	AFFTC ATTN: SSD-Tech Lib Edwards AFB, CA 93523
1	AFATL/DLYV Eglin AFB, FL 32542
1	Commander US Army Materiel Command ATTN: AMCDE 5001 Eisenhower Avenue Alexandria, VA 22333
1	Aerojet Solid Propulsion Co. ATTN: P. Micheli Sacramento, CA 95813
1	AFATL/DLODL ATTN: Tech Lib Eglin AFB, FL 32542-5000
1	AFFDL ATTN: TST-Lib Wright-Patterson AFB, OH 45433
1	Aerodyne Research, Inc. Bedford Research Park ATTN: V. Yousefian Bedford, MA 01730
1	Commander US Army Materiel Command ATTN: DCRSF-E, Safety Office 5001 Eisenhower Avenue Alexandria, VA 22333

No. Of Copies	Organization
1	Atlantic Research Corporation ATTN: M. K. King 5390 Cherokee Avenue Alexandria, VA 22314
1	AVCO Everett Rsch Lab ATTN: D. Stickler 2385 Revere Beach Parkway Everett, MA 02149
2	Calspan Corporation ATTN: Tech Library P. O. Box 400 Buffalo, NY 14225
1	Foster Miller Associates ATTN: A. Erickson 135 Second Avenue Waltham, MA 02154
1	ENKI Corporation 9015 Fullbright Avenue Chatsworth, CA 91311
1	General Applied Sciences Lab ATTN: J. Erdos Merrick & Stewart Avenues Westbury Long Island, NY 11590
1	General Electric Company Armament Systems Dept. ATTN: M. J. Bulman, Room 1311 Lakeside Avenue Burlington, VT 05401
1	Hercules, Inc. Allegany Ballistics Laboratory ATTN: R. B. Miller P. O. Box 210 Cumberland, MD 21501

DISTRIBUTION LIST

No. Of Copies	Organization
1	Hercules, Inc Bacchus Works ATTN: K. P. McCarty P. O. Box 98 Magna, UT 84044
1	Hercules, Inc. Eglin AFB Laboratory AFATL DLDL ATTN: R.L. Simmons P.O. Box 1646 Eglin AFB, FL 32542
1	IITRI ATTN: M. J. Klein 10 W. 35th Street Chicago, IL 60616
2	Lawrence Livermore Laboratory ATTN: M. S. L-355, A. Buckingham M. Finger P. O. Box 808 Livermore, CA 94550
1	Olin Corporation Badger Army Ammunition Plant ATTN: R. J. Thiede Baraboo, WI 53913
1	Olin Corporation Smokeless Powder Operations ATTN: R. L. Cook P.O. Box 222 St. Marks, FL 32355
1	Paul Gough Associates, Inc. ATTN: P. S. Gough P. O. Box 1614, Portsmouth, NH 03801
2	Thiokol Corporation Wasatch Division ATTN: J. Peterson Tech Library P.O. Box 524 Brigham City, UT 84302
1	Princeton Combustion Research Lab., Inc. ATTN: M. Summerfield 475 US Highway One North Princeton, NJ 08852
1	Physics International Company 2700 Merced Street San Leandro, CA 94577
2	Rockwell International Rocketdyne Division ATTN: BA08 J. E. Flanagan J. Gray 6633 Canoga Avenue Canoga Park, CA 91304
1	Science Applications, Inc. ATTN: R. B. Edelman 23146 Cumorah Crest Woodland Hills, CA 91364
1	Scientific Research Assoc. Inc. ATTN: H. McDonald P.O. Box 498 Glastonbury, CT 06033
3	Thiokol Corporation Huntsville Division ATTN: D. Flanigan R. Glick Tech Library Huntsville, AL 35807
1	Commander US Army Development & Employment Agency ATTN: MODE-TED-SAB Fort Lewis, WA 98433

DISTRIBUTION LIST

No. Of Copies	Organization
2	Thiokol Corporation Elkton Division ATTN: R. Biddle Tech Lib. P. O. Box 241 Elkton, MD 21921
2	United Technologies Chemical Systems Division ATTN: R. Brown Tech Library P. O. Box 358 Sunnyvale, CA 94086
1	Universal Propulsion Company ATTN: H. J. McSpadden Black Canyon Stage 1 Box 1140 Phoenix, AZ 85029
1	Veritay Technology, Inc. ATTN: E. B. Fisher P. O. Box 22 Bowmansville, NY 14026
1	California Institute of Tech 204 Karman Lab Main Stop 301-46 ATTN: F.E. Culick 1201 E. California St. Pasadena, CA 91109
1	Battelle Memorial Institute ATTN: Tech Library 505 King Avenue Columbus, OH 43201
1	Brigham Young University Dept. of Chemical Engineering ATTN: M. Beckstead Provo, UT 84601

No. Of Copies	Organization
1	California Institute of Tech Jet Propulsion Laboratory ATTN: L. D. Strand 4800 Oak Grove Drive Pasadena, CA 91103
1	Professor H. Krier University of Illinois Mech/Industrial Engr Dept 144 MEB, 1206 W. Green Street Urbana, IL 61801
1	University of Massachusetts Dept. of Mechanical Engineering ATTN: K. Jakus Amherst, MA 01002
1	University of Minnesota Dept. of Mechanical Engineering ATTN: E. Fletcher Minneapolis, MN 55455
1	Case Western Reserve University Division of Aerospace Sciences ATTN: J. Tien Cleveland, OH 44135
3	Georgia Institute of Tech School of Aerospace Eng. ATTN: B. T. Zinn E. Price W. C. Strahle Atlanta, GA 30332
1	Institute of Gas Technology ATTN: D. Gidaspow 3424 S. State Street Chicago, IL 60616

DISTRIBUTION LIST

No. Of Copies	Organization
1	Johns Hopkins University Applied Physics Laboratory Chemical Propulsion Information Agency ATTN: T. Christian Johns Hopkins Road Laurel, MD 20707
1	Massachusetts Institute of Technology Dept of Mechanical Engineering ATTN: T. Toong Cambridge, MA 02139
1	Pennsylvania State College Applied Research Lab ATTN: G. M. Faeth P. O. Box 30 State College, PA 16801
1	Pennsylvania State University Dept. Of Mechanical Engineering ATTN: K. Kuo University Park, PA 16802
1	Purdue University School of Mechanical Engineering ATTN: J. R. Osborn TSPC Chaffee Hall West Lafayette, IN 47906
1	Rensselaer Polytechnic Inst. Department of Mathematics Troy, NY 12181
1	Rutgers University Dept. of Mechanical and Aerospace Engineering ATTN: S. Temkin University Heights Campus New Brunswick, NJ 08903
1	SRI International Propulsion Sciences Division ATTN: Tech Library 333 Ravenswood Avenue Menlo, Park, CA 94025
1	Stevens Institute of Technology Davidson Laboratory ATTN: R. McAlevy, III Castle Point Station Hoboken, NJ 07030
2	Los Alamos Scientific Laboratory ATTN: T3, D. Butler M. Division, B. Craig P. O. Box 1663 Los Alamos, NM 87544
1	University of Southern California Mechanical Engineering Dept. ATTN: OHE200, M. Gerstein Los Angeles, CA 90007
2	University of Utah Dept. of Chemical Engineering ATTN: A. Baer G. Flandro Salt Lake City, UT 84112
1	Washington State University Dept. of Mechanical Engineering ATTN: C. T. Crowe Pullman, WA 99163
1	AFWL/SUL Kirtland AFB, NM 87117

Aberdeen Proving Ground

Dir, USAMSAA
  ATTN: AMXSY-D
        AMXSY-MP, H. Cohen
Cdr, USATECOM
  ATTN: AMSTE -TO-F
Cdr, CSTA
  ATTN: STECS-AA, S. Walton
                  G. Rice
                  D. Lacey
                  C. Herud
Dir, USAHEL
  ATTN: J. Weisz
Cdr, CRDC, AMCCOM
  ATTN: SMCCR-RSP-A
        SMCCR-MU
        SMCCR-SPS-IL

USER EVALUATION SHEET/CHANGE OF ADDRESS

This Laboratory undertakes a continuing effort to improve the quality of the reports it publishes. Your comments/answers to the items/questions below will aid us in our efforts.

1. BRL Report Number____________________________Date of Report____________

2. Date Report Received____

3. Does this report satisfy a need? (Comment on purpose, related project, or other area of interest for which the report will be used.)__________________

4. How specifically, is the report being used? (Information source, design data, procedure, source of ideas, etc.)____________________________________

5. Has the information in this report led to any quantitative savings as far as man-hours or dollars saved, operating costs avoided or efficiencies achieved, etc? If so, please elaborate.____

6. General Comments. What do you think should be changed to improve future reports? (Indicate changes to organization, technical content, format, etc.)

CURRENT ADDRESS

Name

Organization

Address

City, State, Zip

7. If indicating a Change of Address or Address Correction, please provide the New or Correct Address in Block 6 above and the Old or Incorrect address below.

OLD ADDRESS

Name

Organization

Address

City, State, Zip

(Remove this sheet along the perforation, fold as indicated, staple or tape closed, and mail.)

FOLD HERE

ector
Army Ballistic Research Laboratory
N: AMXBR-OD-ST
rdeen Proving Ground, MD 21005-5066

NO POSTAGE
NECESSARY
IF MAILED
IN THE
UNITED STATES

OFFICIAL BUSINESS
IALTY FOR PRIVATE USE, $300

BUSINESS REPLY MAIL
FIRST CLASS PERMIT NO 12062 WASHINGTON, DC

POSTAGE WILL BE PAID BY DEPARTMENT OF THE ARMY

Director
US Army Ballistic Research Laboratory
ATTN: AMXBR-OD-ST
Aberdeen Proving Ground, MD 21005-9989

FOLD HERE

END

FILMED

5-85

DTIC